



## **Phase and Amplitude Control of Dipole Crabbing Modes in Multi-Cell Cavities**

Amos C. Dexter and Graeme C. Burt  
**COCKCROFT INSITUTE**

*correspondance to*

Engineering Department, Lancaster University, Lancaster, LA1 4YR, UK

### **ABSTRACT**

This report sets out the established theory of driving a mode in a beam loaded, multi-cell cavity via a waveguide coupling and derives associated envelope equations from which time domain solutions are developed. Time domain solution allows accurate simulation with realistic microphonic spectra, beamloading, drive amplifier characteristics, controller and measurement errors to be encompassed. A computer code that uses the model is used to compute limits on phase and amplitude stability of a dipole mode as a function of disturbance and control system latency for a superconducting cavity being developed for use as a crab cavity for the ILC. A crab cavity is a deflection cavity operated with a  $90^\circ$  phase shift with respect to the beam so that the front of a bunch gets kicked one way whilst the back gets kicked the other way.

## CONTENTS

1.	Background	3
2.	Report Organisation	3
3.	Modelling Cavity Filling	5
4.	Waveguide Driven Circuit Model	6
5.	Steady State for a Single Cavity Mode	8
6.	Single Mode Resonant Loss Free Operation	9
7.	Beamloading	9
8.	Cavity Response to Beamloading	11
9.	The Envelope Equations	13
10.	Single Mode Diagonalisation	14
11.	Approximate Envelope Equations for the Multimode Case	16
12.	Definition of shunt impedance for the accelerating mode	17
13.	Definition of shunt impedance for dipole $TM_{1np}$ modes	18
14.	Crab Cavity Beam-loading from offset Bunches	21
15.	Voltage Increment needed for Envelope Equations	23
16.	Power Requirement for Beam loading	28
17.	Beam Loading Simulation – an illustration	30
18.	The Controller	32
19.	Single mode simulations for ILC bunch parameters	33
19.1	$Q_e = 10^6$ (no microphonics, no measurement error, severe random beamloading)	33
19.2	$Q_e = 3 \times 10^6$ (no microphonics, no meas. err., severe random beamloading)	36
19.3	Oscillatory offset (no microphonics)	38
19.4	Oscillatory offset and microphonics	42
20.	Gain Optimisation	45
21.	The Stability Limit	46
21.1	Analysis for Proportional Control	46
21.2	Analysis for Proportional Integral Control	51
22.	Ultimate Phase Performance for the Single Mode Cavity	57
22.1	No measurement error, Latency = 0.5 $\mu$ s, Update = 0.5 $\mu$ s, vary Q	59
22.2	Measurement error = 0.005 degrees, Latency = 0.5 $\mu$ s, Update = 0.5 $\mu$ s, vary Q	61
22.3	No measurement error, Latency = 1 $\mu$ s, Update = 1 $\mu$ s, vary Q	63
22.4	No microphonics	65
22.5	No beam, no microphonics	65
22.6	Measurement error = 0.005 degrees, Latency = 1 $\mu$ s, Update = 1 $\mu$ s, vary Q	66
22.7	Reduce Microphonic frequency from 230 Hz to 23 Hz	68
22.8	Measurement error = 0.005 degrees, Latency = 1.5 $\mu$ s, Update = 1.5 $\mu$ s, vary Q	69
22.9	Measurement error = 0.005 degrees, Latency = 3.0 $\mu$ s, Update = 1.0 $\mu$ s, vary Q	71
23.	Three Mode Simulation for ILC Cavities	73
23.1	Microphonics and oscillatory beamloading but no measurement error	73
23.2	Measurement error, microphonics and oscillatory beamloading	76
24.	Conclusions	78
25.	References	79
26.	Acknowledgements	79
27.	Appendix 1 Code for direct integration (see section 6)	80
28.	Appendix 2 Code for direct integration with controller	85
29.	Appendix 3 Code to integrate envelope equations	90

## 1. Background

The work described in this report has arisen from a requirement to predict the phase and amplitude control performance of superconducting crab cavities as required for the ILC [1].

The major output from the work is the computer code given in appendix III. It was unclear at the outset as to whether a satisfactory estimation of the phase and amplitude control performance could be made from an analytical analysis and hence we proceeded with the development of a code. The report contains derivations of the equations used and solved by code. It should be noted that many of the equations derived in the report are well known and can be found in similar but not necessarily identical forms elsewhere.

The code models the control of a multi-cell crab cavity with microphonics and beamloading, driven by an amplifier of limited bandwidth and in response to filtered measurements from an output coupler. Microphonics is included by specifying the natural frequency of the cavity as a function of time. The code does not include any coupling where electromagnetic forces drive mechanical vibrations [2]. Power consumption is not a key issue for the ILC crab cavities hence the cavity can be filled slowly well before the bunch arrives. This removes the requirement for the code to give an accurate representation of Lorentz detuning and potential electromechanical resonances. The code does not include noise from the electronic circuits of the LLRF system.

The code anticipates that a digital controller will be utilised and typical control loop delays assumed in simulations are consistent available digital processing technology [3]. The code shows how far controller gain must be reduced from the stability limit associated with controller time delays in the presence of unpredictable disturbances. The important disturbances are microphonics and beamloading. Beamloading for a crab cavity is likely to be unpredictable as it depends on the lateral offset of a bunch [4]. Microphonics is likely to be predictable however the analysis determines the limit of control when microphonics is managed by a PI controller that does not look forward or predict response.

## 2. Report Organisation

A large part of the report relates to the equations used by the code and simulations results demonstrating its outputs for a range of simplified or exaggerated situations which demonstrate qualitative validity. Sections 1 to 15 set up the equations.

Key equations with respect to the code are:-

- the enveloped equations (11.3a) and (11.3b) which are solved by the code,
- the equivalent circuit beamloading equations (7.3) and (7.3) and the consequential cavity beamloading equations (15.26) and (15.27),
- the PI controller with delayed action defined by equations (18.1) and (18.2),

Other useful results which are not needed by the code but can be used for design and code validation are:-

- the equations which determine the cavity power requirement from beamloading as a function of bunch offset and cavity parameters given in section 16,
- the stability limit for proportional control with fixed delay and periodic update (21.13),
- the stability limit for proportional control with fixed delay and rapid update (21.27),
- the stability limit for PI control with fixed delay and rapid update (21.41)
- an empirical estimate for (21.41) is given in (21.42)
- an empirical estimate for PI control with fixed delay and periodic update (21.45)

Distributed through the report are examples using ILC crab cavity proposed, parameters.

Shunt impedance,  $R/Q$ , bunch parameters, gradient, stored energies and power requirements are first given at the end of section 14. Discussion of the choice of external  $Q$  is given in section 16.

Input to the code detailing likely control system parameters and Microphonic spectra are first given in the table on figure 12 in section 19.

Section 8 is included as an illustration of beamloading and computes its results from the full time dependent differential equations for the cavity rather than from the envelope equations. An important part of our code validation procedure was the checking the co-incidence of results from integration of the full time dependent equations and integration of the envelope equations. Section 17 is provided as an illustration showing that beamloading has been correctly implemented.

The code went through various stages of development. A version of the code which assumed that the cavity only had excitation of one mode only was developed first. Including results for the analysis of a single mode cavity allows one to see more clearly the effect of adjacent modes when the multi-cell cavity is analysed. The single mode analysis is relevant to the testing of the phase control system performed with single cell cavities [3]. (*During the course of the project insufficient resources were available for the manufacture of a full nine cell cavity and its cryomodule.*) The simulations in section 19 for single mode cavity excitation have been chosen to illustrate how phase and amplitude control depends independently on beam-loading, microphonics and external  $Q$ . The results also illustrate the control action being taken by the power amplifiers.

Section 20 illustrates how control performance depends on gain in preparation for a more comprehensive study in sections 21 and 22. Section 21 derives analytic formulae for the stability limit of proportional control and proportional integral control.

Section 22 gives the first results from systematic application of the code for cases which are relevant to the ILC crab cavity and similar systems, albeit cavities where the operating mode is well separated from other modes. The first important result determined in section 22.1 and section 22.2 is that the phase control performance is likely to be independent of the external  $Q$  (determined by input coupler). This is not a result we had anticipated and is only true for certain parameter ranges. The following sub-sections of section 22 indicate the position of optimum performance with respect to the stability limit as a function of measurement errors, latency, microphonics and beam-loading. Due to project time constraints the coverage of the parameter space involved and interpretation of the result is sparse.

Section 23 presents some analyses for the ILC crab cavity where adjacent modes to the operating mode have a significant effect on the control performance. The simulations in this report make assumptions on the level and frequencies of of microphonics. Real microphonic data will not be available until the the cavities have been tested in a horizontal cryomodule.

### 3. Modelling Cavity Filling

A general layout for a driven superconducting cavity might be drawn as

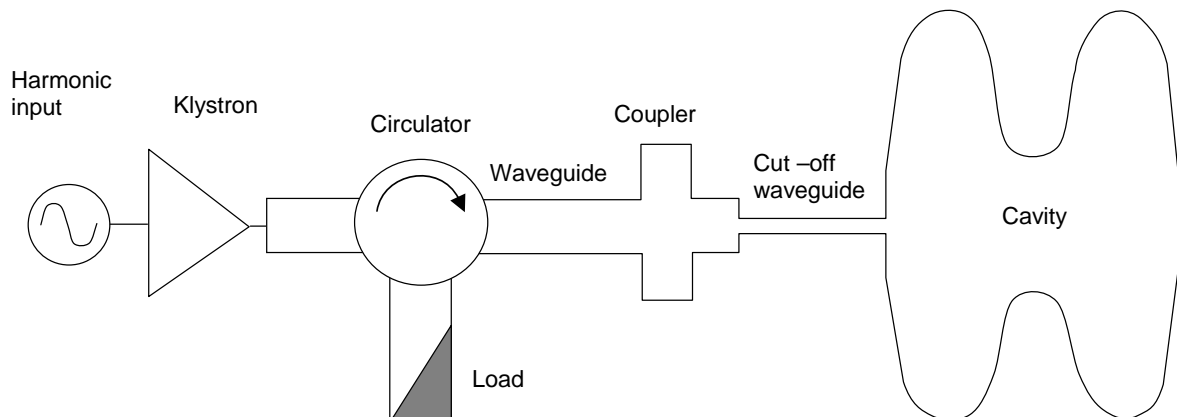


**Figure 1** Cavity Drive Schematic

At each step in the waveguide the impedance changes, i.e. the ratio of the voltage to current changes and there could be some reflection of power. Where the reflected power from successive transitions cancel, all the power travels forward. This means that if the new section has higher impedance than the previous section, the voltage is higher and the current is smaller but the power flow stays the same. When reflected power cancels, the system is matched and the sequence of transitions has a pure transformer action.

To get large voltage transformations it is sometimes useful to use a short waveguide section that is beyond cut-off. The cut off section still transmits and reflects power without energy storage or modifying the frequency hence still acts as part of the transformer.

Often all this complication is reduced to the equivalent circuit

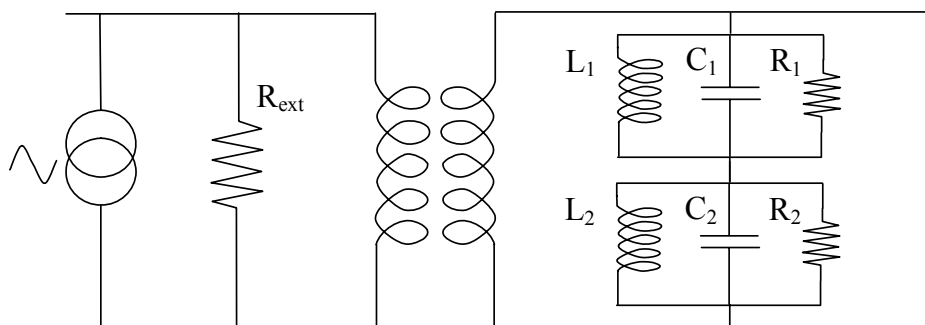


**Figure 2** Equivalent circuit for a cavity with two mode

Modelling the cavity modes as lumped parallel resonant circuits in series is valid provided the cavity is only excited at frequencies that don't excite modes that are not included in the model. A cavity can do one of three things, it can reflect energy and it can store energy and it can re-emit energy as a function of the phase and amplitude of the incoming wave. These properties can all be represented by a parallel lumped circuit.

The difficulty with simplification to this level is that one cannot explicitly see forward and reflected power in the waveguide. Here we will use a modified formulation where the waveguide is explicit. Explicit representation of transformer is omitted as an appropriate voltage transformation is achieved with the correct coupler design.

#### 4. Waveguide Driven Circuit Model

The time evolution of a cavity mode obeys the same differential equation as a parallel lumped circuit [5]. Where a cavity has the potential to resonate at a number of frequencies each mode adds a voltage contribution at the coupler and hence the modes are modelled as parallel resonators in series as shown in figure 3.

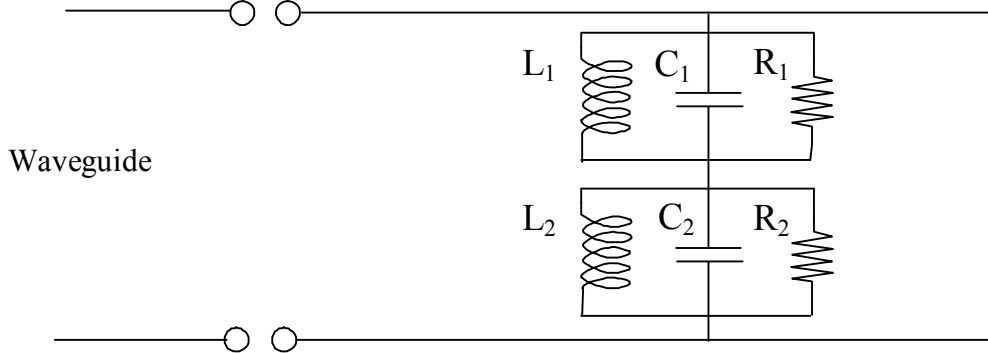


**Figure 3** Simplified equivalent circuit

At the terminal the voltage in the waveguide must equal the voltage in the lumped circuit. Along the waveguide the voltage and current satisfies the equations

$$\frac{\partial V}{\partial z} = -L_{\text{wg}} \frac{\partial I}{\partial t} \quad \text{and} \quad \frac{\partial I}{\partial z} = -C_{\text{wg}} \frac{\partial V}{\partial t}$$

hence

$$\frac{\partial^2 V}{\partial z^2} = L_{\text{wg}} C_{\text{wg}} \frac{\partial^2 V}{\partial t^2}$$

where  $C_{\text{wg}}$  is the capacitance per unit length and  $L_{\text{wg}}$  is the inductance per unit length.

For a fixed frequency source of angular frequency  $\omega$  the voltage along the waveguide is given as

$$V(z, t) = \mathcal{F} \exp \{ j(kz - \omega t) \} + \mathcal{R} \exp \{ -j(kz + \omega t) \} \quad (4.1)$$

where  $k = \omega \sqrt{L_{\text{wg}} C_{\text{wg}}}$

and  $\mathcal{F}$  is the amplitude of the forward wave and  $\mathcal{R}$  is the amplitude of the reflected wave.

The current on the waveguide is therefore given as

$$I(z, t) = \mathcal{F} \frac{\omega C_{\text{wg}}}{k} \exp \{ j(kz - \omega t) \} - \mathcal{R} \frac{\omega C_{\text{wg}}}{k} \exp \{ -j(kz + \omega t) \}$$

this can be written as

$$I(z, t) = \frac{1}{Z_{\text{wg}}} [\mathcal{F} \exp \{ j(kz - \omega t) \} - \mathcal{R} \exp \{ -j(kz + \omega t) \}] \quad (4.2)$$

where  $Z_{\text{wg}} = \sqrt{\frac{L_{\text{wg}}}{C_{\text{wg}}}}$  (4.3)

If the terminal between the cavity and the waveguide is at  $z = 0$  then the current in the waveguide equals the sum of the currents through the equivalent circuit components of each series resonator (i.e. we get an equation for each resonator / mode) hence

$$\frac{1}{L_i} \int V_i dt + C_i \frac{dV_i}{dt} + \frac{V_i}{R_i} = \frac{1}{Z_{wg}} \{F - \mathcal{R}\} \exp(-j\omega t) \quad (4.4)$$

where  $V_i$  is the voltage for the  $i$ th mode and with respect to the model in figure 3 is the voltage across one of the parallel resonators.

From (4.1) and adding series voltages for each mode the voltage at  $z = 0$  is given as

$$V = \sum_{\text{modes}} V_i = (F + \mathcal{R}) \exp(-j\omega t) \quad (4.5)$$

Eliminating the reflected power between (4.4) and (4.5) gives

$$\frac{1}{L_i} \int V_i dt + C_i \frac{dV_i}{dt} + \frac{V_i}{R_i} + \frac{1}{Z_{wg}} \sum_{j=1}^N V_j = \frac{2F}{Z_{wg}} \exp(-j\omega t) \quad (4.6)$$

If the coupling to different modes is dissimilar then  $Z_{wg}$  takes a different value for each mode. This equation determines the modal voltages in the cavity as a function of the amplitude of the forward wave in the waveguide.

Now define the natural frequency of the  $i^{\text{th}}$  mode as

$$\omega_i = \frac{1}{\sqrt{L_i C_i}} \quad (4.7)$$

To evaluate  $Z_{wg}$  we write

$$Q_{ei} = \frac{\omega_i U_{\text{stored}}}{P_{\text{emitted}}} = \frac{\frac{1}{2} \omega_i C_i V_i^2}{\frac{1}{2} (V_i^2 / Z_{wgi})} = \omega_i Z_{wgi} C_i \quad (4.8)$$

$$Q_{oi} = \frac{\omega_i U_{\text{stored}}}{P_{\text{diss}}} = \frac{\frac{1}{2} \omega_i C_i V_i^2}{\frac{1}{2} (V_i^2 / R_i)} = \omega_i R_i C_i \quad (4.9)$$

where  $U$  is an energy,  $P$  is a power and diss is an abbreviation for dissipation in the cavity).

Hence dividing (4.8) and (4.9) we have that

$$\frac{Q_{ei}}{Q_{oi}} = \frac{Z_{wgi}}{R_i} \quad (4.10)$$

which can be re-arranged as

$$Z_{wgi} = \left( \frac{R}{Q_{oi}} \right)_C Q_{ei} \quad (4.11)$$

i.e.  $Z_{wgi}$  is the product of the external  $Q$  with the  $R/Q$  of the bare cavity. The suffix  $C$  is used to denote the circuit definition of  $R/Q$ . Note that  $Z_{wgi}$  is not that of the physical waveguide from the RF generator as represented in figure 2 by the transmission line from the current source to the transformer. The transformer models the coupler which transforms the voltage.

Differentiation of (4.6) and division by  $C_i$  gives

$$\frac{d^2 V_i}{dt^2} + \frac{\omega_i}{\omega_i R_i C_i} \frac{dV_i}{dt} + \frac{\omega_i}{\omega_i Z_{wg} C_i} \sum_{j=1}^N \frac{dV_j}{dt} + \frac{1}{L_i C_i} V_i = \frac{2\omega_i}{\omega_i Z_{wgi} C_i} \frac{d}{dt} \{F \exp(-j\omega t)\} \quad (4.12)$$

and using (4.7) to (4.11) in (4.12) gives

$$\frac{d^2 V_i}{dt^2} + \frac{\omega_i}{Q_{oi}} \frac{dV_i}{dt} + \frac{1}{Q_{ei}} \omega_i \sum_{j=1}^N \frac{dV_j}{dt} + \omega_i^2 V_i = \frac{2\omega_i}{Q_{ei}} \frac{d}{dt} \{F \exp(-j\omega t)\} \quad (4.13)$$

defining

$$\frac{1}{Q_{Li}} = \frac{1}{Q_{oi}} + \frac{1}{Q_{ei}} \quad (4.14)$$

equation (4.12) becomes

$$\frac{d^2 V_i}{dt^2} + \frac{\omega_o}{Q_{Li}} \frac{dV_i}{dt} + \frac{1}{Q_{ei}} \omega_i \sum_{\substack{j=1 \\ j \neq i}}^N \frac{dV_j}{dt} + \omega_o^2 V_i = \frac{2\omega_o}{Q_e} \frac{d}{dt} \{F \exp(-j\omega t)\} \quad (4.15)$$

## 5. Steady State for a Single Cavity Mode

The steady state solution of (4.6) for a single mode ( $N = 1$ ) has to be of the form

$$V(t) = \mathcal{V} \exp(-j\omega t) \quad (5.1)$$

where  $\mathcal{V}$  is complex (i.e. has a phase shift from the forward power).

Solving (4.6) for the single mode case and omitting the suffix gives

$$\left\{ -\frac{1}{j\omega L} - j\omega C + \left( \frac{1}{R} + \frac{1}{Z_{wg}} \right) \right\} \mathcal{V} = \frac{2F}{Z_{wg}} \quad (5.2)$$

Power dissipated in the cavity  $P_c$  is given by

$$P_c = \frac{\mathcal{V}\mathcal{V}^*}{2R} \quad (5.3)$$

Power carried by the forward wave  $P_f$  is given as

$$P_f = \frac{FF^*}{2Z_{wg}} \quad (5.4)$$

Hence multiplying each side of (5.2) by its complex conjugate and substituting from (5.3) and (5.4) gives

$$\left\{ \left( \frac{1}{\omega L} - \omega C \right)^2 + \left( \frac{1}{R} + \frac{1}{Z_{wg}} \right)^2 \right\} R P_c = 4 \frac{P_f}{Z_{wg}} \quad (5.5)$$

hence as expected

$$P_c = \frac{4P_f}{Z_{wg} R \left\{ \left( \frac{1}{\omega L} - \omega C \right)^2 + \left( \frac{1}{R} + \frac{1}{Z_{wg}} \right)^2 \right\}} \quad (5.5)$$

## 6. Single Mode Resonant Loss Free Operation

At resonance when

$$\omega = \omega_o = \frac{1}{\sqrt{LC}}$$

then

$$P_c = \frac{4 Z_{wg} R P_f}{(R + Z_{wg})^2} \quad (6.1)$$

and from (5.2)

$$\mathcal{V} = \frac{2R\mathcal{F}}{Z_{wg} + R} \quad (6.2)$$

For a loss free cavity  $R \rightarrow \infty$  so

$$\mathcal{V} = 2\mathcal{F} \quad (6.3)$$

High voltages are achieved in the cavity by an impedance change not shown in figure 3.

From (4.5) and (5.1)

$$\mathcal{V} = \mathcal{F} + \mathcal{R} \quad (6.4)$$

hence for a lossless cavity (6.3) and (6.4) give

$$\mathcal{F} = \mathcal{R} \quad (6.5)$$

as expected.

Away from steady state we must solve the differential equation (4.6) or equivalently (4.15).

## 7. Beamloading

If a charged bunch moves through a cavity it leaves its image charge  $q_m$  where it enters the cavity and collects some more where it leaves, see figure 4. Importantly the bunch then carries the new image charge with it as it moves on leaving an opposite charge behind.

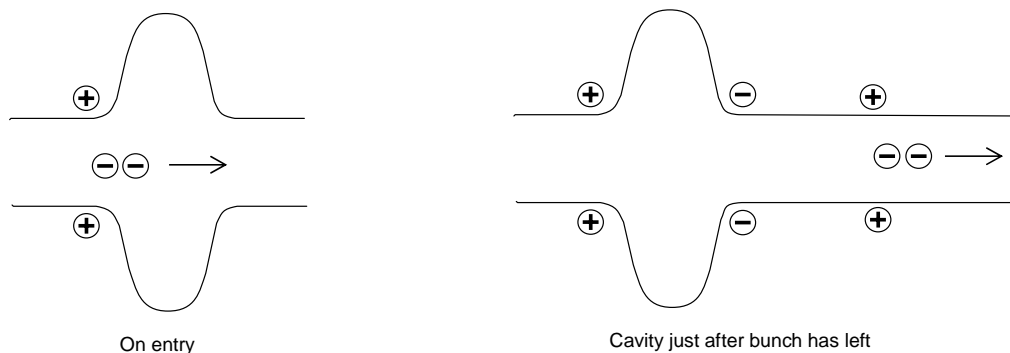


**Figure 4** Image charge illustrating beamloading

Beam loading can be simulated by allowing a current impulse to flow into the equivalent circuit. If this impulse is very short compared to the period of the cavity then its only action is to change the charge across the capacitance  $C$ . For this case the voltage  $V$  jumps instantaneously to a new value. Consequently as an alternative to modelling beamloading with an additional current source in the equivalent circuit we can also model beamloading by letting the voltage jump each time a bunch passes through the cavity. With respect to a numerical solution of equation (4.6) over millions of RF cycles it is easier to let the voltage jump rather than to input short current pulses as a source term. If the time over which the

voltage is allowed to jump is zero, then in equation (4.6) the integral of the voltage is unchanged allowing the differential of  $V$  immediately after the discontinuity to be determined and hence the numerical solution of (4.6) through the discontinuity to be determined. If the cavity is already excited, the charge that moves across adds to the charge that is already there hence the energy is increased as

$$U + \delta U = \frac{1}{2} \frac{(q_m + \delta q_m)^2}{C} \quad \text{so that} \quad \delta U \approx \frac{1}{2} \frac{2q_m \delta q_m}{C} = V \delta Q \quad (7.1)$$

The new voltage in the cavity after the charge has passed must be determined by phasor addition i.e.

$$\underline{V}_{\text{final}} = \frac{1}{C} (q_m + \delta q_m) \quad (7.2)$$

(Note that at any instant the charge is always in phase with the voltage i.e.  $q_m = C\underline{V}$ .)

Suppose that the phase of the cavity charge with respect to some reference is  $\theta$  and the phase of the image charge added by beamloading is  $\alpha$  then from figure 4a we see that

$$\text{Re}(V_{\text{final}}) = \frac{1}{C} (q_m \cos \theta + \delta q_m \cos \alpha) \quad (7.3)$$

$$\text{Im}(V_{\text{final}}) = \frac{1}{C} (q_m \sin \theta + \delta q_m \sin \alpha) \quad (7.4)$$

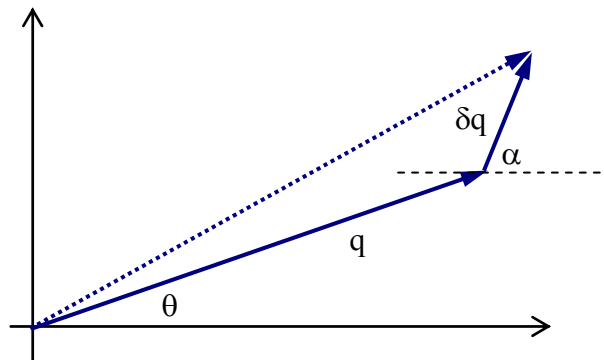


**Figure 4a** Phasor addition of image charge

The phase  $\alpha$  for the incremental addition of charge is determined by the difference between the peak of the reference phase and the reference phase when the bunch is at the centre of the cavity.

A proof can be constructed from the time reversal symmetry of electrodynamics when there are no system losses. The argument goes as follows,

- 1) Let the bunch travel through the cavity and induce a field.
- 2) At some time in the future when the bunch is a long way down the beam pipe let time run backwards.
- 3) After the bunch has gone back through the cavity and into the beam pipe again time reversal symmetry gives us zero field in the cavity.
- 4) The bunch extracts maximum energy from the cavity when it is at the centre of the cavity when the field is maximum (one might question whether this is exactly true for all energies?)
- 5) For the bunch to extract all the energy from the cavity this must be the same as extracting the maximum energy hence the bunch must return to see a field maximum.

6) By time reversal symmetry, the return position and the cavity phase is perfectly synchronised with the forward position and the cavity phase hence the bunch must have been at the centre of the cavity to correspond to a field maximum on the forward path.

Note that time reversal symmetry works for both the relativistic and non relativistic cases.<sup>1</sup>

The quantity  $\delta q_m$  is the charge added to the effective capacitance of the mode. It is of course related to the charge that passes through the cavity. This relationship will be determined for a dipole mode in section 15.

## 8. Cavity Response to Beamloading

Equation (6.4) is valid away from steady state hence if the cavity voltage  $\mathcal{V}$  jumps and the forward wave amplitude  $\mathcal{F}$  stays the same then the amplitude of the reflected wave  $\mathcal{R}$  increases so that the system starts returning towards steady state. From (6.4) we have that

$$\mathcal{R} = \mathcal{V} - \mathcal{F} \quad (8.1)$$

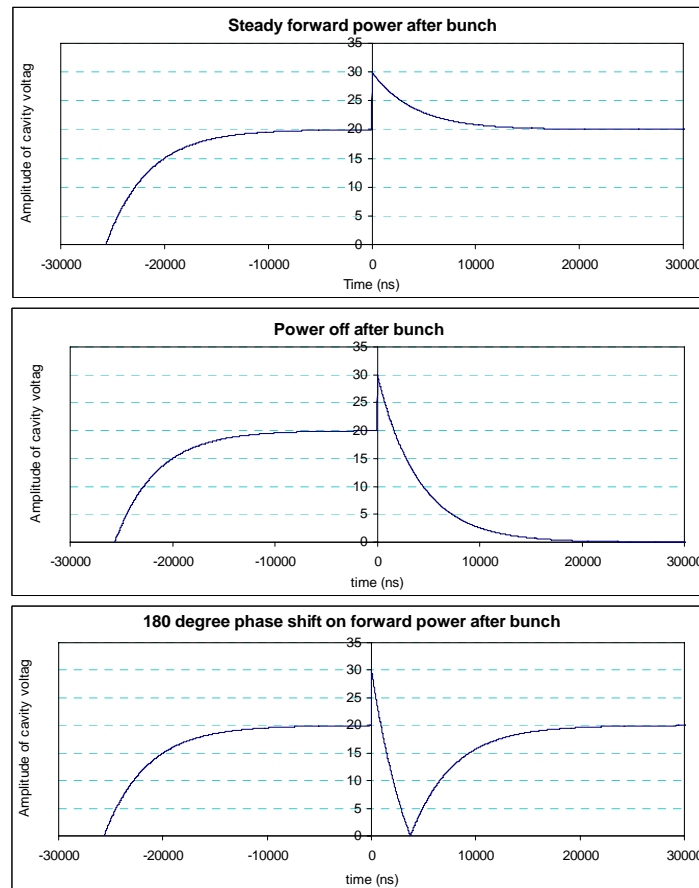
The cavity can start moving back towards steady state faster if the amplitude of the reflected wave is increased. Turning the forward power off will increase the reflected power. Indeed phase shifting the forward power by  $180^\circ$  gives an even greater reflected power and hence the rate at which the system starts returning to steady state is even higher. Effectively phase shifting the forward power by  $180^\circ$  sucks power out of the cavity at an enhanced rate.

Superconducting accelerator, cavity cells are typically designed so that the charged bunches traverse the cavity in half an RF cycle. In this instance the bunch can be simulated by supplying current to the effective capacitance of the cavity cell for half a cycle so that the integrated current is equal to the bunch charge. If the time dependence of the electric field at the centre of a cavity cell is taken to be  $\sin \omega t$  and the bunch is phased to receive maximum acceleration or de-acceleration then the beam load current will be supplied between  $\omega t = 0$  and  $\omega t = \pi$ . This means that the peak of the average beam current coincides with the peak voltage. At resonance the integral term in (4.6) cancels the differential term implying that the peak voltage is in phase with the drive current. Taken together one sees that the peak beam load current is in phase with the drive when the accelerator is providing maximum acceleration.

Equation (4.15) is easily integrated numerically for the initial fill and after the passage of a bunch which kicks the voltage for the three cases described above. These cases where (i) when the drive is constant, (ii) when the drive is switched off as the bunch kicks the cavity and (iii) when the phase of the forward power is shifted by  $180^\circ$  as the bunch kicks the cavity. These cases are shown in figure 5.

---

<sup>1</sup> (We have checked the result using a MAGIC simulation of a symmetric pill box cavity for a mildly relativistic bunch.)



**Figures 5a, 5b & 5c** Response to beam-load impulse at  $t = 0$ . Frequency=3.9 GHz,  
 $Q=5 \times 10^4$

The charts were produced with 180 iterations per period. The phase shift remained close to zero to better than 0.1 degrees. Increasing the number of iterations per period reduced phase errors towards zero. The program used to compute figure 5 is given in Appendix 1.

In a second calculation the forward power was controlled by a PI (Proportional Integral) controller, the response is shown in figure 6. For the case shown the amplitude of the peak forward power was limited to a maximum of 110% of that used for figures 5.

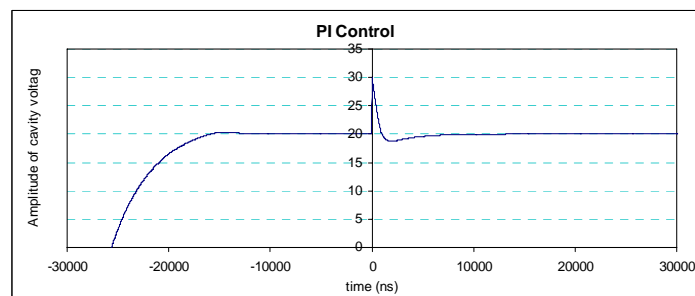


**Figure 6** Response to beam-load impulse at  $t = 0$  with PI control. Frequency=3.9 GHz,  
 $Q=5 \times 10^4$  max amplitude of input = 11

Note that the initial recovery is at the rate obtained with  $180^\circ$  phase shift in figure 5c.

For a multi-cell cavity beamloading can be modelled by applying a periodic current waveform to an appropriate equivalent circuit. The duration will be determined by the time it takes for the bunch to pass through  $N$  cells and the period by twice the time it takes the bunch to pass through one cell. The precise waveform can only be determined by a full electromagnetic simulation. If in the solution one is only interested in the behaviour of a

single mode then one extracts the Fourier component of the current waveform that excites that mode. The net effect of the current will be to change the voltage phasor of the mode. Simulation of beamloading can therefore still be modelled by discrete changes in the cavity voltage phasor.

## 9. The Envelope Equations

The solution of the differential equation (4.15) is only fast with a modern PC. For high Q calculations it is difficult to obtain phase prediction with an accuracy of milli-degrees. A faster solution technique is to assume a solution of the form

$$V_m(t) = \{A_{mr}(t) + jA_{mi}(t)\} \exp\{-j\omega t\} \quad (9.1)$$

where m is the index that runs over modes,  $A_{mr}(t)$  and  $A_{mi}(t)$  are slowly varying functions of time and  $\omega$  is the drive frequency [6]. A similar form is assumed for  $\mathcal{F}$ . It will be seen that when the assumed solution is substituted into the differential equation, second derivatives can be neglected. Differentiating the RHS of (4.15) gives

$$\frac{d^2 V_m}{dt^2} + \frac{\omega_m}{Q_{om}} \frac{dV_m}{dt} + \omega_m^2 V_m + \frac{\omega_m}{Q_{em}} \sum_{j=1}^N \frac{dV_j}{dt} = \frac{2\omega_m}{Q_{em}} (\dot{\mathcal{F}} - j\omega \mathcal{F}) \exp(-j\omega t) \quad (9.2)$$

Differentiation of (9.1) gives

$$\frac{dV_m}{dt} = \left( \dot{A}_{mr} - j\omega A_{mr} + j\dot{A}_{mi} + \omega A_{mi} \right) \exp\{-j\omega t\} \quad (9.3)$$

second differentiation gives

$$\frac{d^2 V_m}{dt^2} = \left( \ddot{A}_{mr} - 2j\omega \dot{A}_{mr} - \omega^2 A_{mr} + j\ddot{A}_{mi} + 2\omega \dot{A}_{mi} - j\omega^2 A_{mi} \right) \exp\{-j\omega t\} \quad (9.4)$$

Substituting (9.3) and (9.4) in (9.2), cancelling a factor of  $\exp(-j\omega t)$  and separating into real and imaginary parts gives the envelope equations as

$$\begin{aligned} \left( \ddot{A}_{mr} + 2\omega \dot{A}_{mi} - \omega^2 A_{mr} \right) + \frac{\omega_m}{Q_{om}} \left( \dot{A}_{mr} + \omega A_{mi} \right) + \frac{\omega_m}{Q_{em}} \sum_{j=1}^N \left( \dot{A}_{jr} + \omega A_{ji} \right) + \omega_m^2 A_{mr} \\ = \frac{2\omega_m}{Q_{em}} \left( \dot{\mathcal{F}}_r + \omega \mathcal{F}_i \right) \end{aligned} \quad (9.5a)$$

$$\begin{aligned} \left( \ddot{A}_{mi} - 2\omega \dot{A}_{mr} - \omega^2 A_{mi} \right) + \frac{\omega_m}{Q_{om}} \left( \dot{A}_{mi} - \omega A_{mr} \right) + \frac{\omega_m}{Q_{em}} \sum_{j=1}^N \left( \dot{A}_{ji} - \omega A_{jr} \right) + \omega_m^2 A_{mi} \\ = \frac{2\omega_m}{Q_{em}} \left( \dot{\mathcal{F}}_i - \omega \mathcal{F}_r \right) \end{aligned} \quad (9.6a)$$

Now  $\omega_o$  and  $\omega$  are big numbers whilst  $\dot{A}$  and  $\ddot{A}$  are not so big as A is a slowly varying envelope function. This means that in (9.5a) and (9.6a) the second derivative terms i.e.  $\ddot{A}$  are an order of magnitude smaller than all the other terms, i.e. we retain order  $\omega$  and  $\omega^2$  though we shall see that order  $\omega^2$  cancels. Later we will also take  $Q_L$  as large but not yet.

Eliminating 2<sup>nd</sup> derivatives in (9.5a) and (9.6a) they become

$$\begin{aligned}
2\omega \dot{A}_{mi} + \frac{\omega_m}{Q_{om}} \dot{A}_{mr} + \frac{\omega_m}{Q_{em}} \sum_{j=1}^N \dot{A}_{jr} + \frac{\omega\omega_m}{Q_{om}} A_{mi} + \frac{\omega\omega_m}{Q_{em}} \sum_{j=1}^N A_{ji} + (\omega_m^2 - \omega^2) A_{mr} \\
= \frac{2\omega_m}{Q_{em}} (\dot{\mathcal{F}}_r + \omega \mathcal{F}_i)
\end{aligned} \tag{9.5b}$$

$$\begin{aligned}
-2\omega \dot{A}_{mr} + \frac{\omega_m}{Q_{om}} \dot{A}_{mi} + \frac{\omega_m}{Q_{em}} \sum_{j=1}^N \dot{A}_{ji} - \frac{\omega\omega_m}{Q_{om}} A_{mr} - \frac{\omega\omega_m}{Q_{em}} \sum_{j=1}^N A_{jr} + (\omega_m^2 - \omega^2) A_{mi} \\
= \frac{2\omega_m}{Q_{em}} (\dot{\mathcal{F}}_i - \omega \mathcal{F}_r)
\end{aligned} \tag{9.6b}$$

## 10. Single Mode Diagonalisation

For the case of a single mode equation (9.5b) and (9.6b) can be diagonalised exactly. In this section we drop the suffix m.

Eliminating  $\dot{A}_i$  by  $\frac{\omega_o}{Q_L} \times (7.5b) - 2\omega \times (7.6b)$  gives

$$\begin{aligned}
\left\{ 4\omega^2 + \left(\frac{\omega_o}{Q_L}\right)^2 \right\} \dot{A}_r + (\omega^2 + \omega_o^2) \frac{\omega_o}{Q_L} A_r + \left\{ \left(\frac{\omega_o}{Q_L}\right)^2 - 2(\omega_o^2 - \omega^2) \right\} \omega A_i \\
= \frac{2\omega_o^2}{Q_e Q_L} (\dot{\mathcal{F}}_r + \omega \mathcal{F}_i) - \frac{4\omega\omega_o}{Q_e} (\dot{\mathcal{F}}_i - \omega \mathcal{F}_r)
\end{aligned} \tag{10.1a}$$

Eliminating  $\dot{A}_r$  by  $2\omega \times (7.5b) + \frac{\omega_o}{Q_L} \times (7.6b)$  gives

$$\begin{aligned}
\left\{ 4\omega^2 + \left(\frac{\omega_o}{Q_L}\right)^2 \right\} \dot{A}_i + (\omega^2 + \omega_o^2) \frac{\omega_o}{Q_L} A_i - \left\{ \left(\frac{\omega_o}{Q_L}\right)^2 - 2(\omega_o^2 - \omega^2) \right\} \omega A_r \\
= \frac{2\omega_o^2}{Q_e Q_L} (\dot{\mathcal{F}}_i - \omega \mathcal{F}_r) + \frac{4\omega_o\omega}{Q_e} (\dot{\mathcal{F}}_r + \omega \mathcal{F}_i)
\end{aligned} \tag{10.1b}$$

Dividing (10.1a) and (10.1b) by  $\omega_o^3$  they can be written as

$$\begin{aligned}
\left\{ \left(\frac{2\omega}{\omega_o}\right)^2 + \left(\frac{1}{Q_L}\right)^2 \right\} \frac{1}{\omega_o} \dot{A}_r + \left(\frac{\omega^2}{\omega_o^2} + 1\right) \frac{1}{Q_L} A_r + \left\{ \left(\frac{1}{Q_L}\right)^2 - \frac{2\omega}{\omega_o} \left(\frac{\omega_o}{\omega} - \frac{\omega}{\omega_o}\right) \right\} \frac{\omega}{\omega_o} A_i \\
= \frac{2}{Q_e Q_L} \left(\frac{1}{\omega_o} \dot{\mathcal{F}}_r + \frac{\omega}{\omega_o} \mathcal{F}_i\right) - \frac{4}{Q_e} \frac{\omega}{\omega_o} \left(\frac{1}{\omega_o} \dot{\mathcal{F}}_i - \frac{\omega}{\omega_o} \mathcal{F}_r\right)
\end{aligned} \tag{10.2a}$$

$$\left\{ \left( \frac{2\omega}{\omega_0} \right)^2 + \left( \frac{1}{Q_L} \right)^2 \right\} \frac{1}{\omega_0} \dot{A}_i + \left( \frac{\omega^2}{\omega_0^2} + 1 \right) \frac{1}{Q_L} A_i - \left\{ \left( \frac{1}{Q_L} \right)^2 - \frac{2\omega}{\omega_0} \left( \frac{\omega_0}{\omega} - \frac{\omega}{\omega_0} \right) \right\} \frac{\omega}{\omega_0} A_r \quad (10.2b)$$

$$= \frac{2}{Q_e Q_L} \left( \frac{1}{\omega_0} \dot{\mathcal{F}}_i - \frac{\omega}{\omega_0} \mathcal{F}_r \right) + \frac{4}{Q_e} \frac{\omega}{\omega_0} \left( \frac{1}{\omega_0} \dot{\mathcal{F}}_r + \frac{\omega}{\omega_0} \mathcal{F}_i \right)$$

For superconducting cavities  $Q_L$  and  $Q_e$  are invariably made very large (to benefit from its superconducting properties) hence the equations after multiplication by  $\omega_0^2/4\omega^2$  approximate to

$$\frac{1}{\omega_0} \dot{A}_r + \frac{1}{4} \left( 1 + \frac{\omega_0^2}{\omega^2} \right) \frac{1}{Q_L} A_r - \frac{1}{2} \left( \frac{\omega_0}{\omega} - \frac{\omega}{\omega_0} \right) A_i = - \frac{1}{Q_e} \frac{\omega_0}{\omega} \left( \frac{1}{\omega_0} \dot{\mathcal{F}}_i - \frac{\omega}{\omega_0} \mathcal{F}_r \right) \quad (10.3a)$$

$$\frac{1}{\omega_0} \dot{A}_i + \frac{1}{4} \left( 1 + \frac{\omega_0^2}{\omega^2} \right) \frac{1}{Q_L} A_i + \frac{1}{2} \left( \frac{\omega_0}{\omega} - \frac{\omega}{\omega_0} \right) A_r = \frac{1}{Q_e} \frac{\omega_0}{\omega} \left( \frac{1}{\omega_0} \dot{\mathcal{F}}_r + \frac{\omega}{\omega_0} \mathcal{F}_i \right) \quad (10.3b)$$

These equations have been integrated for the same parameters as figure 6, results are given in figure 7. The program is given in appendix 2.

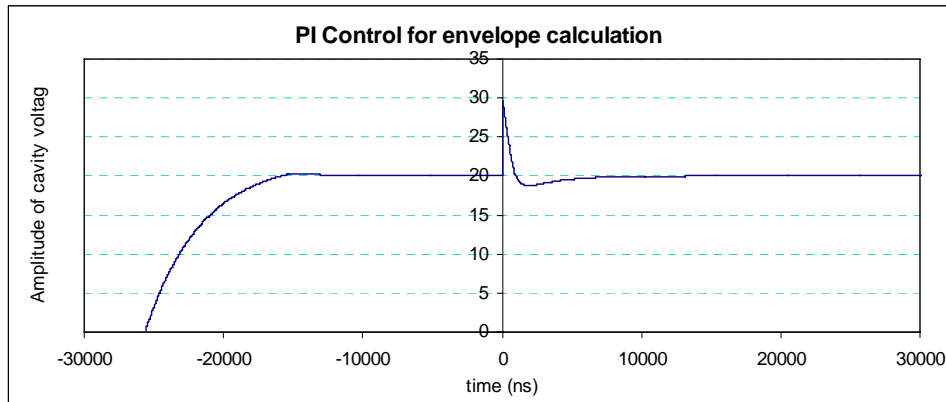


**Figure 7** Response to beam-load impulse at  $t = 0$  with PI control by integrating the envelope equations. Frequency=3.9 GHz,  $Q=5 \times 10^4$  max amplitude of input = 11

## 11. Approximate Envelope Equations for the Multimode Case

For the multi-mode case we go back to considering equations (9.5b) and (9.6b). In superconducting cavities  $Q_{Lm}$  and  $Q_{em}$  are always going to be large ( $\sim 10^6$ ) hence terms in  $1/Q^2$  can always be neglected where they are multiplied by the same power of  $\omega$ . This observation allows us to diagonalise the derivative terms of (9.5b) and (9.6b) by substituting (9.6b) into (9.5a) and (9.5a) into (9.6b) neglecting powers  $1/Q^2$ .

$$2\omega \dot{A}_{mi} + \frac{1}{2Q_{om}} \frac{\omega_m}{\omega} (\omega_m^2 - \omega^2) A_{mi} + \frac{1}{2Q_{em}} \frac{\omega_m}{\omega} \sum_{j=1}^N (\omega_j^2 - \omega^2) A_{ji} + \frac{\omega\omega_m}{Q_{om}} A_{mi} + \frac{\omega\omega_m}{Q_{em}} \sum_{j=1}^N A_{ji} + (\omega_m^2 - \omega^2) A_{mr} = \frac{2\omega_m}{Q_{em}} (\dot{F}_r + \omega F_i) \quad (11.1a)$$

$$-2\omega \dot{A}_{mr} - \frac{1}{2Q_{om}} \frac{\omega_m}{\omega} (\omega_m^2 - \omega^2) A_{mr} - \frac{1}{2Q_{em}} \frac{\omega_m}{\omega} \sum_{j=1}^N (\omega_j^2 - \omega^2) A_{jr} - \frac{\omega\omega_m}{Q_{om}} A_{mr} - \frac{\omega\omega_m}{Q_{em}} \sum_{j=1}^N A_{jr} + (\omega_m^2 - \omega^2) A_{mi} = \frac{2\omega_m}{Q_{em}} (\dot{F}_i - \omega F_r) \quad (11.1b)$$

Combing terms and normalising the differentials in (11.1a) and (11.1b) and swapping the order of (11.1a) and (11.1b) gives

$$\frac{\dot{A}_{mr}}{\omega_m} + \frac{1}{4Q_{om}} \left( \frac{\omega_m^2}{\omega^2} + 1 \right) A_{mr} + \frac{1}{4Q_{em}} \sum_{j=1}^N \left( \frac{\omega_j^2}{\omega^2} + 1 \right) A_{jr} - \left( \frac{\omega_m}{\omega} - \frac{\omega}{\omega_m} \right) \frac{A_{mi}}{2} = -\frac{1}{Q_{em}} \left( \frac{\dot{F}_i}{\omega} - F_r \right) \quad (11.2a)$$

$$\frac{\dot{A}_{mi}}{\omega_m} + \frac{1}{4Q_{om}} \left( \frac{\omega_m^2}{\omega^2} + 1 \right) A_{mi} + \frac{1}{4Q_{em}} \sum_{j=1}^N \left( \frac{\omega_j^2}{\omega^2} + 1 \right) A_{ji} + \left( \frac{\omega_m}{\omega} - \frac{\omega}{\omega_m} \right) \frac{A_{mr}}{2} = \frac{1}{Q_{em}} \left( \frac{\dot{F}_r}{\omega} + F_i \right) \quad (11.2b)$$

For Runge Kutta Solution we write these equations in the form

$$\dot{A}_{mr} = -\frac{\omega_m}{4Q_{om}} \left( \frac{\omega_m^2}{\omega^2} + 1 \right) A_{mr} - \frac{\omega_m}{4Q_{em}} \sum_{j=1}^N \left( \frac{\omega_j^2}{\omega^2} + 1 \right) A_{jr} + (\omega_m^2 - \omega^2) \frac{A_{mi}}{2\omega} - \frac{\omega_m}{\omega Q_{em}} (\dot{F}_i - \omega F_r) \quad (11.3a)$$

$$\dot{A}_{mi} = -\frac{\omega_m}{4Q_{om}} \left( \frac{\omega_m^2}{\omega^2} + 1 \right) A_{mi} - \frac{\omega_m}{4Q_{em}} \sum_{j=1}^N \left( \frac{\omega_j^2}{\omega^2} + 1 \right) A_{ji} - (\omega_m^2 - \omega^2) \frac{A_{mr}}{2\omega} + \frac{\omega_m}{\omega Q_{em}} (\dot{F}_r + \omega F_i) \quad (11.3b)$$

which is of the form

$$\dot{A}_r(m) = -f_o(m)g_1(m)A_r(m) - f_e(m) \sum_{j=1}^N g_1(j)A_r(j) + g_2(m)A_i(m) - g_3(m)(\dot{F}_i - \omega F_r) \quad (11.4a)$$

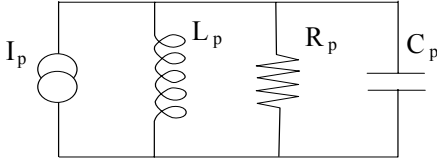
$$\dot{A}_i(m) = -f_o(m)g_1(m)A_i(m) - f_e(m) \sum_{j=1}^N g_1(j)A_i(j) - g_2(m)A_i(m) + g_3(m)(\dot{F}_r + \omega F_i) \quad (11.4b)$$

where

$$f_o(m) = \frac{\omega_m}{4Q_{om}} \quad f_e(m) = \frac{\omega_m}{4Q_{em}} \quad g_1(m) = \left( \frac{\omega_m^2}{\omega^2} + 1 \right) \quad g_2(m) = \frac{(\omega_m^2 - \omega^2)}{2\omega} \quad g_4(m) = \frac{\omega_m}{\omega Q_{em}}$$

## 12. Definition of shunt impedance for the accelerating mode

For a parallel resonant circuit where  $R_p$  is the shunt impedance (resistance),



the stored energy  $U_{\text{stored}}$  is given as

$$U_{\text{stored}} = \frac{C V_{\text{peak}}^2}{2} \quad (12.1)$$

and the dissipated energy  $P_{\text{diss}}$  is given as

$$P_{\text{diss}} = \frac{V_{\text{peak}}^2}{2R_p} \quad (12.2)$$

hence the Q factor is given as

$$Q = \frac{\omega U_{\text{stored}}}{P_{\text{diss}}} = R_p \sqrt{\frac{C_p}{L_p}} \quad (12.3)$$

Note also that

$$\frac{R_p}{Q} = \sqrt{\frac{L_p}{C_p}} = \frac{1}{\omega C_p} \quad (12.4)$$

The  $R$  over  $Q$  written as  $(R/Q)$  applies to a parallel resonant circuit and not to a series resonant circuit as for a series resonant circuit one has that

$$Q = \frac{\omega U_{\text{stored}}}{P_{\text{diss}}} = \frac{\frac{1}{2} \omega L_s I_{\text{peak}}^2}{\frac{1}{2} R_s I_{\text{peak}}^2} = \frac{1}{R_s} \sqrt{\frac{L_s}{C_s}} \quad (12.5)$$

The R/Q takes different values for different modes. It is an important figure of merit as it determines how much energy a charged bunch passing through a cavity will deliver to its associated mode. This result will be derived in a later section.

For accelerator cavities the shunt impedance  $R_c$  is often defined in a different way. It is defined such that

$$P_{\text{diss}} = \frac{V_c^2}{R_c} \quad (12.6)$$

where  $V_c$  is the voltage that accelerates the beam. For a cavity mode with a uniform electric field along the beam axis and for a charged bunch travelling at the velocity of light and at a phase such that the electric field is maximum when the bunch is at the centre of the cavity

$$V_c = \frac{V_{\text{peak}}}{d} \int_{-d/2c}^{d/2c} \cos(\omega t) c dt = V_{\text{peak}} \frac{\sin\left(\frac{\omega d}{2c}\right)}{\frac{\omega d}{2c}} \leq \frac{2}{\pi} V_{\text{peak}} \quad (12.7)$$

where the cavity length is  $d$  and  $V_{\text{peak}}$  is the end to end voltage on the axis. The maximum acceleration voltage is achieved when

$$\frac{\omega d}{2c} = \frac{\pi}{2} \quad (12.8)$$

Equating (12.2) and (12.6)

$$\frac{V_c^2}{R_c} = \frac{V_{\text{peak}}^2}{2R_p} \quad (12.9)$$

For a cavity of optimum length (maximum acceleration voltage) equations (12.7) and (12.9) give

$$\frac{R_c}{R_p} = 2 \left( \frac{2}{\pi} \right)^2 = 0.8106 \quad (12.10)$$

i.e. the accelerator definition of shunt impedance is close to the external circuit shunt impedance.

Eliminating  $U_{\text{diss}}$  between (12.3) and (12.6) we can also write

$$Q = \frac{\omega U_{\text{stored}}}{P_{\text{diss}}} = \frac{\omega R_c U_{\text{stored}}}{V_c^2} \quad (12.11)$$

hence

$$\frac{R_c}{Q} = \frac{V_c^2}{\omega U_{\text{stored}}} \quad (12.12)$$

### 13. Definition of shunt impedance for dipole $TM_{1np}$ modes

For dipole and higher order modes the maximum voltage between two points on the cavity walls no longer occurs on the axis, indeed there is no electric field on the axis hence the end to end voltage on the axis is zero. The concept of a peak longitudinal voltage  $V_{\text{peak}}$  still exists hence equation (12.2) can still be used to define a shunt impedance. Supposing that  $V_{\text{peak}}$  for occurs at radius  $a$  (and in a direction appropriate to the dipole) then equation (12.2) could be used to define a shunt impedance  $R_{px}$  as

$$P_{\text{diss}} = \frac{V_{\text{peak}}^2(a)}{2R_{\text{px}}} \quad (13.1)$$

Note that  $a$  is often taken as the beam pipe radius.

Taking  $m = 0$  for an accelerating mode,  $m = 1$  for a dipole mode,  $m = 2$  for a quadrupole mode etc., the variation of the axial electric field  $E_z$  out from the centre varies with radius as  $r^m$  hence one has that<sup>2</sup>

$$V_{\text{peak}}(r) = \frac{r^m}{a^m} V_{\text{peak}}(a) \quad (13.2)$$

Using (12.3) and (13.1) the Q factor might be expressed as

$$Q = \frac{\omega U_{\text{stored}}}{P_{\text{diss}}} = \frac{2\omega R_{\text{px}} U_{\text{stored}}}{V_{\text{peak}}^2(a)} \quad (13.3)$$

Hence the R upon Q might be written as

$$\frac{R_{\text{px}}}{Q} = \frac{V_{\text{peak}}^2(a)}{2\omega U_{\text{stored}}} \quad (13.4)$$

This definition of the shunt impedance and its associated R/Q is inconvenient as it relates to a potential in the cavity far from beam axis and which does not immediately relate to the deflecting properties of the mode. The definition of the shunt voltage for a dipole cavity is instead defined by the equation

$$P_{\text{diss}} = \frac{V_{\text{cz}}^2(a)}{\left(\frac{a\omega}{c}\right)^2 R_{\text{d}}} \quad (13.5)$$

where  $V_{\text{cz}}(a)$  is the voltage that a bunch moving parallel to the axis at radius  $a$  experiences including transit time effects. From (13.5) and the definition of Q given in (4.9) one gets that

$$\frac{R_{\text{d}}}{Q} = \frac{V_{\text{cz}}^2(a)}{\omega \left(\frac{a\omega}{c}\right)^2 U_{\text{stored}}} \quad (13.6)$$

The usefulness of this definition comes from a relationship between the on axis transverse kick  $V_{\perp}$  to the off axis longitudinal kick  $V_z(a)$  derived from the Panofsky Wenzel theorem i.e.

$$V_{\text{cz}}(a) = j \frac{a\omega}{c} V_{\perp} \quad (13.7)$$

Using (13.7) equation (13.6) becomes

$$\frac{R_{\text{d}}}{Q} = \frac{|V_{\perp}|^2}{\omega U_{\text{stored}}} \quad (13.8)$$

---

<sup>2</sup> This only strictly applies if the cavity is azimuthally symmetric.

This equation conveniently has the same form as (12.12). Note that for quadrupole and higher order modes there is no transverse kick for on axis particles hence (13.8) only applies to dipole modes.

For higher modes one normally defines the shunt impedance as

$$R_m = \frac{V_{cz}^2(a)}{\left(\frac{a\omega}{c}\right)^{2m} U_{\text{diss}}} = \frac{V_{cz}^2(a)}{\left(\frac{2\pi a}{\lambda}\right)^{2m} U_{\text{diss}}}$$

where  $\lambda$  is the free space wavelength at the frequency of the mode. If  $a$  is at a radius where the field is maximum, then the factor  $\left(\frac{2\pi a}{\lambda}\right)$  is going to be close and probably slightly more than one. This estimation is based on the simplistic assumption that the peak field will be a quarter of a wavelength from the field null occurring on the axis.

To derive equation (13.7) from the Panofsky Wenzel theorem [7] one writes

$$V_z(a) = \int_0^{d/c} E_z(a) \exp(j\omega t) c dt \approx a \int_0^{d/c} \nabla_{\perp} E_z(0) \exp(j\omega t) c dt = a \int_0^d \nabla_{\perp} E_z(0) \exp(j\omega z/c) dz \quad (13.9)$$

where the first approximation comes from a Taylor expansion for small radius  $a$ . Note that this approximation is not useful for quadrupole and higher modes. The Panofsky Wenzel theorem can be stated as

$$\int_0^d F_{\perp} \exp(j\omega z/v) dz = -j q \frac{v}{\omega} [E_{\perp} \exp(j\omega z/v)]_0^d + j q \frac{v}{\omega} \int_0^d \nabla_{\perp} E_z \exp(j\omega z/v) dz \quad (13.10)$$

where  $v$  is the velocity of the bunch which will be taken to be the velocity of light  $c$ . The first term on the RHS vanishes assuming the electric field in the beam pipe vanishes, i.e. the mode is cut-off.

Combining (13.9) and (13.10) gives

$$V_z(a) = -j \frac{a\omega}{qv} \int_0^d F_{\perp} \exp(j\omega z/v) dz \quad (13.11)$$

The transverse momentum kick is given as force  $\times$  time hence the deflection energy kick is the velocity of light  $\times$  the momentum kick so that the deflection voltage kick  $V_{\perp}$  is the energy kick divided by the charge hence

$$V_{\perp} = \frac{1}{q} \int_0^{d/c} F_{\perp} \exp(j\omega t) c dt = \frac{1}{q} \int_0^d F_{\perp} \exp(j\omega z/c) dz \quad (13.12)$$

Definition (13.12) in result (13.11) gives the earlier result (13.7).

Note that the use of a voltage kick or energy rather than a momentum kick is very dangerous as the new energy of the bunch is not the initial energy plus the energy kick, voltage kicks must be combined as momenta.

Re-arranging equation (13.6) to give the stored energy in terms of the R/Q on gets

$$U_{\text{stored}} = \frac{V_{\text{cz}}^2(a)}{\omega \left( \frac{a\omega}{c} \right)^2 \frac{R_d}{Q}} \quad (13.13)$$

Later this expression will be needed for an arbitrary radius hence utilising the relationship (13.2) for the case of a dipole ( $m = 1$ ) equation (13.13) becomes

$$U_{\text{stored}} = \frac{V_{\text{cz}}^2(r)}{\omega \left( \frac{r\omega}{c} \right)^2 \frac{R_d}{Q}} \quad (13.14)$$

i.e. we are not restricted to radius  $a$ .

#### 14. Crab Cavity Beam-loading from offset Bunches

A crab cavity is a deflection cavity operated with a  $90^\circ$  phase shift [8]. The fields that acts on an offset bunch in a pillbox dipole cavity radius excited in a  $TM_{110}$  mode are given by

$$E_z = E_o J_1 \left( \frac{u_{11}r}{a} \right) \cos \phi \exp(j\omega t) \quad (14.1a)$$

$$H_r = j E_o \sqrt{\frac{\epsilon_o}{\mu_o}} \frac{\omega_{110} a^2}{c r u_{11}^2} J_1 \left( \frac{u_{11}r}{a} \right) \sin \phi \exp(j\omega t) \quad (14.1b)$$

$$H_\phi = j E_o \sqrt{\frac{\epsilon_o}{\mu_o}} \frac{\omega_{110} a}{c u_{11}^2} J_1' \left( \frac{u_{11}r}{a} \right) \cos \phi \exp(j\omega t) \quad (14.1c)$$

$$E_r = E_\phi = H_z = 0 \quad (14.1d)$$

where

$$\omega_{110} = \frac{c u_{11}}{a} \quad (14.1e)$$

and where  $u_{11}$  is the first root of  $J_1(x)$

Importantly the longitudinal electric field is  $90^\circ$  out of phase with the magnetic field. For a crab cavity the charged bunch is at the centre of the cavity when the magnetic field is zero. This means that the longitudinal electric field is maximized and hence equation (12.7) applies. The electric field that bunches see is therefore determined by (13.14) i.e.

$$V_{\text{cz}}(r) = \frac{r\omega}{c} \sqrt{\omega \frac{R_d}{Q} U_{\text{stored}}} \quad (14.2)$$

It should be noted that for a deflection cavity as opposed to a crab cavity the cosine in (12.7) is replaced with a sine and hence the integrated voltage and hence the beam-loading is zero.

Equation (14.2) is easy to understand as from (12.4)

$$\omega \frac{R_d}{Q} \sim \frac{1}{C_d}$$

hence (14.2) just re-states the relationship between the charge, the peak voltage at  $r = c/\omega$  that an electron sees for optimum cavity length and stored energy of a capacitor.

For the FNAL CKM 3.9 GHz cavity the  $R_d/Q$  of a single cell has been determined by McAshan & Wanzenberg [9]. They use a slightly different definition for  $R_d/Q$  that is given here. Our definition is based on that used in Padamsee's book [10]. From equation 14 in [9]

$$\left(\frac{R}{Q}\right)'_{\text{FNAL}} = \frac{|V_L(r)|^2}{2\omega U \left(\frac{r\omega}{c}\right)^2}$$

where  $V_L(r)$  includes transit time effects hence

$$|V_L(r)| = \frac{r\omega}{c} \sqrt{2\omega \left(\frac{R}{Q}\right)'_{\text{FNAL}} U_{\text{stored}}} \quad (14.2_{\text{FNAL}})$$

comparison with (14.2) gives

$$2\left(\frac{R}{Q}\right)'_{\text{FNAL}} = \frac{R_d}{Q} \quad (14.3)$$

Henceforth we will write

$$\left(\frac{R}{Q}\right)'_{\text{FNAL}} = \left(\frac{R}{Q}\right)_F$$

where the suffix F implies a factor of one half as in the parallel equivalent circuit definition and retain the transit time factor unlike the equivalent circuit definition.

The paper <http://accelconf.web.cern.ch/AccelConf/p01/papers/MPPH129.pdf> gives

$$\left(\frac{R}{Q}\right)_F = 702 \quad \Omega \text{ m}^{-1} \quad (26 \text{ cells})$$

For 1 cell of a multi-cell cavity<sup>3</sup>  $\left(\frac{R}{Q}\right)_F = 27 \quad \Omega$  and with the definition here

$$\frac{R_d}{Q} = 54 \quad \Omega \text{ per cell}$$

for a transverse kick of  $5 \text{ MV m}^{-1}$  and operation at 3.9 GHz the paper gives

$$U_{\text{stored}} = 0.73 \quad \text{J m}^{-1}$$

hence per cell

$$U_{\text{stored}} = 0.0281 \text{ J per cell}$$

From (14.2<sub>FNAL</sub>) one calculates that for a metre length of cavities

$$|V_L(r)| = 4.096 \times 10^8 r \quad \text{V m}^{-1}$$

hence for beam offsets of 0.6 mm and 1 mm the kick per metre length of cavity system is  $2.458 \times 10^5 \text{ V m}^{-1}$  and  $4.096 \times 10^5 \text{ V m}^{-1}$  respectively.

For the ILC [11] the nominal bunch charge is  $3.2 \times 10^{-9} \text{ C}$  hence the energy delivered for 0.6 mm and 1 mm offsets are  $qV = 0.787 \times 10^{-3} \text{ J m}^{-1}$  per bunch and

<sup>3</sup> Because the endcells of a multi-cell cavity have a slightly different shape, for one cell on its own i.e. a cavity made of a single cell of 2 pieces 18.6mm long will have  $R/Q$  nearer to  $40.2 \quad \Omega$  and it will need to be run up to 34.8 mJ to give 5 MV/m deflection.

$qV = 1.311 \times 10^{-3} \text{ J m}^{-1}$  per bunch respectively which give for 3300 bunches 2.6 J and 4.3 J respectively which are bigger than the required energy for the cavity. The high power amplifier has to deliver or extract this amount of energy in 1 ms hence amplifier power requirements are  $2600 \text{ Wm}^{-1}$  and  $4300 \text{ Wm}^{-1}$  respectively plus cavity losses which can be neglected, plus reflection losses associated with any miss-match between  $Q_{\text{beam}}$  and  $Q_{\text{ext}}$ , noting that the impedance of the external circuit can only be matched to the impedance of the beam at one power level. Note that  $4300 \text{ Wm}^{-1}$  corresponds to 165 Watts per cell.

Calculations for a 9 cell CKM cavity planned for the ILC [1] give

$$\left(\frac{R}{Q}\right)_F = 664 \text{ } \Omega \text{ m}^{-1} \quad \text{and the stored energy is } 0.795 \text{ J m}^{-1} \text{ hence we obtain}$$

$|V_L(r)| = 4.157 \times 10^8 \text{ r V m}^{-1}$  which is practically what is obtained for the original design.

For the purpose of understanding the control of phase in a cavity, precise values for  $(R/Q)$  and  $U_{\text{stored}}$  are not necessary. For the computations in subsequent section we use  $(R/Q)_F = 26.5 \text{ } \Omega$  and  $U_{\text{stored}} = 0.0284 \text{ Joules per cell}$ .

## 15. Voltage Increment needed for Envelope Equations

From (14.2)

$$U_{\text{stored}} = \left(\frac{c}{r\omega}\right)^2 \frac{1}{\omega \left(\frac{R_d}{Q}\right)} V_{cz}^2(r) \quad (15.1)$$

where  $V_{cz}(r)$  includes transit time effects for ideal crab cavity phasing. Differentiation gives

$$\delta U_{\text{stored}} = \left(\frac{c}{r\omega}\right)^2 \frac{1}{\omega \left(\frac{R_d}{Q}\right)} 2 V_{cz}(r) \delta V_{cz}(r) \quad (15.2)$$

Equation (7.1) gives

$$\delta U_{\text{stored}} = q V_{\text{seen}} \quad (15.3)$$

where  $q$  is the bunch charge and  $V_{\text{seen}}$  is the voltage experience by the bunch for non-ideal crab cavity phasing. Combining (15.2) and (15.3) gives

$$\delta V_{cz}(r) = \frac{1}{2} \left(\frac{r\omega}{c}\right)^2 \omega \left(\frac{R_d}{Q}\right) \frac{V_{\text{seen}}}{V_{cz}(r)} q \quad (15.4)$$

The voltage that the bunch sees depends on the phase  $\phi$  with which it traverses the cavity with respect to the peak field in the cavity. If the cavity has a uniform longitudinal electric field<sup>4</sup>  $E_z$  along any offset path taken by the bunch then the maximum voltage seen by the bunch is

---

<sup>4</sup> the analysis can be more general with the use of a transit factor that encompasses non-constant  $E_z$

$$V_{cz} = E_z \int_{-\frac{d}{2}}^{\frac{d}{2}} \cos(\omega t) dz \quad (15.5)$$

In this integral  $t = 0$  when  $z = 0$  so that a particle in the crabbing phase gets maximum longitudinal acceleration/retardation depending upon which side of the cavity's axis the beam enters.

If the bunch travels at the velocity of light then  $z = ct$  and if the length of the cavity cell is  $d = \frac{\pi c}{\omega}$  then (15.5) becomes

$$V_{cz} = E_z \int_{-\frac{d}{2}}^{\frac{d}{2}} \cos(\omega t) dz = c E_z \int_{-\frac{2c}{2\omega}}^{\frac{2c}{2\omega}} \cos(\omega t) dt = \frac{\omega d}{\pi} E_z \int_{-\frac{\pi}{2\omega}}^{\frac{\pi}{2\omega}} \cos(\omega t) dt = \frac{2}{\pi} E_z d \quad (15.6)$$

For a bunch that traverses the cavity with phase error  $\phi$  then

$$\begin{aligned} V_{\text{seen}} &= E_z \int_{-\frac{d}{2}}^{\frac{d}{2}} \cos(\omega t - \phi) dz = \frac{\omega d}{\pi} E_z \int_{-\frac{\pi}{2\omega}}^{\frac{\pi}{2\omega}} \cos(\omega t - \phi) dt = \frac{d}{\pi} E_z \left\{ \sin\left(\frac{\pi}{2} - \phi\right) - \sin\left(-\frac{\pi}{2} - \phi\right) \right\} \\ &= \frac{2}{\pi} E_z d \cos \phi \end{aligned} \quad (15.7)$$

hence from (15.6) and (15.7)

$$V_{\text{seen}} = V_{cz}(r_b) \cos \phi \quad (15.8)$$

Where  $r_b$  is the lateral displacement of the beam.

hence (15.4) can be written

$$\delta V_{cz}(r) = \frac{1}{2} \left( \frac{r\omega}{c} \right)^2 \omega \left( \frac{R_d}{Q} \right) \frac{V_{cz}(r_b)}{V_{cz}(r)} q \cos \phi \quad (15.9)$$

From (12.2) with  $m = 1$  we can write

$$\frac{V_{cz}(a)}{a} = \frac{V_{cz}(r)}{r} = \frac{V_{cz}(r_b)}{r_b}$$

Hence (15.9) can be written

$$\delta V_{cz}(r) = \frac{1}{2} \left( \frac{r\omega}{c} \right)^2 \omega \left( \frac{R_d}{Q} \right) \frac{r_b}{r} q \cos \phi$$

Evaluating the voltage increment at radius  $r = a$  for a bunch with an offset  $r_b$  then the cavity kick is therefore

$$\delta V_{cz}(a) = \frac{1}{2} \left( \frac{a\omega}{c} \right)^2 \omega \left( \frac{R_d}{Q} \right) \frac{r_b}{a} q \cos \phi = \frac{1}{2} \frac{a\omega}{c} \frac{r_b\omega}{c} \omega \left( \frac{R_d}{Q} \right) q \cos \phi \quad (15.10)$$

The radius  $a$  is to be determined by ensuring that the stored energy for the equivalent circuit of figure 3 is the same as the stored energy given by (15.1). For the equivalent circuit and using (4.9) gives

$$U_{\text{stored}} = \frac{1}{2} C V_i^2 = \frac{V_i^2}{2\omega \left( \frac{R}{Q_{oi}} \right)_C} \quad (15.11)$$

equating this to the stored energy given for the dipole mode by (15.1) evaluated at radius  $a$  and reverting to the FNAL definition of  $R/Q$  given in (14.3) gives

$$\frac{V_i^2}{2\omega \left(\frac{R}{Q_{oi}}\right)_C} = \left(\frac{c}{a\omega}\right)^2 \frac{1}{2\omega \left(\frac{R}{Q}\right)_F} \left(\frac{2}{\pi}\right)^2 V_z^2(a) \quad (15.12)$$

where we have replaced the  $V_{cz}(a)$  in (15.1) by  $\frac{2}{\pi}V_z(a)$  so that the voltages on each side do not contain the transit time factor.

It is apparent from (15.12) that

$$\text{if } \frac{a\omega}{c} = \frac{2}{\pi} \quad \text{then} \quad \left(\frac{R}{Q_{oi}}\right)_C = \left(\frac{R}{Q}\right)_F \quad (15.13)$$

creating meaning for the circuit voltage  $V_i$ .

Equation (15.10) can now be used to determine the beam loading voltage kick that must be applied to the cavity response equation (4.15) each time a bunch passes through the cavity at phase  $\phi$ . Using (15.13) in (15.10) we evaluate the cavity voltage increment from the initially existing field acting on the bunch  $\delta V_i$  (without the transit time factor) as

$$\delta V_i = \frac{\pi}{2} \delta V_c = \frac{1}{2} \frac{r_b \omega}{c} \omega \left(\frac{R_d}{Q}\right) q \cos \phi = \frac{r_b \omega}{c} \omega \left(\frac{R}{Q}\right)_F q \cos \phi \quad (15.14)$$

### Side Note

*Padamsee [10] gives the beam induced voltage on pg 386 eqn. (19.12) as*

$$\tilde{V}_{br} = \frac{\tilde{i}_b R_a}{2(1+\beta)} = -\frac{I_o R_a}{(1+\beta)} \quad \text{where} \quad \beta = \frac{Q_o}{Q_e}, \quad \tilde{i}_b \text{ is the Fourier component of the}$$

*actual beam current that excites the cavity,  $I_o$  is the time average beam current and  $R_a$  is the shunt impedance of the cavity in the equivalent circuit. This is the steady state voltage attained after many bunches when the external circuit is connected and dissipating the beam current. The minus sign represents the fact that the beam in an accelerator cavity is acting to reduce the voltage with respect to the generator. This equation is not comparable with (15.14).*

The derivation of (15.14) using the integral (15.7) only considered the action of the cavity field on the bunch and not the action of the bunch back on the cavity. Effectively equation (15.14) is a limiting case of equations (7.2) – (7.4) as illustrated in the approximate form of (7.1). The  $\delta V_i$  is not the full change in the voltage but just the change in its component in the direction of the existing field. Note that in equations (7.2) to (7.4) the quantity  $q_m$  was charge added to the cavity mode whereas in (15.3) the quantity  $q$  is the bunch charge. We also note that  $\phi = \alpha - \theta$  i.e.  $\phi$  is the phase of the bunch with respect to the field in the cavity and not the reference.

If we apply the kick (15.14) to the envelope equations we must take account of the fact that the voltage kick is being applied at phase  $\phi$ .

From (7.3) and (7.4) and (9.1) we identify the real and imaginary parts of the field phasor  $\underline{V}_{initial}$  before the bunch passes as

$$A_r = \frac{q_m}{C} \cos \theta \quad (15.15)$$

$$A_i = \frac{q_m}{C} \sin \theta \quad (15.16)$$

and we have that

$$\underline{V}_{\text{initial}}^2 = A_r^2 + A_i^2 \quad (15.17)$$

hence

$$|\underline{V}_{\text{initial}}| = V_{\text{initial}} = \frac{q_m}{C} \quad (15.18)$$

Equations (7.3) and (7.4) can be therefore be written as

$$\text{Re}(V_{\text{final}}) = A_r + \frac{\delta q_m}{C} \cos \alpha \quad (15.19)$$

$$\text{Im}(V_{\text{final}}) = A_i + \frac{\delta q_m}{C} \sin \alpha \quad (15.20)$$

The square of the final voltage phasor is now given as

$$\underline{V}_{\text{final}}^2 = (\underline{V}_{\text{initial}} + \underline{\delta V})^2 = \left( A_r + \frac{\delta q_m}{C} \cos \alpha \right)^2 + \left( A_i + \frac{\delta q_m}{C} \sin \alpha \right)^2 \quad (15.21)$$

Hence expanding and subtracting (15.17) gives

$$\underline{V}_{\text{initial}} \cdot \underline{\delta V} + \frac{1}{2} \delta V^2 = \frac{\delta q_m}{C} (A_r \cos \alpha + A_i \sin \alpha) + \frac{1}{2} \left( \frac{\delta q_m}{C} \right)^2 \quad (15.22)$$

Using (15.18) in (15.15) and (15.16) so that  $A_r$  and  $A_i$  can be replaced with  $\underline{V}_{\text{initial}}$  and the phase angle in (15.22) gives

$$\underline{V}_{\text{initial}} \cdot \underline{\delta V} + \frac{1}{2} \delta V^2 = \frac{\delta q_m}{C} V_{\text{initial}} (\cos \theta \cos \alpha + \sin \theta \sin \alpha) + \frac{1}{2} \left( \frac{\delta q_m}{C} \right)^2 \quad (15.23)$$

Hence as  $\phi = \alpha - \theta$  we have

$$\underline{V}_{\text{initial}} \cdot \underline{\delta V} + \frac{1}{2} \delta V^2 = \frac{\delta q_m}{C} V_{\text{initial}} \cos \phi + \frac{1}{2} \left( \frac{\delta q_m}{C} \right)^2 \quad (15.24)$$

Comparison of this equation with its approximate form given in (15.15) allows us to identify

$$\frac{\delta q_m}{C} = \frac{r_b \omega}{c} \omega \left( \frac{R}{Q} \right)_F q \quad (15.25)$$

Hence from (15.19) and (15.20) beamloading in the envelope equations is determined as

$$A_r(\text{final}) = A_r(\text{initial}) + \frac{r_b \omega}{c} \omega \left( \frac{R}{Q} \right)_F q \cos \alpha \quad (15.26)$$

$$A_i(\text{final}) = A_i(\text{initial}) + \frac{r_b \omega}{c} \omega \left( \frac{R}{Q} \right)_F q \sin \alpha \quad (15.27)$$

By consideration of figure 5 we note that:-

$$\delta V_i = \delta |\underline{V}_i| = \delta A_r \cos \theta + \delta A_i \sin \theta \quad (15.28)$$

where  $\delta A_r = A_r(\text{final}) - A_r(\text{initial})$  and  $\delta A_i = A_i(\text{final}) - A_i(\text{initial})$

Putting our preferred cavity parameters and the ILC bunch charge into (15.14) where

$(R_d/Q) = 53 \Omega$  per cell,  $q = 3.2 \times 10^{-9} \text{ C}$ ,  $f = 3.9 \times 10^9$  gives

$$\delta V_i = 1.697 \times 10^5 r_b \cos \phi \quad (15.29)$$

hence for  $r = 1$  mm and  $\phi = 1$  degree then

$$\delta V_i = 169.7 \text{ Volts per cell} \quad (15.30)$$

From (15.12) and (15.14)

$$V_i = \sqrt{2\omega_o \left( \frac{R}{Q} \right)_F U_{\text{stored}}} \quad (15.31)$$

hence

$$V_i = \sqrt{2 \times 2\pi \times 3.9 \times 10^9 \times 26.5 \times 0.0284} = 1.92 \times 10^5 \text{ Volts per cell} \quad (15.32)$$

hence

$$\frac{\delta V_i}{V_i} \approx 0.88 \times 10^{-3} \quad (15.33)$$

i.e. individual bunches have a negligible effect on the amplitude.

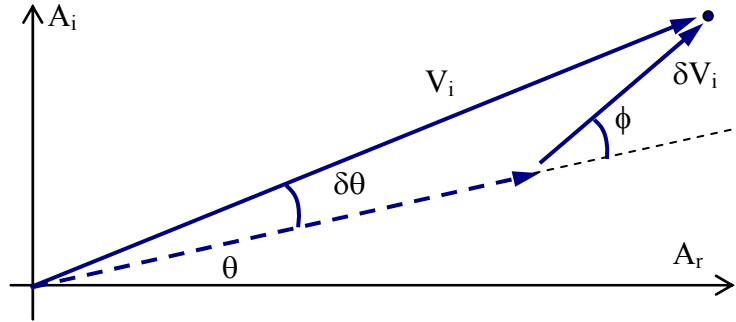


**Figure 4b** Phase addition of image charge giving a voltage increment

By consideration of figure 4b the change in the phase caused by a single bunch is given as

$$\delta\theta = \sin^{-1} \left( \frac{\delta V_i}{V_i} \tan \phi \right) \quad (15.34)$$

where  $\phi = \alpha - \theta$  is the phase error on the bunch with respect to the cavity field. The phase on the cavity phase  $\theta$  should not exceed 0.1 degrees at 3.9 GHz when properly controlled and  $\alpha$  is unlikely to exceed 1 degree (at 3.9 GHz), hence

$$\delta\phi_{\text{cavity}} = \sin^{-1} \left( 0.88 \times 10^{-3} \tan(1) \right) = 0.88 \times 10^{-3} \text{ degrees} \quad (15.35)$$

Phase synchronisation of the ILC crab cavity systems on the positron and electron beam lines needs to be better than 0.124 degrees for a 14 mad crossing angle [12]. If the synchronisation error is composed of three equal uncorrelated components, namely cavity 1 to reference 1, reference 1 to reference 2 and reference 2 to cavity 2 then the synchronisation requirement for each component is  $0.124 / \sqrt{3} = 0.072$  degrees. From (15.35) one concludes that it needs about 80 offset bunches at 1 mm and with a beam to cavity phase error of 1 degree before a change in the cavity phase reaches the limit of acceptability. The ILC bunches are 330 ns apart hence the control system needs to complete its correction on a time scale of 26  $\mu$ s.

## 16. Power Requirement for Beam loading

From (6.1) and (4.10) one has for an unloaded cavity, excited at resonance and in steady state that

$$P_f = \frac{\left(1 + \frac{Z_{wg}}{R}\right)^2}{4 \frac{Z_{wg}}{R}} P_c = \frac{\left(1 + \frac{Q_e}{Q_o}\right)^2}{4 \frac{Q_e}{Q_o}} P_c \quad (16.1)$$

This equation expresses the condition for impedance matching between the waveguide and the cavity.

When a cavity is excited with a beam, the beam can be modelled as an additional shunt resistance  $R_b$  in parallel to the cavity resistance  $R$ . The resistance  $R$  is positive if power is transferred from the cavity to the beam and negative if power is transferred from the beam to the cavity. If beam-loading is high then we can neglect  $R$  with respect to  $R_b$  hence (16.1) can be written

$$P_f = \frac{\left(1 + \frac{Q_e}{Q_b}\right)^2}{4 \frac{Q_e}{Q_b}} P_b \quad (16.2)$$

where

$$Q_b = \frac{\omega U}{P_b} \quad (16.3)$$

The maximum power that the beam can extract is given by

$$P_b = q V_{seen} f_{rep} = q V_z(r) \cos \phi f_{rep} \quad (16.4)$$

where  $f_{rep}$  is the bunch repetition frequency,  $q$  is the bunch charge and  $V_z(r)$  is given by (14.2) i.e.

$$V_z(r) = \frac{r\omega}{c} \sqrt{\omega \frac{R_d}{Q} U_{stored}} \quad (14.2)$$

If  $U_{stored}$  is specified,  $R/Q$  is known and the offset  $r$  is known then the power  $P_b$  can be determined and hence the forward power requirement.

The current ILC design spaces the bunches by 330 ns hence  $f_{rep} = 3.03$  MHz. Putting in values appropriate to the ILC crab cavity one gets

$$q = 3.2 \times 10^{-9} \text{ C}, \quad f_{rep} = 3.03 \times 10^6, \quad U_{stored} = 0.0284 \text{ J per cell} \quad r = 1 \times 10^{-3} \text{ m},$$

$$\frac{R_d}{Q_o} = 53 \Omega \quad \text{and} \quad \phi = 0 \quad \text{gives}$$

$$V_z(1\text{mm}) = 15700 \text{ V}, \quad P_b = 152 \text{ W}, \quad Q_b = 4.57 \times 10^6$$

Figure 8 plots equation (14.2) with these parameters.

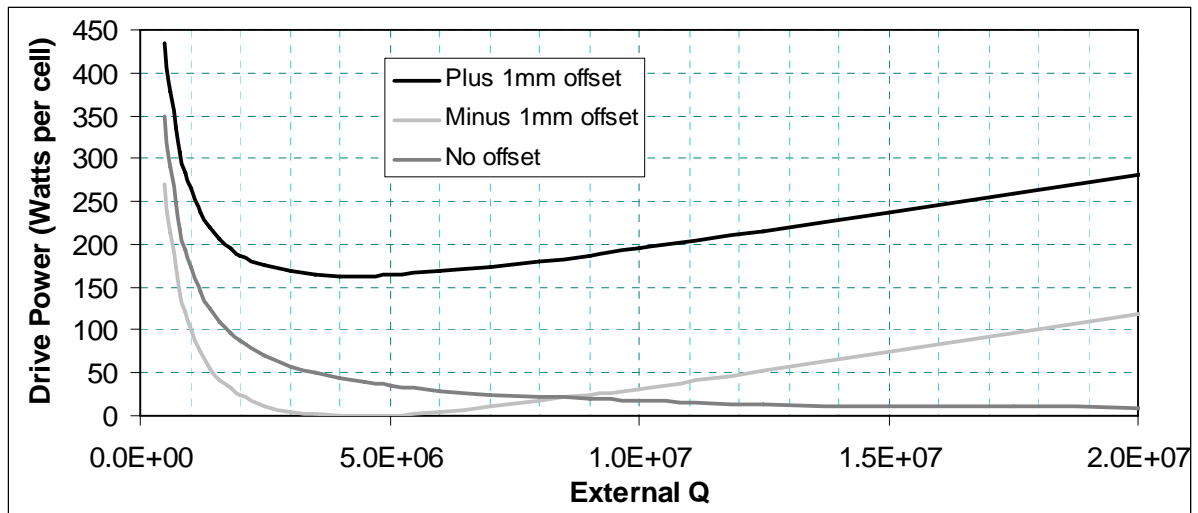


**Figure 8** Drive power as function of  $Q_{\text{ext}}$  for  $\pm 1$  mm beam offset (no microphonics).

For cavity sizes up to nine cells and for drive powers of a few hundred Watts per cell the total power requirement at 3.9 GHz for the proposed ILC crab cavity can be met with either a Klystron, or a TWT or a solid state amplifier. Control of microphonics might be expected to be better the lower the external Q and this will be analysed in later sections. On this basis and provided the amplifier has adequate flexibility one would probably want to aim for an external Q near to  $3 \times 10^6$  hence many of the later calculations use this value as a reference case.

### 17. Beam Loading Simulation – an illustration

Beam loading can be simulated by incrementing the voltage by an appropriate amplitude and phase each time a bunch passes through the cavity. Appendix 3 gives the code for integration of the envelope equations with repetitive beam loading and a controller on the phase and amplitude of the forward wave from the generator. Figures 8 to 11 show illustrative results for highly exaggerated dipole beam loading using an unrealistic 40 mm beam offset, a massive 5 degree timing error and a 15.38  $\mu$ s repetition rate (chosen so that the effect of the beam can be clearly seen in the figures). The external Q has been taken as  $10^6$  and the beam is turned on after  $2.0 \times 10^6$  cycles and off 1 ms later. The controller uses a simple PI algorithm and the control action is applied with a delay of 3900 cycles = 1  $\mu$ s.

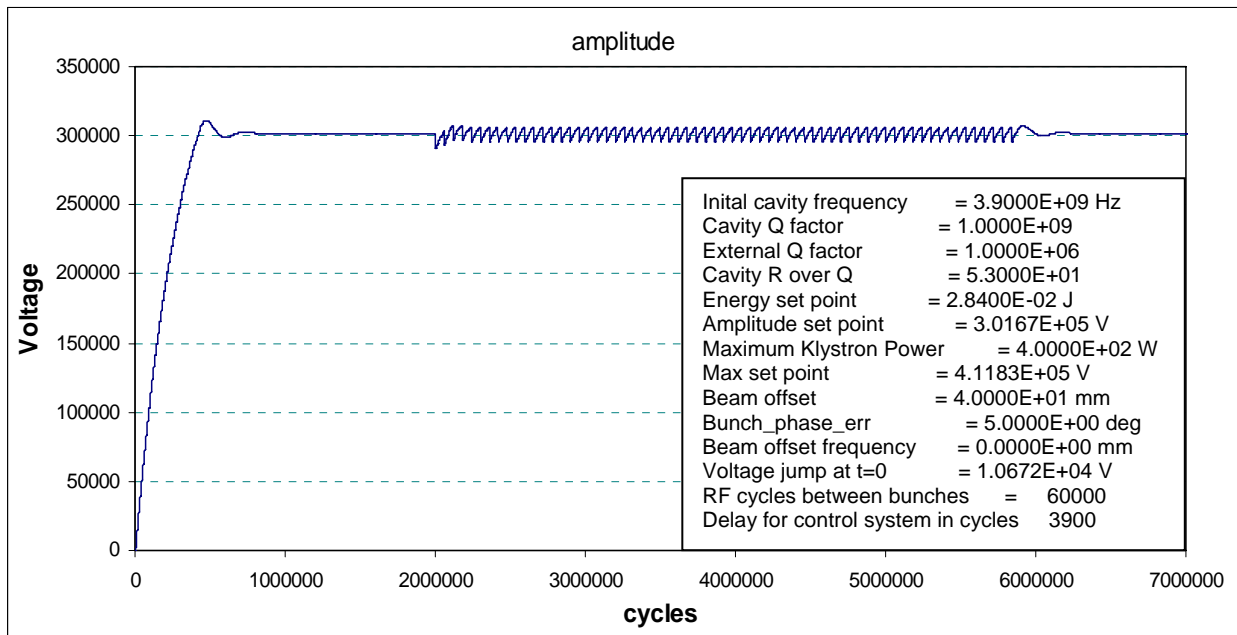


**Figure 8** Cavity voltage after switch on and after arrival of beam

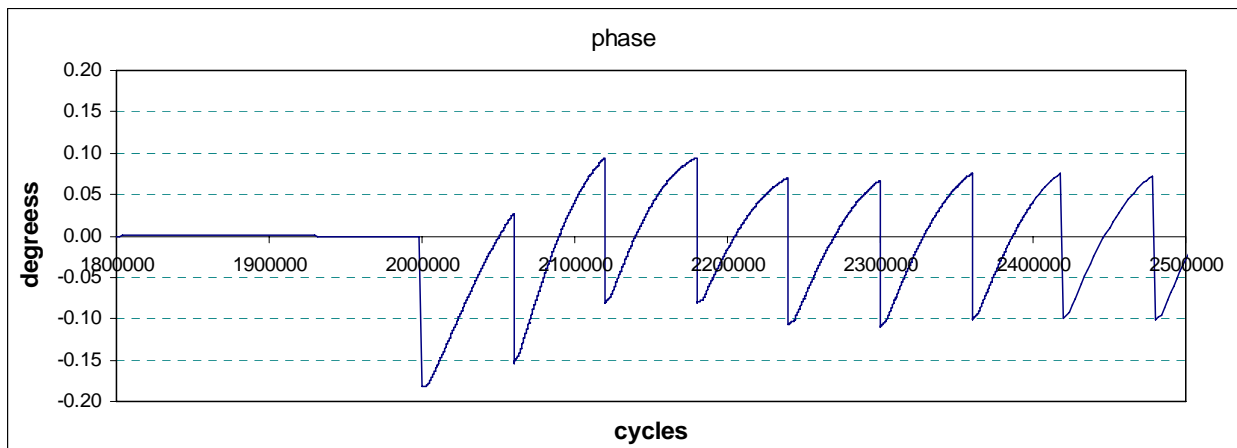


**Figure 9** Cavity phase showing arrival of beam

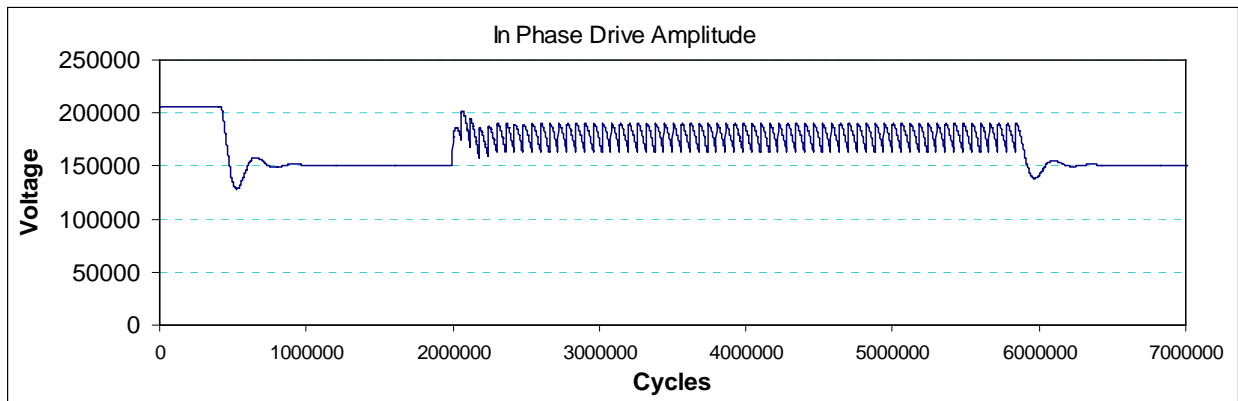


**Figure 10** Amplitude of drive voltage (1:1 transformer ratio) after switch on and after arrival of beam

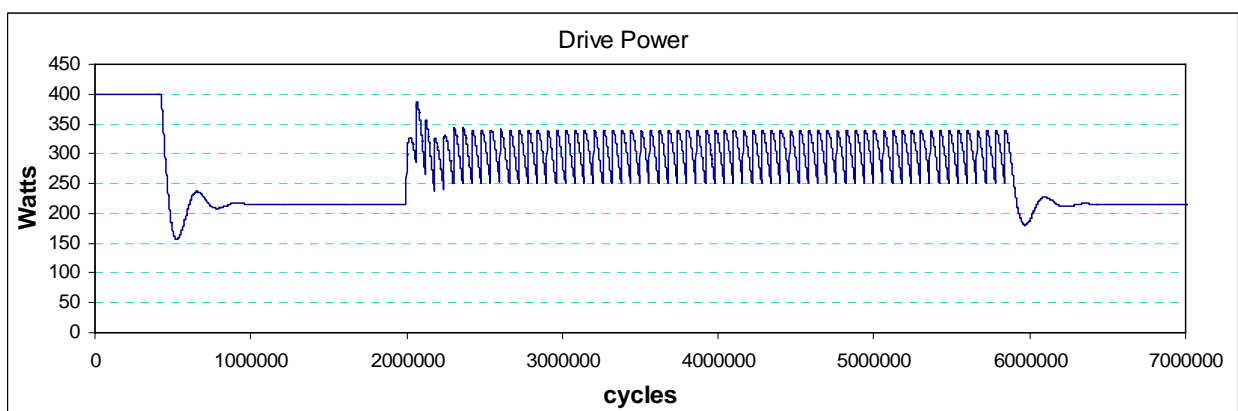


**Figure 11** Input power from drive after switch on and after arrival of beam

Note that the amplifier has been limited to 400 Watts. The control system attempts to correct the phase and amplitude after every bunch.

## 18. The Controller

The controller employed for these and subsequent simulations is a simple PI controller with a delayed action. A differential term is not employed as it is anticipated that noise on measurements of actual cavity fields cannot be adequately suppressed for the differential term to be useful whilst retaining system response. A PI algorithm responds well to random and unpredictable system disturbances such as beam offsets. In high Q superconducting cavities, tiny mechanical vibrations referred to as Microphonics [2] can give significant phase and frequency shifts. Microphonics are typically predictable on the time scale of sub milliseconds and hence predictive, feed-forward algorithms have the potential to out perform the simple PI algorithm. Advanced control algorithms are not considered in this report as microphonic data for the real system would not be available until a full system is tested. Performance with a PI algorithm should be regarded as a baseline performance.

For the multi-mode cavity an issue with the controller is whether by clever filtering one can determine the amplitude and phase of the operating mode. If one can and with reference to the envelope equations (11.2) one determines the drive as

$$\mathcal{F}_r(t + t_{\text{delay}}) = c_{\text{pr}} (V_{\text{sp}} - A_{1r}) + c_{\text{ir}} \left( \frac{\omega}{2\pi} \right) \int_{-\infty}^t dt (V_{\text{sp}} - A_{1r}) \quad (18.1)$$

$$\mathcal{F}_i(t + t_{\text{delay}}) = -c_{\text{pi}} A_{1i} - c_{\text{ii}} \left( \frac{\omega}{2\pi} \right) \int_{-\infty}^t dt A_{1i} \quad (18.2)$$

where  $t_{\text{delay}}$  is the time it takes to measure the error and adjust the amplifier output and  $V_{\text{sp}}$  is the set point voltage required in the cavity. The set point for the phase is zero hence the set point for the out of phase part of the voltage  $A_{1i}$  is also zero.

In the multi-mode software model we assume that the operating mode cannot be measured directly and instead one measures a time average of amplitude and phase of all the modes in the cavity where differing modes have a differing weighting according to their coupling to the output coupler.

The ratio of the integral coefficients  $c_i$  to the proportional coefficients  $c_p$  have been chosen such that the response immediately after rapid cavity filling at full power is slightly under-damped. This choice generally gave a slightly better control of amplitude and phase during the bunch than critical damping.

In some simulations such as those in sections 19.4, 20 and 22 the coefficients for the imaginary part were taken to be several times larger than those for the real part. The idea behind this followed from the fact that the crab cavity would operate at zero phase and better control of phase than amplitude is required. It was later realised that there is no real penalty for having coefficients for the real part equal to those for the imaginary part and the benefit is better control of the amplitude. Equal coefficients are used in sections 19.1, 19.2, 19.3, 21 and 23. Where larger control coefficients have been used for the imaginary part, these coefficients set the stability limit (*see section 21*).

## 19. Single mode simulations for ILC bunch parameters

### 19.1 $Q_e = 10^6$ (no microphonics, no measurement error, severe random beamloading)

This section considers the performance of single mode crab cavities with ILC bunch parameters [11]. Multi-mode cavities are considered in section 23. The first simulations of sections 19.1 and 19.2 focus on the effect of beam loading. The simulation shown in figures 12 to 16 illustrates beam loading response for a far less extreme case than was shown in section 17. Bunch charges and repetition rate are now nominal ILC values. In this simulation the beam is given a random offset with a maximum value of 1 mm and a maximum phase error of 1 degree; ILC actual values at the Crab Cavity location are more likely to be a slowly varying offset to 0.6 mm and beam arrival phase error of up to 0.3 degrees (at 3.9 GHz). The external Q has been set again as  $10^6$  so that results can be compared with calculations in section 16. The offset and phase errors are randomized with a flat distribution to the maximum offsets stated above. The controller has a relatively low gain with respect to the stability limit. The bunch arrives at cycle 500000.

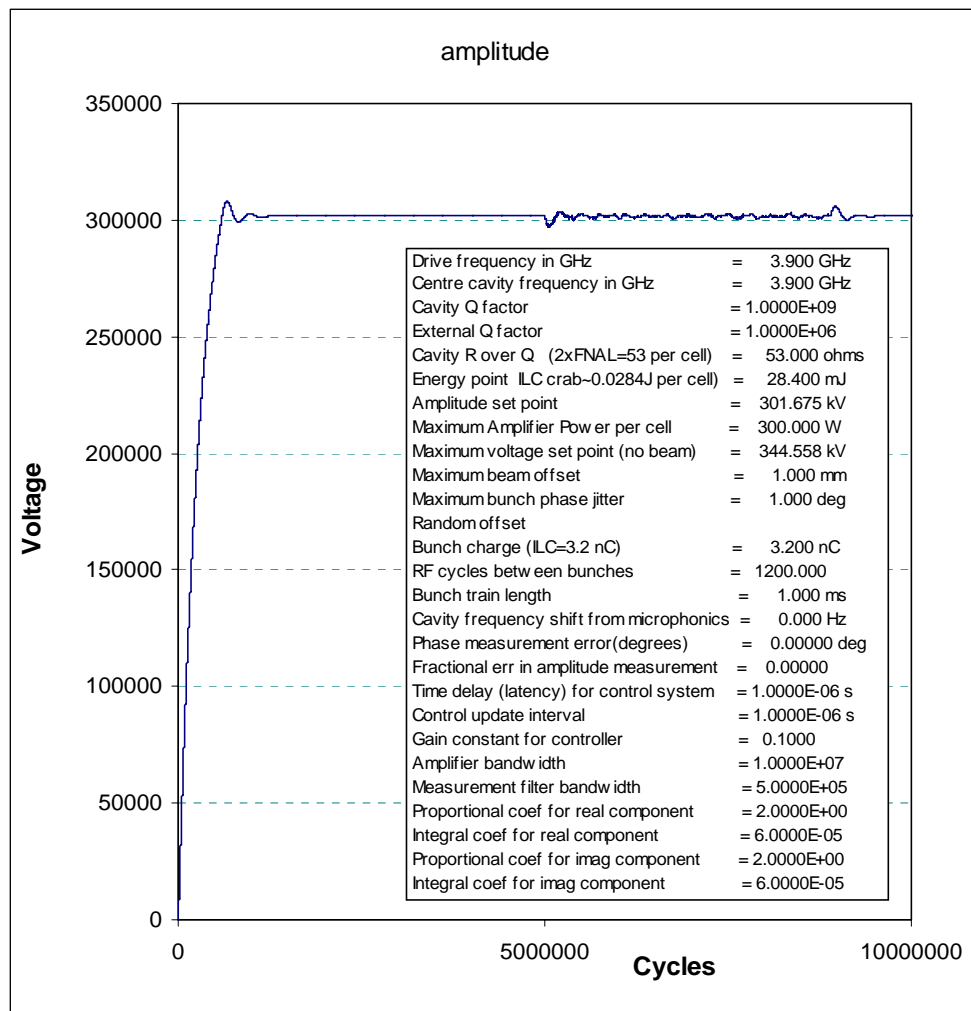


**Figure 12** Cavity voltage after switch on and after arrival of beam

After initial settling, the RMS amplitude fluctuation during the bunch (cycle 5200000 to 8800000) in figure 12 with beam are about 0.2%

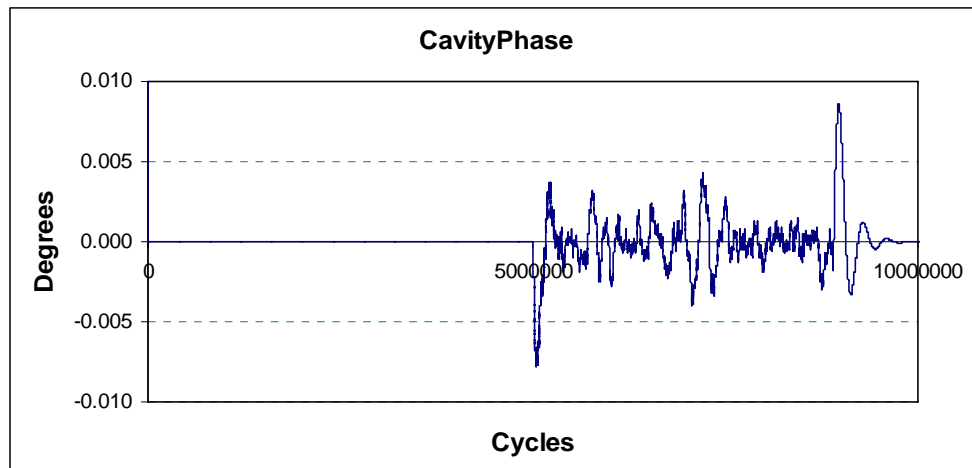


**Figure 13** Cavity phase before and after bunch arrival at 5000000 cycles

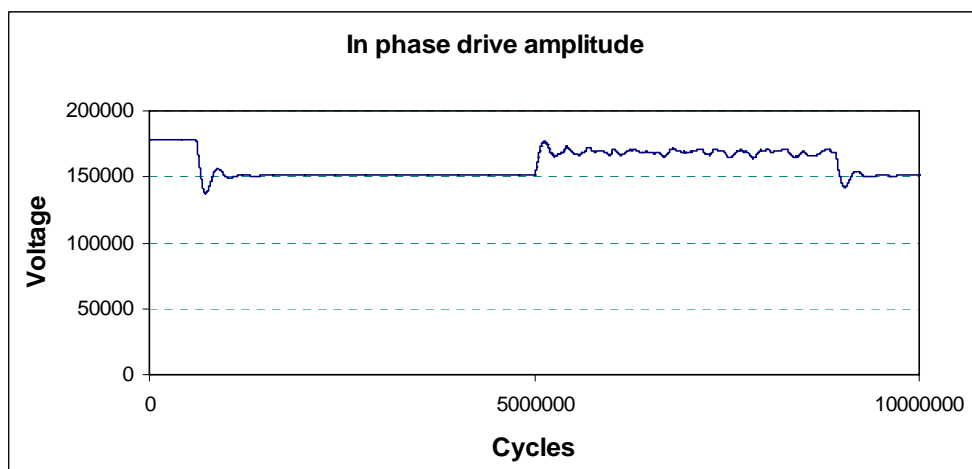


**Figure 14** Amplitude of drive voltage (1:1 transformer ratio). Note that the peak value is limited as the drive amplifier has a maximum output of 300 W.

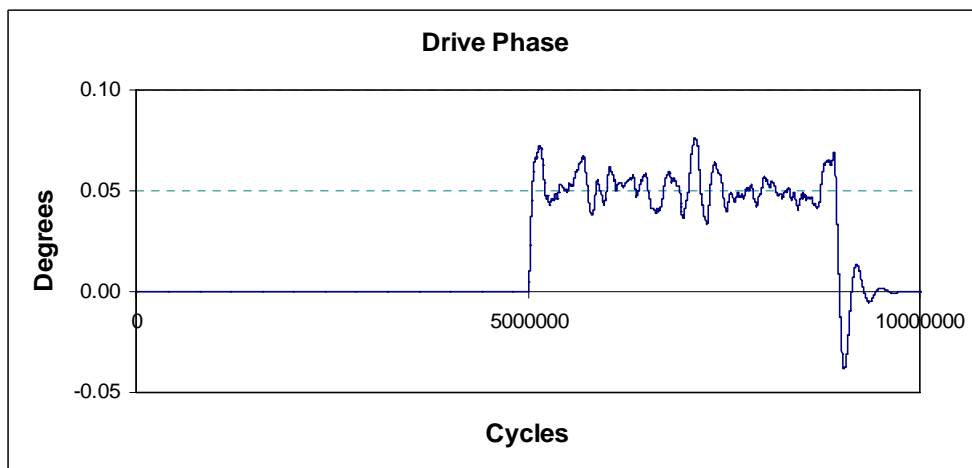


**Figure 15** Phase of drive voltage (1:1 transformer ratio)

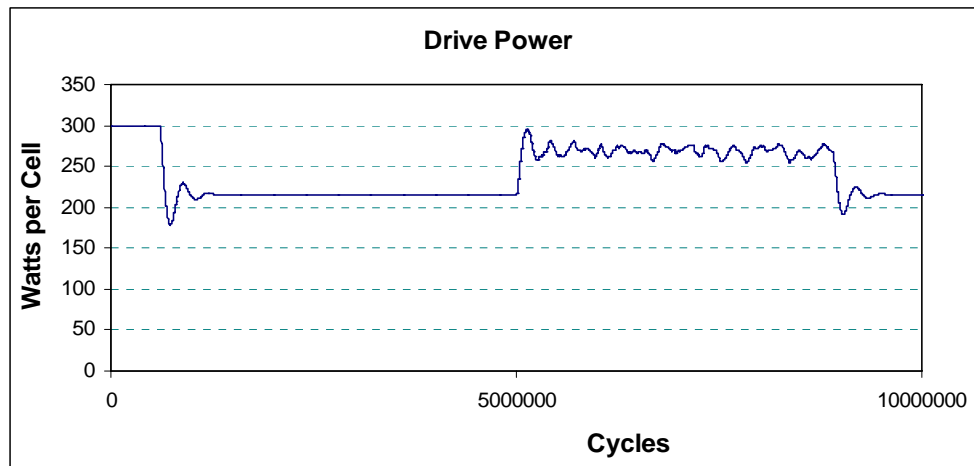
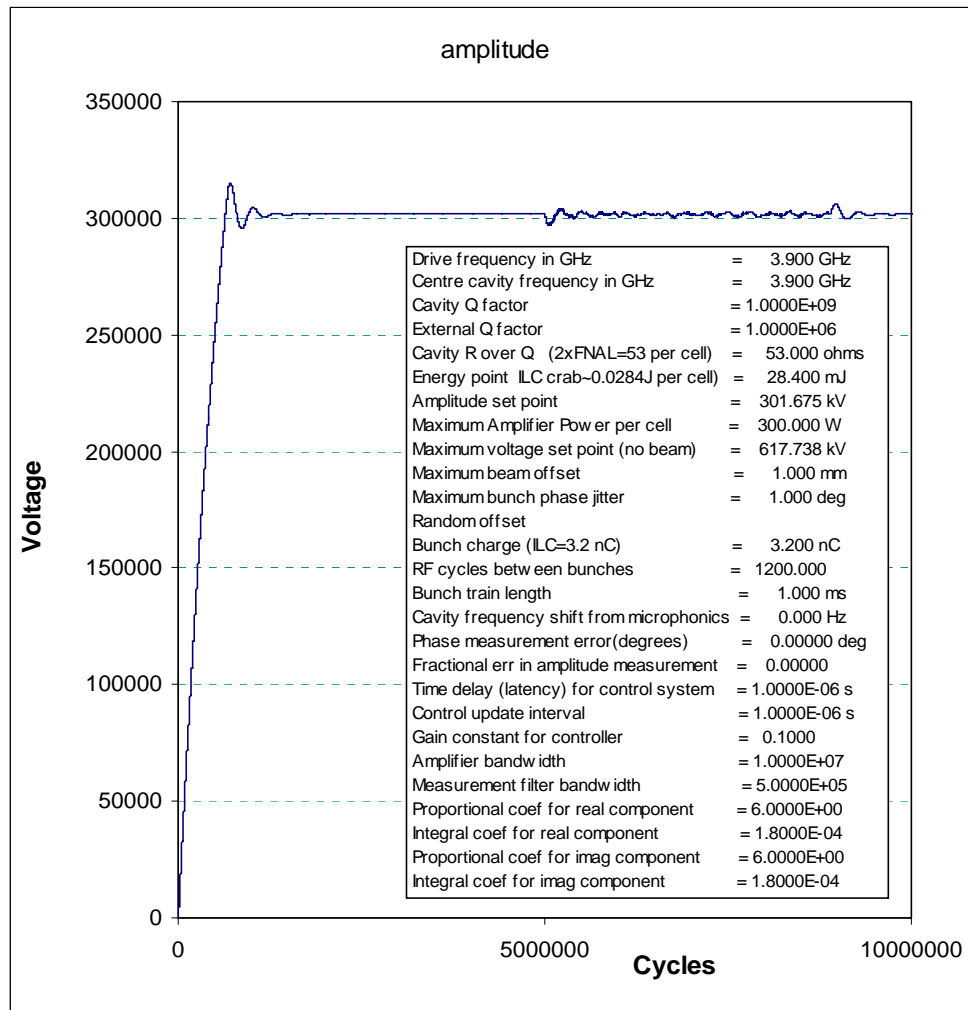


**Figure 16** Input power from drive after switch on and after arrival of beam

Inspection of figure 16 suggests that the drive amplifier needs to respond in a time period of about 50000 RF cycles = 13  $\mu\text{m}$  hence the bandwidth required to compensate for random beam loading is about 100 kHz. The actual bandwidth used for the simulation was 10 MHz.

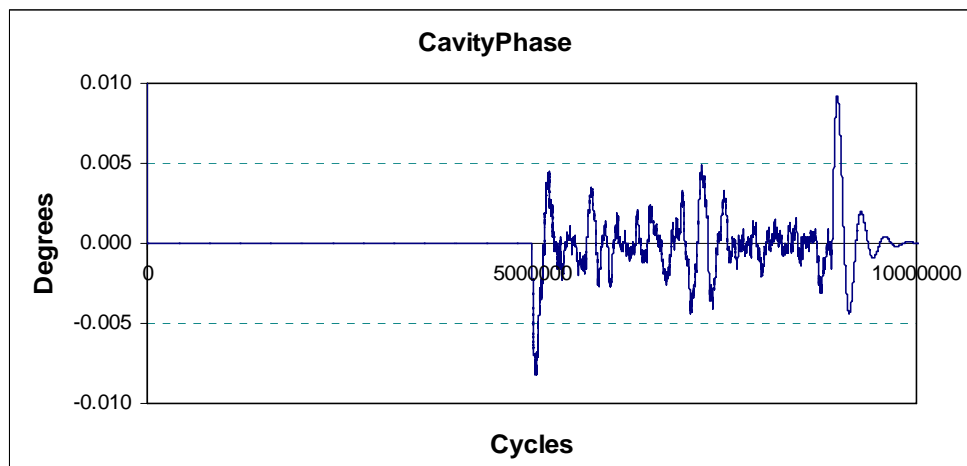
### 19.2 $Q_e = 3 \times 10^6$ (no microphonics, no meas. err., severe random beamloading)

One might guess that increasing the external Q factor of the cavity increases the phase error. The simulations in this section show that this is not necessarily the case if one increases the gain in the same proportion to any increase in Q. The simulation in this section shows that increasing the cavity external Q with respect to the previous calculation reduces power consumption with no other detrimental effect provided the gain is increased. When the external Q is increased from  $10^6$  to  $3 \times 10^6$  the amplitude response as shown in figure 17 is practically unchanged except where the set point is just attained. If gain is not increased then control deteriorates.



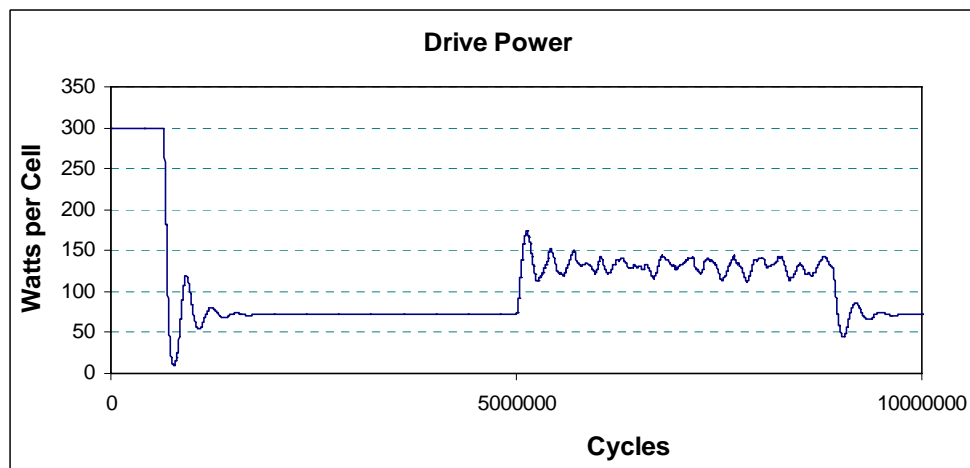
**Figure 17** Cavity amplitude showing fill and full bunch,  $Q_e = 3 \times 10^6$

The phase response of the cavity as shown in figure 18 is also almost identical to the low external Q case of figure 13.



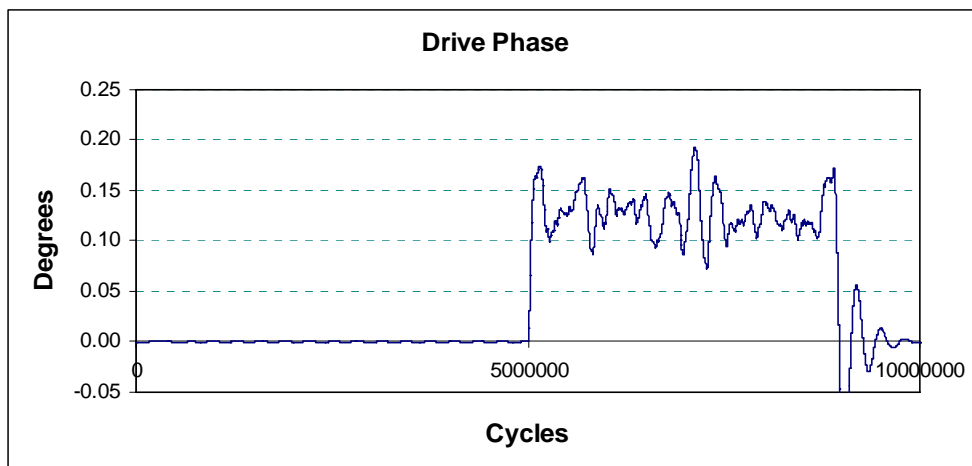
**Figure 18** Cavity phase showing fill and whole bunch,  $Q_e = 3 \times 10^6$

Figure 19 shows the power requirement before and after the beam arrives and should be compared with figure 16. In figure 16 a power requirement of 215 Watts is required before the beam arrives. After the beam arrives this rises to an average value of 270 Watts. In figure 19 there is a power requirement of 72 Watts before the beam arrives and this rises to an average of 132 Watts once the beam arrives. The power in each case rises by 55 Watts and 60 Watts respectively which is roughly the same as expected. The rise in power is required on a time scale of about 13  $\mu$ s. There would appear to be no disadvantage in having a high external Q of  $3 \times 10^6$  provided the amplifier has the required flexibility of output. In section 14 we determined that the minimum power requirement for a beam offset of 1 mm occurs at  $Q_{\text{external}} = 4.51 \times 10^6$ . For this external Q and for a random offset the power requirement falls to an average of 115 W.



**Figure 19** Input power for fill and whole bunch,  $Q_e = 3 \times 10^6$

Figure 20 plots the phase of the drive, note that it does not average to zero.



**Figure 20** Phase of drive voltage (1:1 transformer ratio) after switch on and after arrival of beam,  $Q_e = 3 \times 10^6$

**19.3 Oscillatory offset (no microphonics)**

Maximum power requirement occurs when the beam offset stays at its maximum offset. The most demanding power requirement is when the beam oscillates slowly from its extreme offset where it is taking power to its extreme offset where it is delivering power. For this case the power supply either has to turn itself on and off or switch its phase. Figures 21 to 23 illustrate the situation where the control algorithm turns the power supply on and off rather than switching phase and moving around zero output. The offset is taken to be sinusoidal with a frequency of 2 kHz so that there are two periods during the bunch. Figure 21 shows the amplitude on an expanded scale. Note that the control coefficients as defined in section 18 are given in a separate box and are written in terms of  $Q_e$  in accordance with the identified scaling.

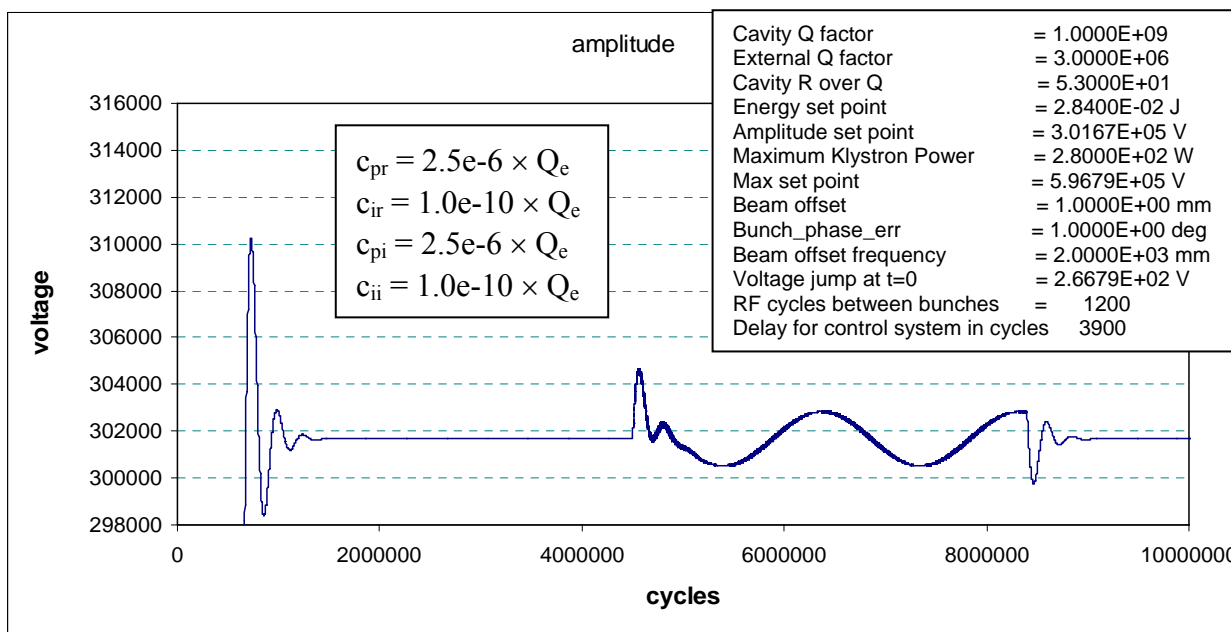


**Figure 21** Cavity amplitude for oscillating beam offset,  $Q_e = 3 \times 10^6$

The simple PI controller keeps amplitude fluctuations to less than 0.8% . Figure 22 shows the power supply response that is needed to achieve this.

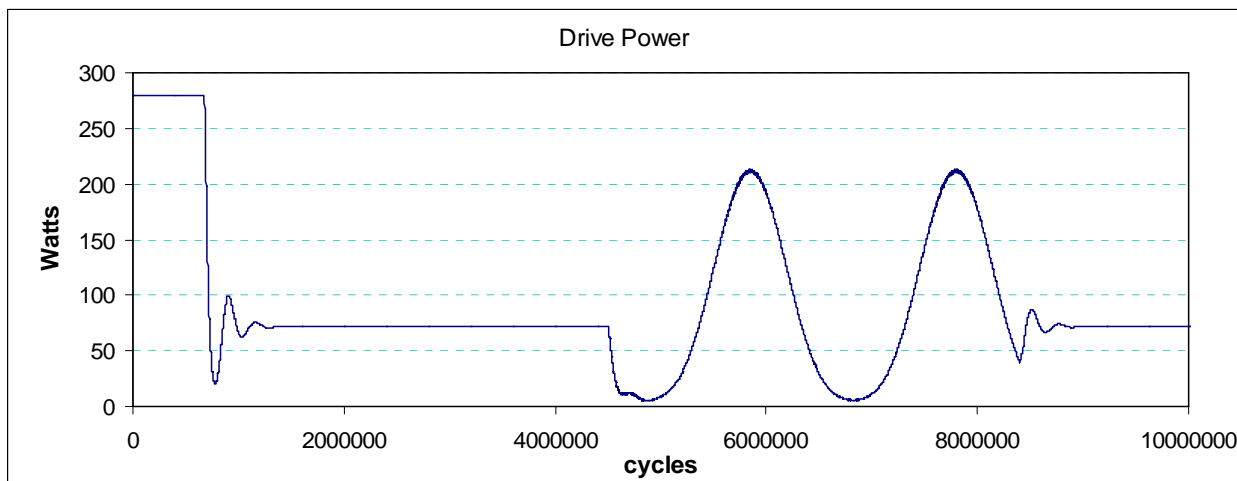


**Figure 22** Input power for oscillating beam offset,  $Q_e = 3 \times 10^6$

The power supply has to turn off and back on again at the oscillation frequency of the beam.

As shown in figure 23 cavity phase can still be maintained within the required tolerance.

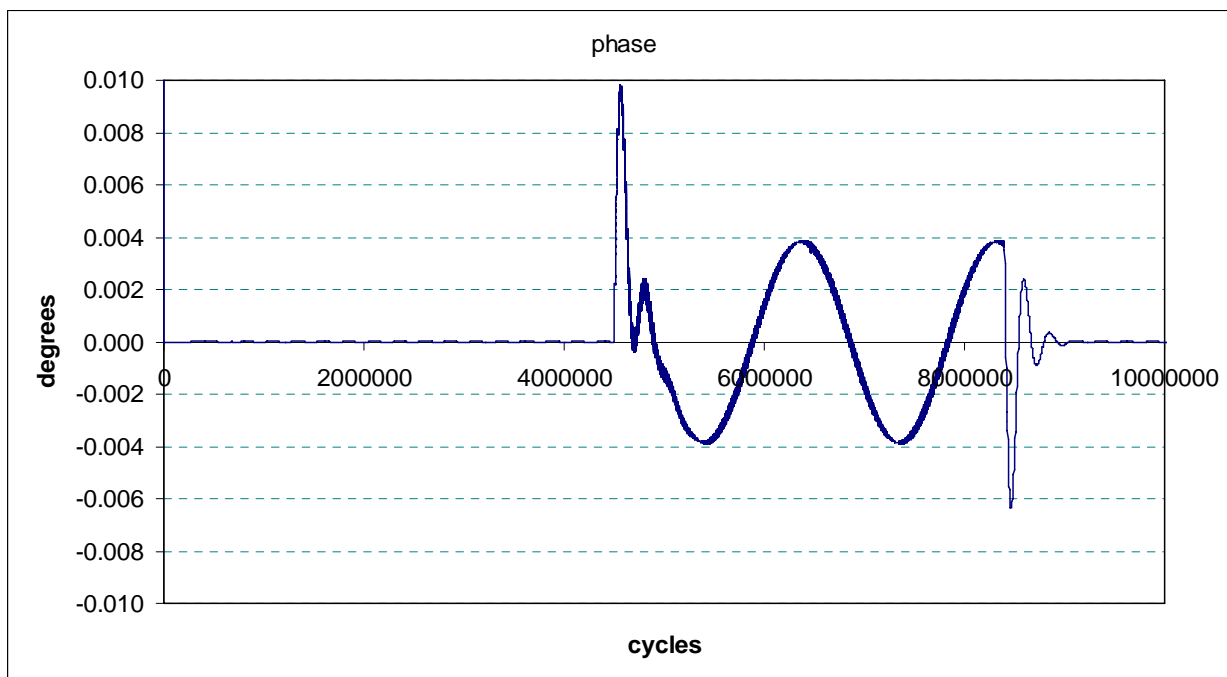


**Figure 23** Cavity phase for oscillating beam offset,  $Q_e = 3 \times 10^6$

If the cavity external  $Q$  is further increased the power supply must reverse its phase. Figures 24 to 28 illustrate this situation for the case of  $Q_{\text{external}} = 1.75 \times 10^7$ . As this external  $Q$  is much higher than the required external  $Q$  for matching the beam load at an offset of 1 mm the amplifier power must be increased. Here it is increase to 400 W per cell. Figure 24 shows the amplitude during cavity filling a period of settling and then during the pulse.

As the power has been increased the initial fill is rapid. Amplitude control is satisfactory. Figures 25, 26 and 27 show the amplifier power output, its drive amplitude and its drive phase respectively.

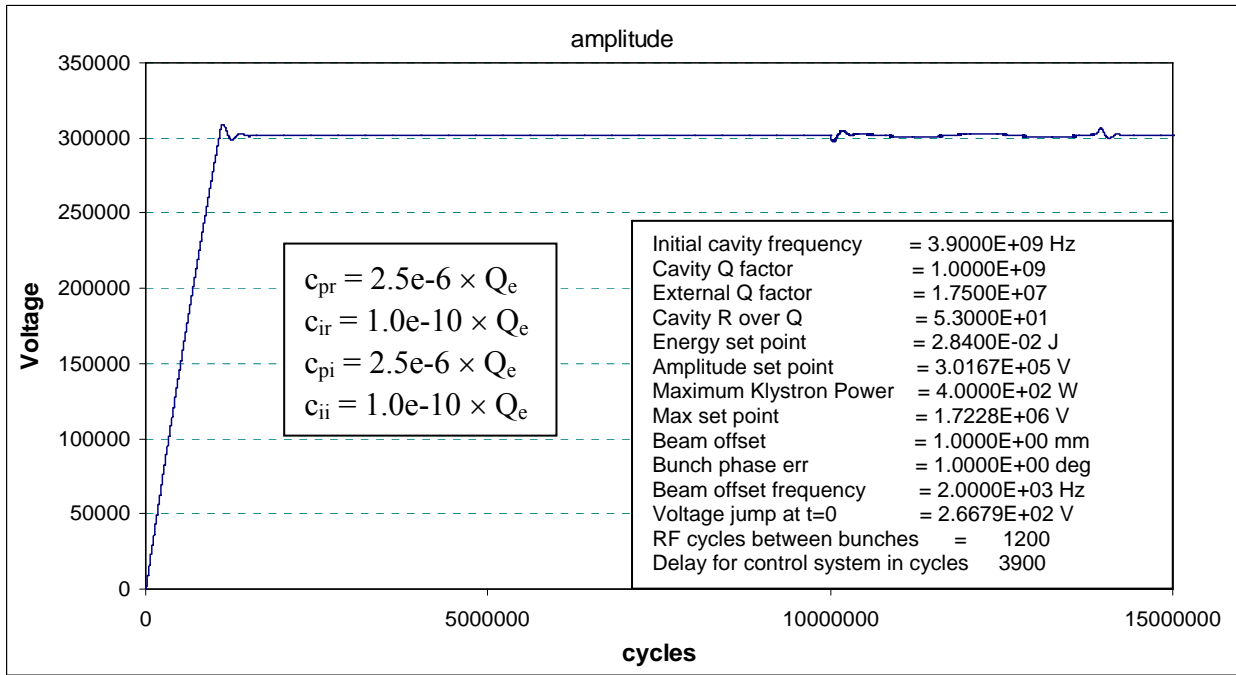


**Figure 24** Cavity amplitude for oscillating beam offset,  $Q_e = 1.75 \times 10^7$

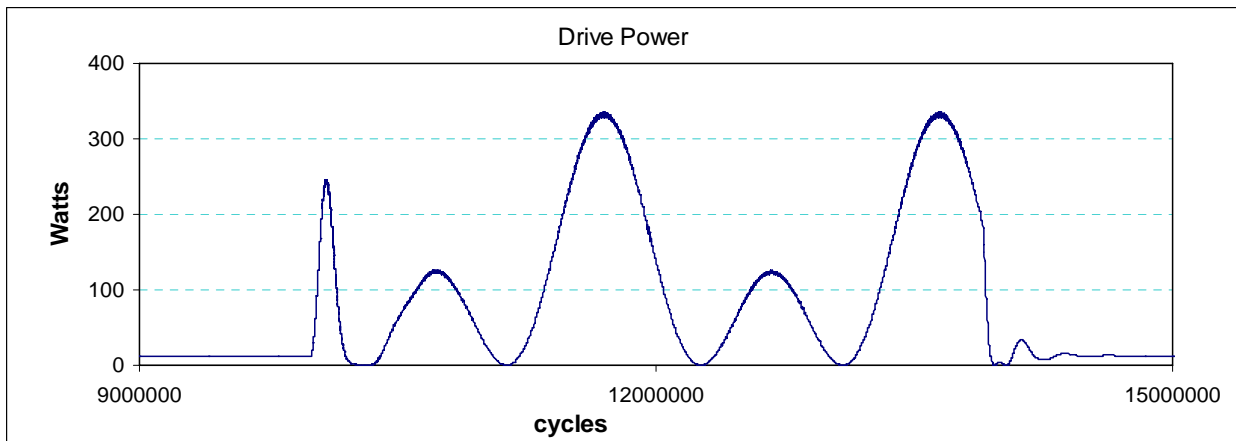


**Figure 25** Drive power during bunch for oscillating beam offset,  $Q_e = 1.75 \times 10^7$

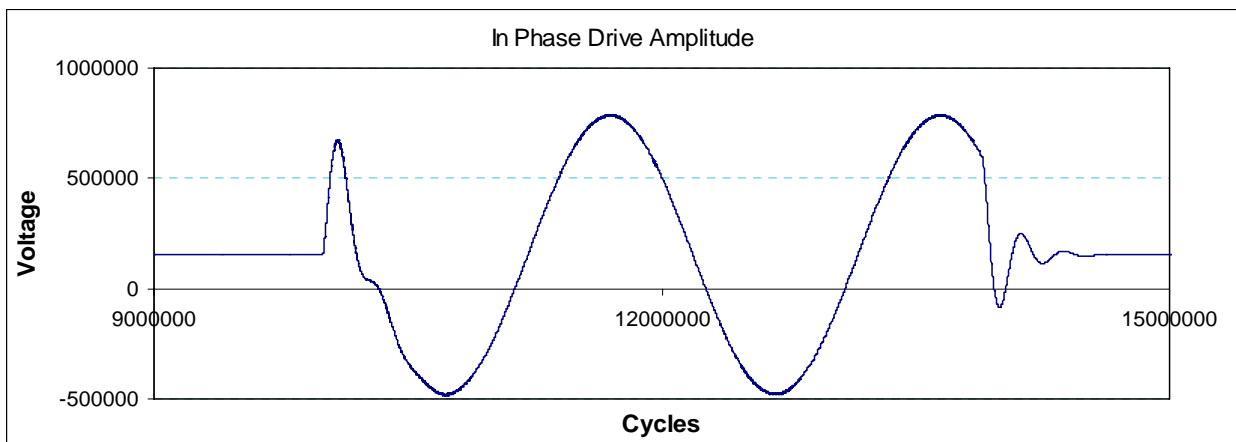


**Figure 26** In phase drive amp. during bunch for oscillating beam offset,  $Q_e = 1.75 \times 10^7$

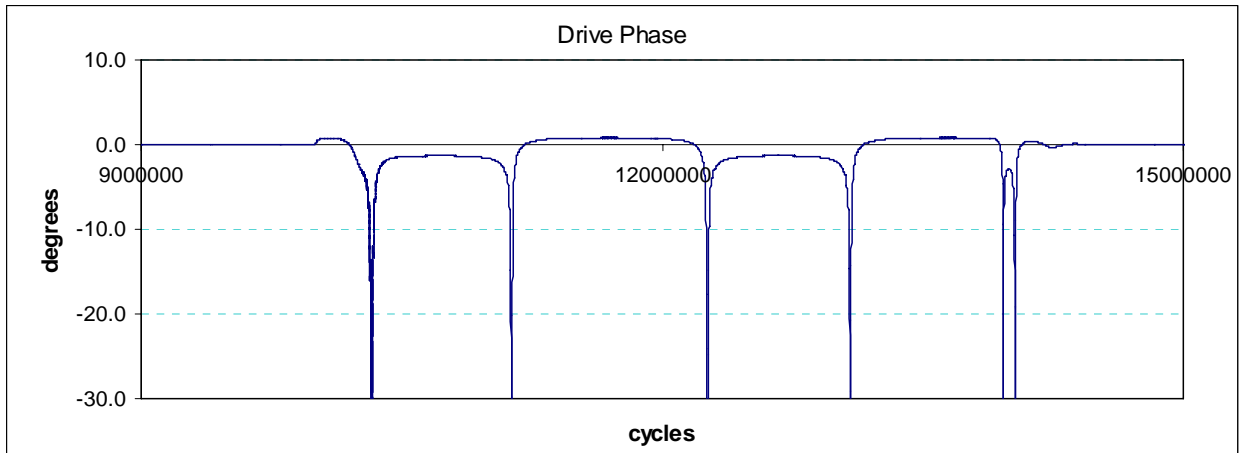


**Figure 27** Drive phase during bunch for oscillating beam offset,  $Q_e = 1.75 \times 10^7$

Figure 28 shows that for the higher external  $Q$ , control of the cavity phase and using the same controller parameters which include a scaling factor of  $Q_e$  is nominally the same. Accuracy of phase control depends primarily on the gain of the controller. When the controller has a delayed action, control becomes unstable when the gain (or indeed the integral term in the controller) rises above a certain level. It will be seen later that the point of instability is almost independent of  $Q_e$  when the control parameters have the scaling factor of  $Q_e$ .

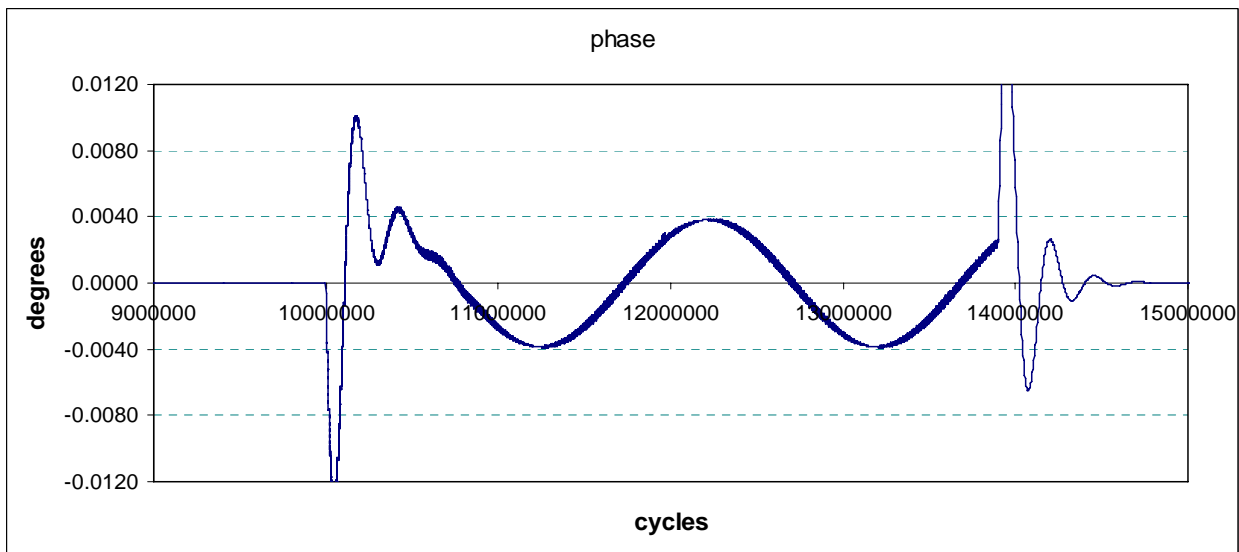


**Figure 28** Cavity phase during bunch for oscillating beam offset,  $Q_e = 1.75 \times 10^7$

### 19.4 Oscillatory offset and microphonics

In this section micro-phonics are simulated by giving the cavity frequency a sinusoidal variation.

The control action on the out of phase drive has been increased to keep the phase errors within the previous margin of  $0.04^\circ$ . Figures 29 to 34 illustrate the effect of a mechanical resonance at 230 Hz that causes a maximum cavity frequency shift of 600 Hz. (See for instance “Microphonics detuning compensation in 3.9 GHz Superconducting Cavities”, Carcagno, Bellantoni et al. FERMILAB-Conf-03/315-E). Note that the control parameters for the quadrature component have been increased by a factor of four with respect to the in phase component for these simulations. The motivation for this was that a higher degree of phase control is required than amplitude control. (*Later we find no disadvantage in equal coefficients*)

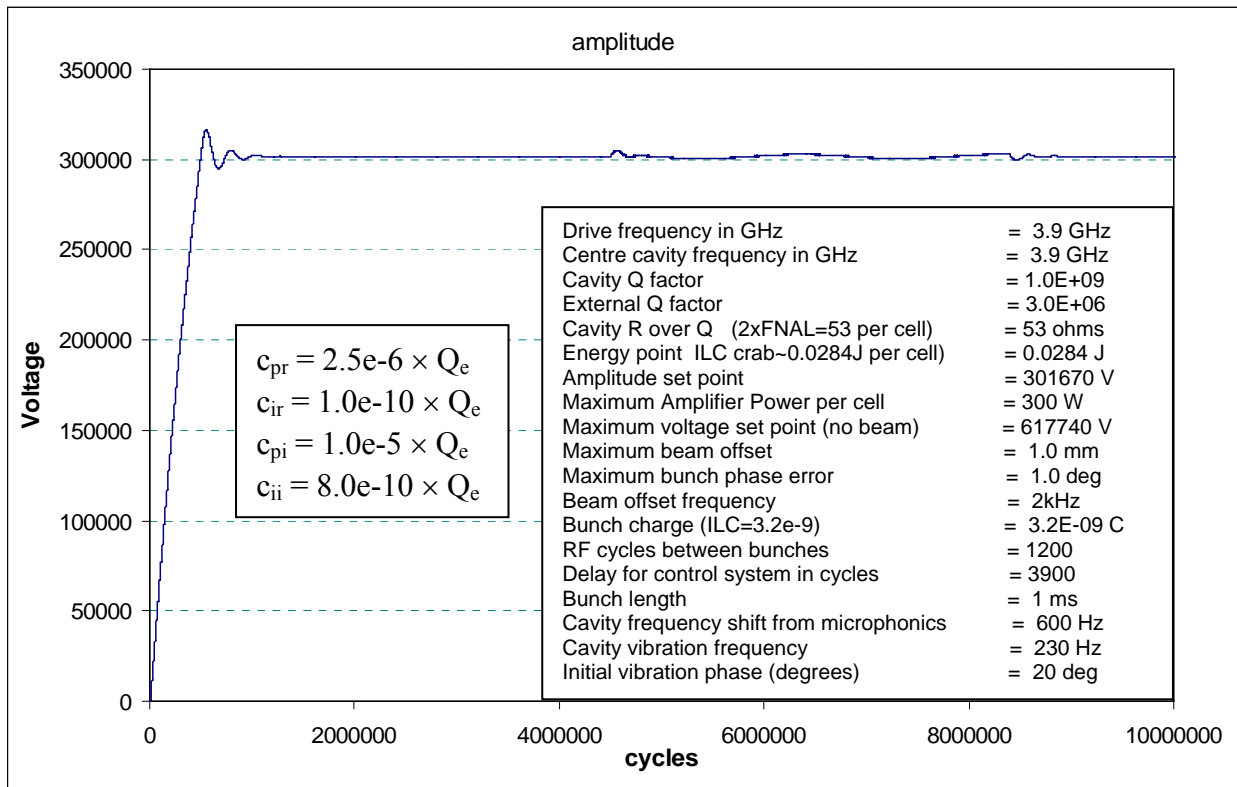


**Figure 29** Cavity amplitude for oscillating beam offset and micrphonics,  $Q_e = 3 \times 10^6$

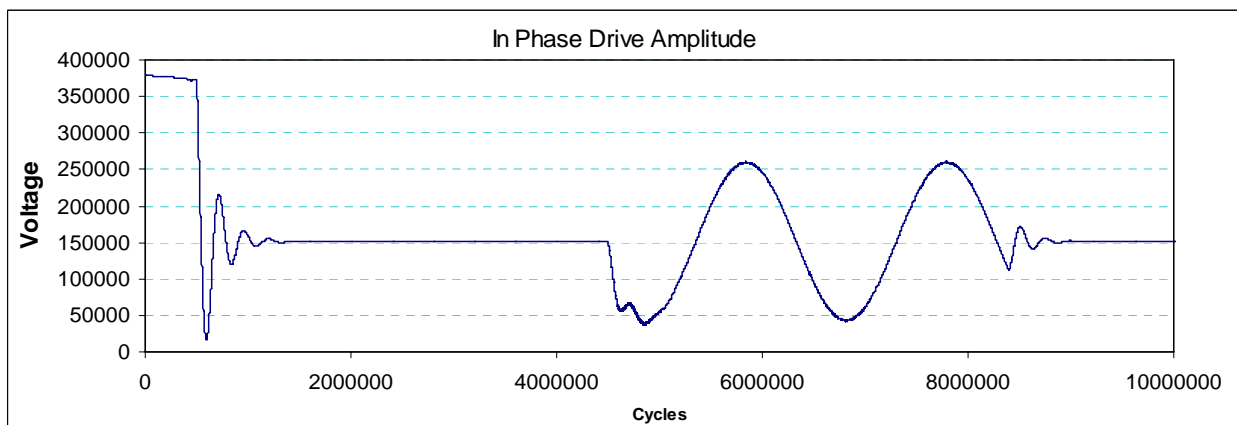


**Figure 30** In phase drive amp. for oscillating beam offset & microphonics,  $Q_e = 3 \times 10^6$

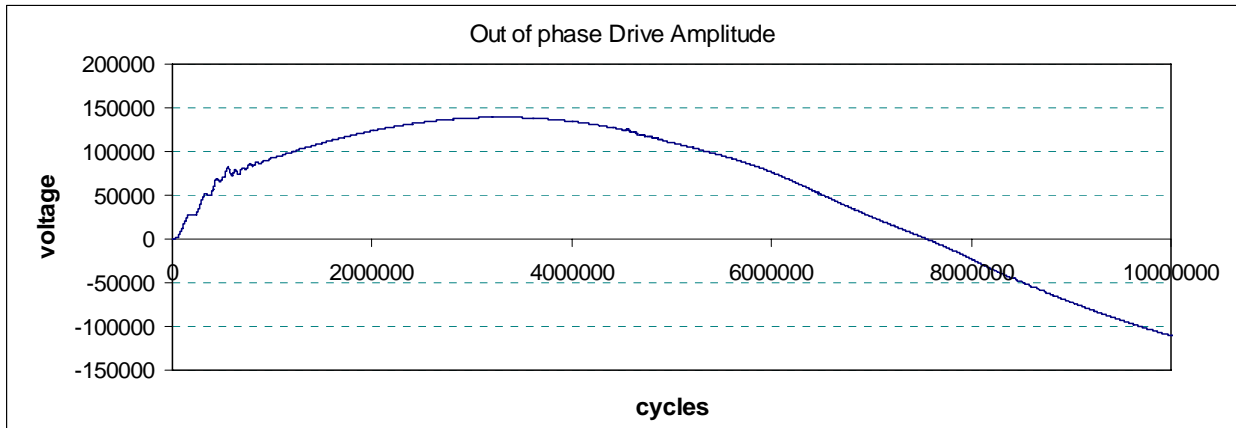


**Figure 31** Out of phase drive ampl. oscillating beam offset & microphonics  $Q_e = 3 \times 10^6$

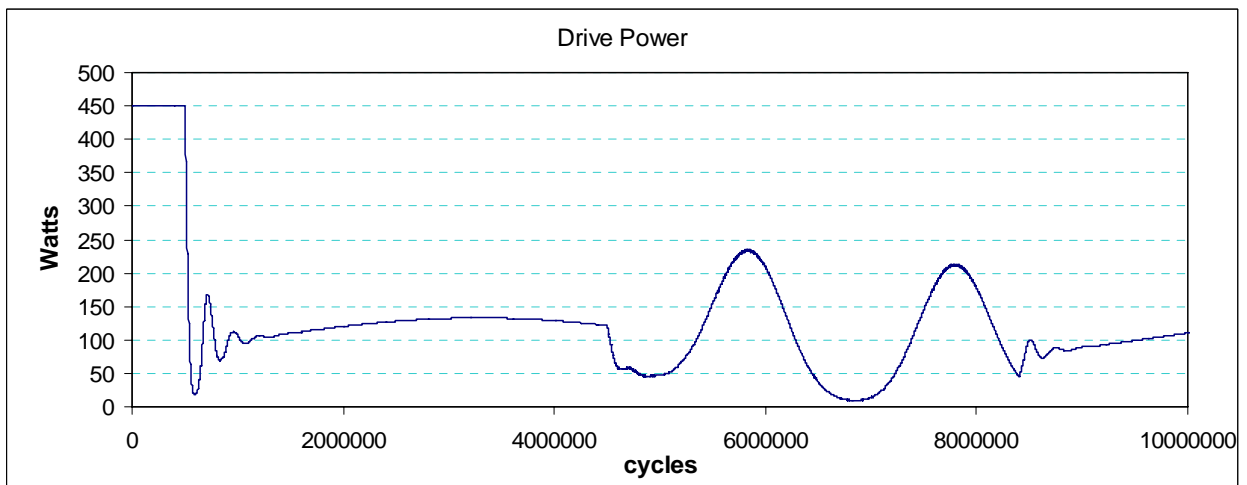


**Figure 32** Out of phase drive power, oscillating beam offset & microphonics  $Q_e = 3 \times 10^6$

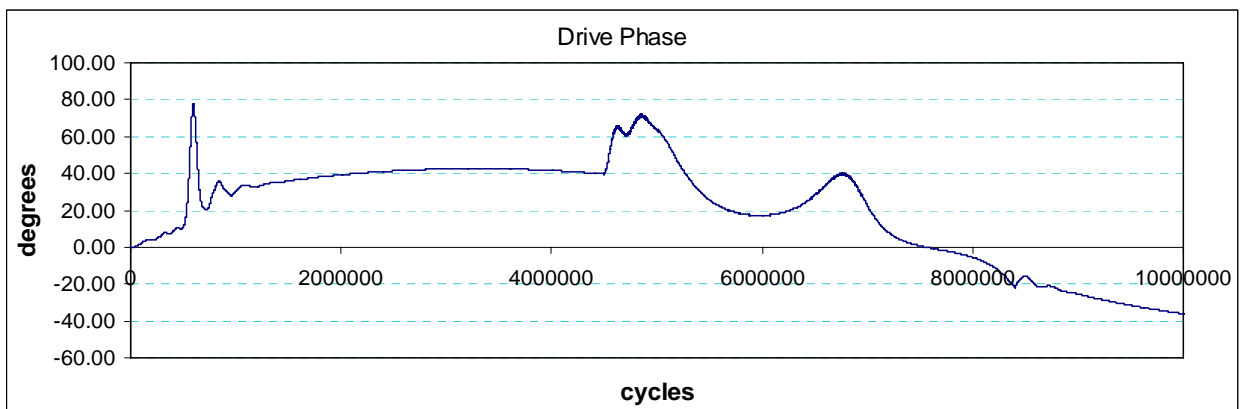


**Figure 33** Out of phase drive phase oscillating beam offset & microphonics  $Q_e = 3 \times 10^6$

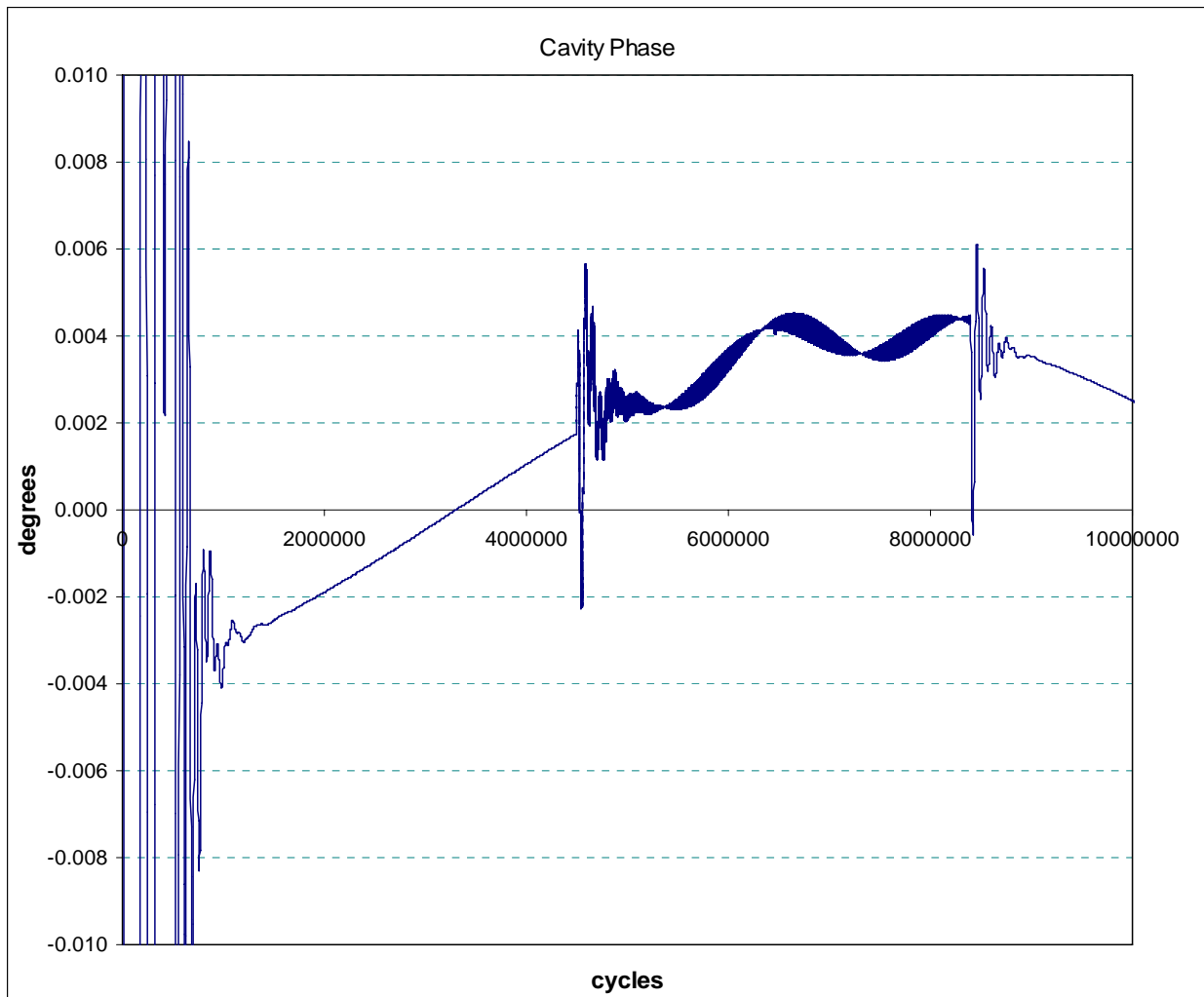


**Figure 34** Cavity phase for oscillating beam offset & microphonics  $Q_e = 3 \times 10^6$

Figures 30 and 31 show that the in phase component of the drive power predominantly corrects beamloading from beam offset and the out of phase component of the drive power corrects microphonics.

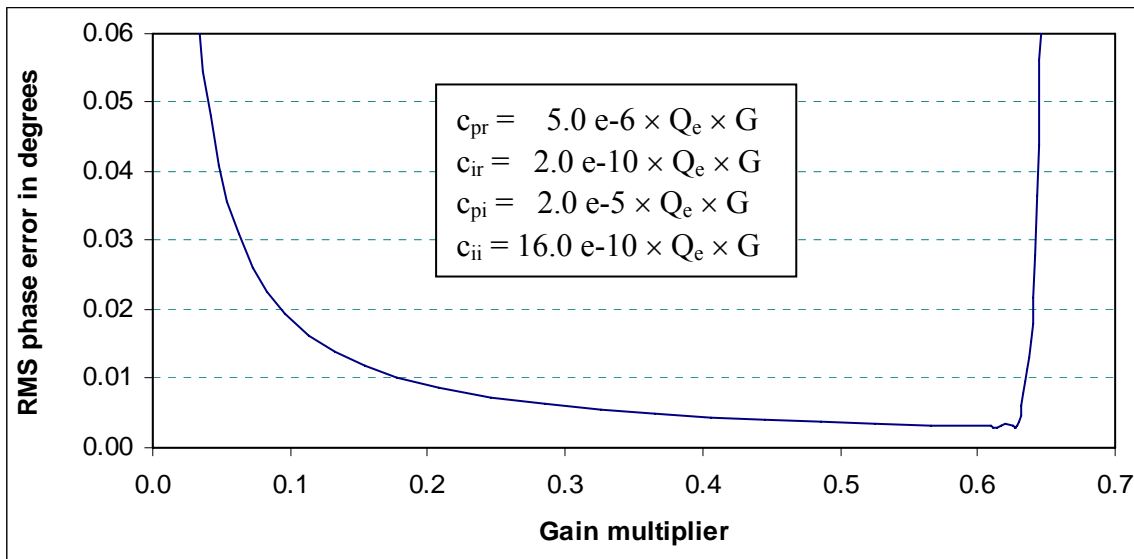
Figure 32 shows how microphonics will push up the power supply requirement. The minimum additional power requirement is given as  $P = U \delta\omega$  where  $U$  is the energy stored in the cavity and  $\delta\omega$  is the cavity detuning [2]. For this simulation  $U = 0.0284$  J and  $\delta\omega = 2\pi \times 600$  Hz hence  $P = 107$  W. Comparing figures 22 and 32 for the period before the bunch arrives the peak power rises from 70 W to 140 W. This is a little less than the prediction of 107 W, however one has to bear in mind that the phase and amplitude control here is not perfect.

Figure 34 suggests that with a sufficiently high gain, phase control to the required stability specification for the ILC crab cavity of 0.05 degrees rms can be achieved. Whether the gain used in the calculation gives a stable control system in practice will depend on measurement jitter at an appropriate sampling rate, delays in the controller and delays in the power supply responding to the new requirement.

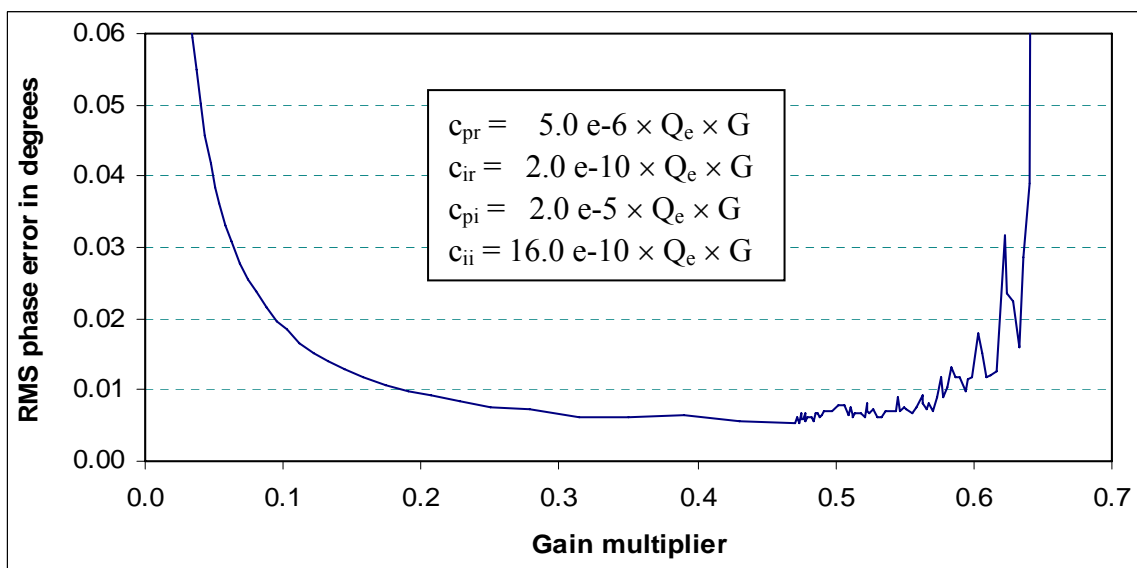
## 20. Gain Optimisation

Figure 35 shows the effect of winding up the gain when the overall delay is fixed at 3900 RF cycles and there are no measurement errors. In this figure a gain  $G = 0.5$  corresponds to the simulation presented in figures 29 - 34 hence the parameters given in the large table on figure 29 apply. Figure 35 shows that by reducing the gain with respect to the previous calculation by a factor of two gives an RMS error that is increased from 0.0036 degrees to 0.0072 degrees. An increase in the gain to 0.63 results in oscillations that degrade the phase. This point is the stability limit for the control algorithm.

Figure 36 shows the effect of including some measurement error. The measurement model used here supposes that the cavity only supports one mode and the output from the probe is taken through a low pass filter whose time constant has been taken equal to the time it takes for the controller to re-compute the required control.



**Figure 35** RMS phase error as a function of controller gain with an oscillating beam offset and microphonics but no measurement errors.  $Q_e = 3 \times 10^6$



**Figure 36** RMS phase error as a function of controller gain with an oscillating beam offset and microphonics and 0.005 degrees and 0.002 phase and amplitude measurement jitter respectively for a 1 MHz bandwidth.  $Q_e = 3 \times 10^6$

## 21. The Stability Limit

Later, figure 40 in section 22 illustrates how the stability limit on gain goes to infinity as the time delay in the control system goes to zero. Section 22.5 shows that the stability limit still exists in the absence of beamloading and microphonic disturbances. This means that the stability limit can be analysed from equations (10.2) with  $\omega = \omega_0$  which give

$$\left\{ 4 + \left( \frac{1}{Q_L} \right)^2 \right\} \frac{1}{\omega_0} \dot{A}_r + \frac{2}{Q_L} A_r + \left( \frac{1}{Q_L} \right)^2 A_i = \frac{2}{Q_e Q_L} \left( \frac{1}{\omega_0} \dot{\mathcal{F}}_r + \mathcal{F}_i \right) - \frac{4}{Q_e} \left( \frac{1}{\omega_0} \dot{\mathcal{F}}_i - \mathcal{F}_r \right) \quad (21.1a)$$

$$\left\{ 4 + \left( \frac{1}{Q_L} \right)^2 \right\} \frac{1}{\omega_0} \dot{A}_i + \frac{2}{Q_L} A_i - \left( \frac{1}{Q_L} \right)^2 A_r = \frac{2}{Q_e Q_L} \left( \frac{1}{\omega_0} \dot{\mathcal{F}}_i - \mathcal{F}_r \right) + \frac{4}{Q_e} \left( \frac{1}{\omega_0} \dot{\mathcal{F}}_r + \mathcal{F}_i \right) \quad (21.1b)$$

For typical accelerator cavities we can invariably neglect terms of order  $1/Q^2$ . The drive is also expected to be a slowly varying function with respect to the cavity frequency  $\omega_0$  hence the terms  $\dot{\mathcal{F}}/\omega_0$  can also be neglected. This means that for the stability analysis we consider the equations

$$\frac{1}{\omega_0} \dot{A}_r + \frac{1}{2Q_L} A_r = \frac{\mathcal{F}_r}{Q_e} \quad (21.2a)$$

$$\frac{1}{\omega_0} \dot{A}_i + \frac{1}{2Q_L} A_i = \frac{\mathcal{F}_i}{Q_e} \quad (21.2b)$$

where the force terms are delayed. As equations (21.2) are identical we need only consider one of them hence we will consider the first equation.

### 21.1 Analysis for Proportional Control

Formal methods for the determination of the stability limit of time-delay systems when the input is sampled and the output is updated in step changes are very complicated, they involve Z transforms and the solution of equations with infinite numbers of roots. Here we do not attempt such a complicated analysis. Firstly we make an estimate from the simple rule that positive feed back must be avoided for the system with periodic update. This estimate turns out to be in exact correspondence with the full model when the measurement filter is turned off, the amplifier has instantaneous response and the update interval equals the delay time (latency). Secondly we will make an estimate using Laplace transform methods assuming continuous update and hence should allow a larger delay for the same gain. In this section we confine ourselves to proportional control and in the next second we consider proportional integral control.

#### 21.1.1 Simple method

A minimum requirement for stability is that the error  $\varepsilon = A_r - V_{sp}$  does not change its sign in the time it takes before the force  $\dot{\mathcal{F}}$  finishes acting and gets updated, note that  $V_{sp}$  is the set point defined in (18.1). If the error did change sign before the force finishes acting, the next force to be applied will be the value at the start of the previous delay interval and will reinforce the error for the whole delay period plus the overshoot period. In this case the error grows rather than oscillating about zero as shown in figure 37.

Suppose initially the control system is off and there is an error  $\varepsilon = A_r - V_{sp}$ . At time  $t_0$  the control system is switched on and a force is applied that starts reducing the error to zero, see figure 37.

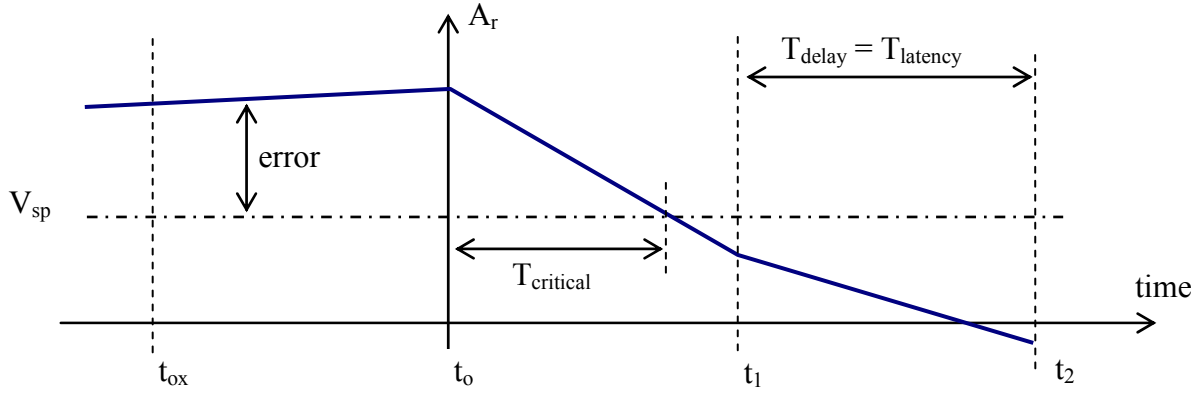


**Figure 37** Control delay timing

Define the time  $T_{critical}$  as the time it would take this force to bring the error to zero so that

$$T_{critical} = -\frac{A_r(t_0) - V_{sp}}{\dot{A}_r(t_0)} \quad (21.3)$$

For (21.2a) the minimum stability condition is therefore determined as

$$T_{latency} < -\frac{A_r(t_0) - V_{sp}}{\dot{A}_r(t_0)} \quad \text{for } A_r(t_0) - V_{sp} \neq 0 \quad (21.4)$$

which is the same as

$$-\frac{\dot{A}_r(t_0)}{A_r(t_0) - V_{sp}} < \frac{1}{T_{latency}} \quad \text{for } A_r(t_0) - V_{sp} \neq 0 \quad (21.5)$$

Equation (21.2a) re-arranges to give

$$\frac{\dot{A}_r}{A_r} = \frac{\omega_o}{Q_e} \left( \frac{\mathcal{F}_r}{A_r} - \frac{Q_e}{2Q_L} \right) \quad (21.6)$$

Substituting (21.6) in (21.5) to remove  $\dot{A}_r$  gives

$$-\frac{\omega_o}{Q_e} \left( \frac{\mathcal{F}_r}{A_r} - \frac{Q_e}{2Q_L} \right) \left( \frac{A_r}{A_r - V_{sp}} \right) < \frac{1}{T_{latency}}$$

where all values are evaluated at  $t_0$ . Hence

$$-\frac{\mathcal{F}_r}{A_r - V_{sp}} < \frac{Q_e}{\omega_o T_{latency}} - \frac{Q_e}{2Q_L} \frac{A_r}{A_r - V_{sp}} \quad (21.7)$$

For the case of proportional control i.e. when  $c_{ir} = 0$ , putting the force from (18.1) in equation (21.7) gives

$$\frac{c_{pr}}{Q_e} \left\{ \frac{A_r(t_0 - T_{delay}) - V_{sp}}{A_r(t_0) - V_{sp}} \right\} < \frac{1}{\omega_o T_{latency}} - \frac{A_r(t_0)}{2Q_L \{A_r(t_0) - V_{sp}\}} \quad (21.8)$$

From (21.2) and (18.1) the steady state error is determined from

$$\frac{A_r}{2Q_L} = \frac{c_{pr}(V_{sp} - A_r)}{Q_e} \quad (21.9)$$

which re-arranges to give  $\frac{c_{pr}}{Q_e} = \frac{A_r}{2Q_L(A_r - V_{sp})}$  providing an estimate of the third term in

(21.8). Using this estimate, the stability limit for proportional control becomes

$$\frac{c_{pr}}{Q_e} \left\{ 1 + \frac{A_r(t_o - T_{delay}) - V_{sp}}{A_r(t_o) - V_{sp}} \right\} < \frac{1}{\omega_o T_{latency}} \quad \text{for } A_r(t_o) - V_{sp} \neq 0 \quad (21.10)$$

From the diagram one can see that at the stability limit the field oscillates about the set point with a period of  $4T_{critical}$  and when

$$A_r(t_o) - V_{sp} \neq 0 \quad \text{then} \quad A_r(t_o - T_{delay}) - V_{sp} \approx 0 \quad (21.11)$$

hence (21.10) gives

$$\frac{c_{pr}}{Q_e} < \frac{1}{\omega_o T_{latency}} \quad (\text{for proportional control}) \quad (21.12)$$

For 3.9 GHz and a latency of 1  $\mu$ s then  $\frac{c_{pr}}{Q_e} < 4.08 \times 10^{-5}$

Formulae (21.12) can also be expressed in the more familiar format often given with reference to phase lock loops. Writing  $Q_e = \omega_o / \delta\omega$  where  $\delta\omega$  is the cavity bandwidth, equation (21.12) becomes

$$c_{pr} < \frac{1}{\text{bandwidth} \times T_{latency}} \quad (\text{for PI control}) \quad (21.13)$$

The stability limit for the ILC Tesla cavities and performance with adaptive feed-forward control algorithm has been recently discussed by Elmar Vogel [13].

### 21.1.2 Numerical result for periodic update

Figure 38 shows the numerical computation where only proportional control is used, the measurement filter is off and the amplifier has infinite bandwidth. The stability limit appears

at  $G = 2.04$  hence  $\frac{c_p}{Q_e} = 4.08 \times 10^{-5}$ .

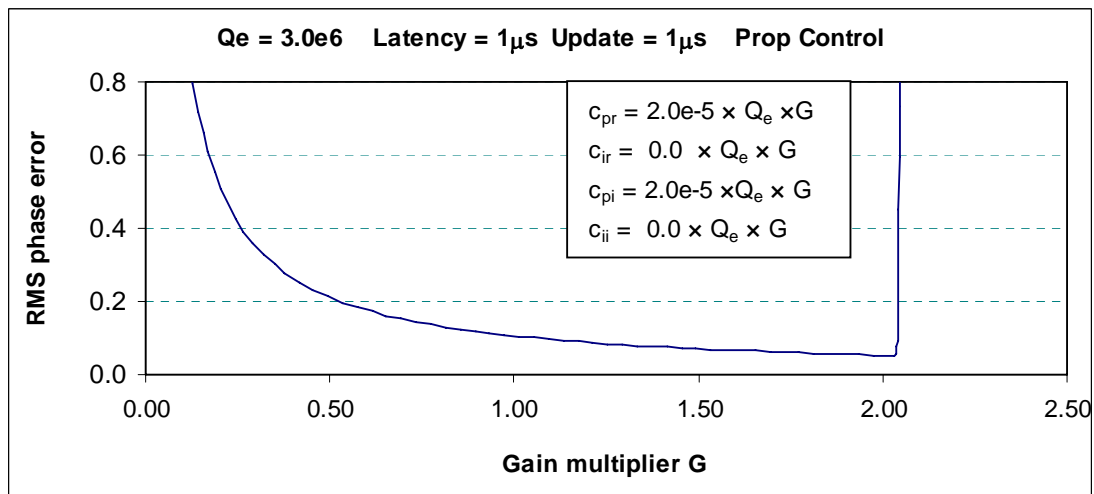


**Figure 38** Stability limit for proportional control only

### 21.1.3 Laplace transform method for proportional control

From the system equation (21.2) and the controller (18.1) with  $c_i = 0$

$$\frac{Q_e}{\omega_o} \dot{A}_r + \frac{Q_e}{2Q_L} A_r = -c_p \{ A_r(t - T_{\text{delay}}) - V_{\text{sp}} \} \quad (21.14)$$

The Laplace transform method gives the stability limit for this differential equation as written but takes no account of the periodic update associated with a digital control system, i.e. whilst the action is delayed a new force is determined at every instant from the delayed data. Taking the Laplace transform of (21.14) gives

$$\frac{Q_e}{\omega_o} s \tilde{A} + \frac{Q_e}{2Q_L} \tilde{A} = -c_p \tilde{A} e^{-sT_{\text{delay}}} + c_p \frac{V_{\text{sp}}}{s} \quad (21.15)$$

$$\text{Hence } \tilde{A} = \frac{\frac{c_p}{Q_e} \frac{V_{\text{sp}}}{s}}{\frac{s}{\omega_o} + \frac{1}{2Q_L} + \frac{c_p}{Q_e} e^{-sT_{\text{delay}}}} \quad (21.16)$$

For stability we require that the roots of the denominator lie in the left hand plane. Given that we already know that the equation moves from a region of stability to a region of instability as  $c_p$  is increased it is reasonable to assume that the point of instability is given by one of the roots of the denominator, i.e. of

$$\frac{s}{\omega_o} + \frac{1}{2Q_L} + \frac{c_p}{Q_e} e^{-sT_{\text{delay}}} = 0 \quad (21.17)$$

As the roots are complex roots it is convenient to set

$$s = \sigma + j\lambda \quad (21.18)$$

where  $\sigma$  and  $\lambda$  are real numbers. Putting (21.18) in (21.17) and setting real and imaginary parts to zero gives

$$\frac{\sigma}{\omega_o} + \frac{1}{2Q_L} + \frac{c_p}{Q_e} e^{-\sigma T_{\text{delay}}} \cos \lambda T_{\text{delay}} = 0 \quad (21.19)$$

$$\frac{\lambda}{\omega_o} - \frac{c_p}{Q_e} e^{-\sigma T_{\text{delay}}} \sin \lambda T_{\text{delay}} = 0 \quad (21.20)$$

It is convenient to eliminate the sine and cosine terms in (21.19) and (21.20), doing this gives

$$\left( \frac{\sigma}{\omega_o} + \frac{1}{2Q_L} \right)^2 + \left( \frac{\lambda}{\omega_o} \right)^2 = \left( \frac{c_p}{Q_e} \right)^2 e^{-2\sigma T_{\text{delay}}} \quad (21.21)$$

The roots move into the LHP when  $\sigma = 0$  hence from (21.21) the value of  $\lambda$  at the point of instability is given as

$$\lambda = \pm \omega_o \sqrt{\left( \frac{c_p}{Q_e} \right)^2 - \left( \frac{1}{2Q_L} \right)^2} \quad \text{when } \sigma = 0 \quad (21.22)$$

From (21.20)

$$T_{\text{delay}} = \frac{1}{\lambda} \sin^{-1} \left( \frac{\lambda Q_e}{\omega_o c_p} \right) + 2\pi n \quad \text{when } \sigma = 0 \quad (21.23)$$

or from (21.19)

$$T_{\text{delay}} = \frac{1}{\lambda} \cos^{-1} \left( \frac{Q_e}{2Q_L c_p} \right) + 2\pi n \quad \text{when } \sigma = 0 \quad (21.24)$$

and where  $n$  is a positive or negative integer. As expected there are an infinite number of solutions and each one represents a pole crossing the axis. Stability is for the smallest value of  $T_{\text{delay}}$  as this corresponds to the last pole crossing into the left hand plane.

The maximum proportional control coefficient is determined by solving (21.22) and (21.23) for  $c_p$  when  $n = 0$ .

From the approximate analysis we expect that the maximum  $\frac{c_{pr}}{Q_e} \approx 4.0 \times 10^{-5}$  which is much

bigger than  $\frac{1}{2Q_L} \approx 1.667 \times 10^{-7}$  for the planned cavity hence

$$\lambda \approx \pm \omega_o \frac{c_p}{Q_e} \quad \text{for last root with typical values} \quad (21.25)$$

$$\omega_o T_{\text{delay}} \approx \frac{Q_e}{c_p} \sin^{-1}(1) = \frac{\pi Q_e}{2 c_p} \quad (21.26)$$

$$\text{or } \frac{c_p}{Q_e} < \frac{\pi}{2\omega_o T_{\text{delay}}} \quad (\text{for proportional control}) \quad (21.27)$$

For 3.9 GHz and a latency of 1  $\mu\text{s}$  then  $\frac{c_{pr}}{Q_e} < 6.41 \times 10^{-5}$

which is a factor  $0.5\pi$  better than the value for periodic update after each latency period.

#### 21.1.4 Numerical result for proportional control with rapid update

Figure 39 shows the numerical computation where only proportional control is used and update is rapid. The stability limit appears at  $G = 3.19$  hence  $\frac{c_p}{Q_e} = 6.38 \times 10^{-5}$ .

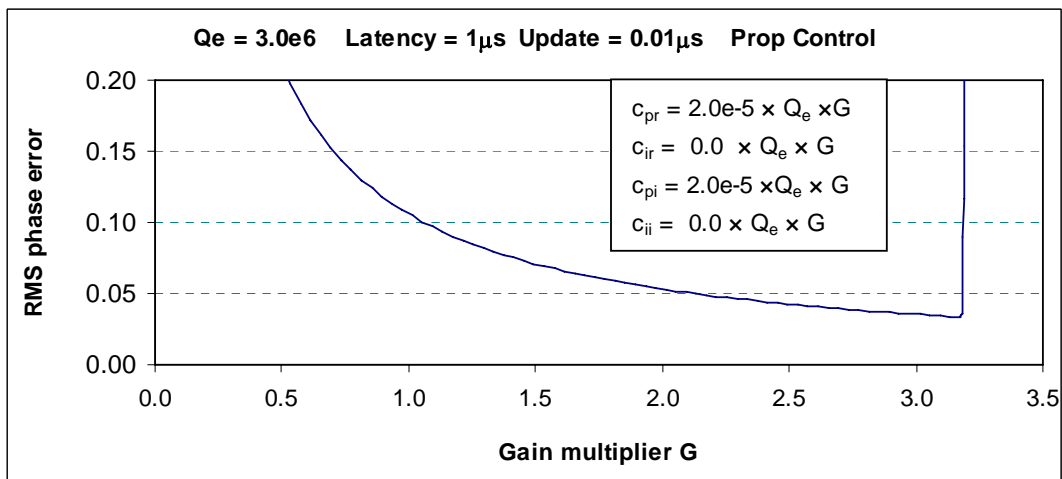


**Figure 38** Stability limit for proportional control only

## 21.2 Analysis for Proportional Integral Control

### 21.2.1 Laplace transform method for PI control

From the system equation (21.2) and the controller (18.1)

$$\frac{Q_e}{\omega_o} \dot{A}_r + \frac{Q_e}{2Q_L} A_r = -c_p \{ A_r(t - T_{\text{delay}}) - V_{\text{sp}} \} - c_i \frac{\omega}{2\pi} \int_{-\infty}^t \{ A_r(t' - T_{\text{delay}}) - V_{\text{sp}} \} dt' \quad (21.28)$$

Differentiation gives

$$\frac{Q_e}{\omega_o} \ddot{A}_r + \frac{Q_e}{2Q_L} \dot{A}_r = -c_p \dot{A}_r(t - T_{\text{delay}}) - c_i \left( \frac{\omega}{2\pi} \right) \{ A_r(t - T_{\text{delay}}) - V_{\text{sp}} \} \quad (21.29)$$

Laplace transform of (21.29) gives

$$\frac{Q_e}{\omega_o} s^2 \tilde{A} + \frac{Q_e}{2Q_L} s \tilde{A} = -(c_p s + c_i f) \tilde{A} e^{-sT_{\text{delay}}} + c_i f \frac{V_{\text{sp}}}{s} \quad (21.30)$$

where  $f = \frac{\omega}{2\pi}$  is the drive frequency, hence

$$\tilde{A} = \frac{c_i f \frac{V_{\text{sp}}}{s}}{\frac{Q_e}{\omega_o} s^2 + \frac{Q_e}{2Q_L} s + (c_p s + c_i f) e^{-sT_{\text{delay}}}} \quad (21.31)$$

For stability we require that the roots of the denominator lie in the left hand plane. Given that we already know that the equation moves from a region of stability to a region of instability as  $c_p$  and  $c_i$  are increased it is reasonable to assume that the point of instability is given by one of the roots of the denominator, i.e. of

$$\frac{s^2}{\omega_o} + \frac{s}{2Q_L} + \frac{(c_p s + c_i f)}{Q_e} e^{-sT_{\text{delay}}} = 0 \quad (21.32)$$

As the roots are complex roots it is convenient to set

$$s = \sigma + j\lambda \quad (21.33)$$

where  $\sigma$  and  $\lambda$  are real numbers. Putting (21.33) in (21.32) and setting real and imaginary parts to zero gives

$$\frac{\sigma^2 - \lambda^2}{\omega_o} + \frac{\sigma}{2Q_L} + \frac{(c_p \sigma + c_i f)}{Q_e} e^{-\sigma T_{\text{delay}}} \cos \lambda T_{\text{delay}} + \frac{c_p \lambda}{Q_e} e^{-\sigma T_{\text{delay}}} \sin \lambda T_{\text{delay}} = 0 \quad (21.34)$$

$$\frac{2\lambda \sigma}{\omega_o} + \frac{\lambda}{2Q_L} + \frac{c_p \lambda}{Q_e} e^{-\sigma T_{\text{delay}}} \cos \lambda T_{\text{delay}} - \frac{c_p \sigma + c_i f}{Q_e} e^{-\sigma T_{\text{delay}}} \sin \lambda T_{\text{delay}} = 0 \quad (21.35)$$

The roots move into the LHP when  $\sigma = 0$  hence from (21.34) and (21.35) the value of  $\lambda$  at the point of instability is determined from

$$\frac{-\lambda^2}{\omega_o} + \frac{c_i f}{Q_e} \cos \lambda T_{\text{delay}} + \frac{c_p \lambda}{Q_e} \sin \lambda T_{\text{delay}} = 0 \quad (21.36)$$

and

$$\frac{\lambda}{2Q_L} + \frac{c_p \lambda}{Q_e} \cos \lambda T_{\text{delay}} - \frac{c_i f}{Q_e} \sin \lambda T_{\text{delay}} = 0 \quad (21.37)$$

Eliminating  $\sin \lambda T_{\text{delay}} = 0$  between (21.36) and (21.37) gives

$$-\lambda^2 \left( \frac{1}{\omega_o} - \frac{c_p}{2Q_L c_i f} \right) + \frac{c_i f}{Q_e} \left( 1 + \lambda^2 \frac{c_p^2}{f^2 c_i^2} \right) \cos \lambda T_{\text{delay}} = 0 \quad (21.38)$$

Eliminating  $\cos \lambda T_{\text{delay}} = 0$  between (21.36) and (21.37) gives

$$-\left( \frac{\lambda^3 c_p}{\omega_o c_i f} + \frac{\lambda}{2Q_L} \right) + \frac{c_i f}{Q_e} \left( 1 + \lambda^2 \frac{c_p^2}{f^2 c_i^2} \right) \sin \lambda T_{\text{delay}} = 0 \quad (21.39)$$

Elimination of the cosine and sine terms in (21.38) and (21.39) gives

$$\lambda^4 \left( \frac{1}{\omega_o} - \frac{c_p}{2Q_L c_i f} \right)^2 + \lambda^2 \left( \frac{\lambda^2 c_p}{\omega_o c_i f} + \frac{1}{2Q_L} \right)^2 = \left( \frac{c_i f}{Q_e} \right)^2 \left( 1 + \lambda^2 \frac{c_p^2}{c_i^2 f^2} \right)^2$$

hence

$$\lambda^6 \left( \frac{c_p}{\omega_o c_i f} \right)^2 + \lambda^4 \left\{ \left( \frac{1}{\omega_o} + \frac{c_p}{2Q_L c_i f} \right)^2 - \frac{c_p}{\omega_o c_i f Q_L} - \left( \frac{c_p^4}{Q_e^2 c_i^2 f^2} \right) \right\} + \lambda^2 \left\{ \frac{1}{4Q_L^2} - \frac{2c_p^2}{Q_e^2} \right\} - \left( \frac{c_i f}{Q_e} \right)^2 = 0$$

which simplifies to

$$\lambda^6 \left( \frac{c_p}{\omega_o c_i f} \right)^2 + \lambda^4 \left\{ \left( \frac{1}{\omega_o} \right)^2 + \left( \frac{c_p}{2Q_L c_i f} \right)^2 - \left( \frac{c_p^4}{Q_e^2 c_i^2 f^2} \right) \right\} + \lambda^2 \left\{ \frac{1}{4Q_L^2} - \frac{2c_p^2}{Q_e^2} \right\} - \left( \frac{c_i f}{Q_e} \right)^2 = 0$$

or

$$\lambda^6 + \lambda^4 \left\{ \left( \frac{c_i f}{c_p} \right)^2 + \left( \frac{\omega_o}{2Q_L} \right)^2 - \left( \frac{\omega_o c_p}{Q_e} \right)^2 \right\} + \lambda^2 \left\{ \left( \frac{\omega_o c_i f}{2Q_L c_p} \right)^2 - 2 \left( \frac{\omega_o c_i f}{Q_e} \right)^2 \right\} - \left( \frac{\omega_o c_i^2 f^2}{Q_e c_p} \right)^2 = 0 \quad (21.40)$$

This cubic equation can be solved exactly though the analytic expression is long. For typical values the equation only has one real root for  $\lambda^2$ . Table 19.1 gives coefficients in (21.40) and the positive solution for  $\lambda$  for a typical choice of control parameters known to give good control.

f	$3.900 \times 10^9$
$\omega_o$	$24.50442 \times 10^9$
$Q_e$	$3.0 \times 10^6$
$Q_L$	$3.0 \times 10^6$
$c_p/Q_e$	$2.0 \times 10^{-5}$
$c_i f/Q_e$	6.240
$c_i f/c_p$	$3.120 \times 10^5$
$\omega_o/(2Q_L)$	$4.084 \times 10^3$
$\omega_o c_p/Q_e$	$4.901 \times 10^5$
$\omega_o c_i f/(2Q_L c_p)$	$2.548 \times 10^4$
$\omega_o c_i f/Q_e$	$1.529 \times 10^{11}$
$\omega_o c_i^2 f^2/(Q_e c_p)$	$4.771 \times 10^{16}$
$\lambda$	$7.074 \times 10^5$

Table 19.1 Parameters for (21.40) known to give good control

It is apparent from the table that all the terms in (21.40) except one have similar magnitudes hence one does not expect a simple approximate formula for its solution.

Once  $\lambda$  has been computed for specific control parameters one can then use (21.38) to determine  $T_{\text{delay}}$ . Re-arranging (21.38) gives

$$T_{\text{delay}} = \frac{1}{\lambda} \cos^{-1} \left\{ \frac{\lambda^2 Q_e}{\omega_o c_i f} \left( \frac{1 - \frac{\omega_o c_p f}{2Q_L c_i}}{1 + \lambda^2 \frac{c_p^2}{c_i^2 f^2}} \right) \right\} \quad (21.41)$$

Putting values from the table above gives

$$T_{\text{delay}} = \frac{1}{7.074 \times 10^5} \cos^{-1} \left\{ 3.273 \left( \frac{1 - 0.013}{1 + 5.141} \right) \right\} = 1.438 \times 10^{-6} \text{ s}$$

Figure 38 gives results for repeated calculations to determine delay times for four values of the proportional control term and for a range of values for the integral term until the stability limit is reached. For this calculation  $Q_e = Q_L = 3 \times 10^6$ .

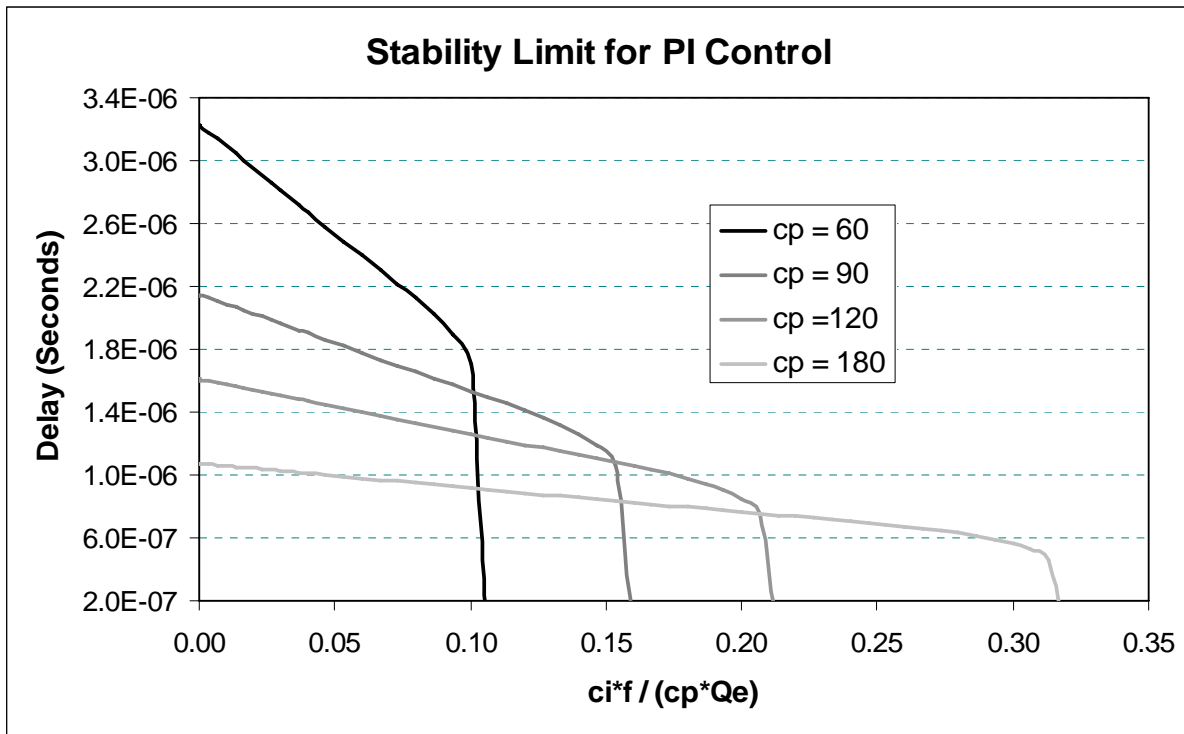


**Figure 39** Stability limit for proportional integral control with rapid update

The intercept on the y axis is determined from (21.27) i.e.

$$T_{\text{delay}}(c_i = 0) = \frac{Q_e}{4f c_p}$$

Since the gradient of the curves in figure 39 are constant to the point where the maximum permissible delay suddenly drops they can be approximated by a simple empirical formula which works out to be

$$T_{\text{delay}} = \frac{Q_e}{4f c_p} \left( 1 - 250 \frac{c_i f}{c_p^2 Q_e} \right) \quad (21.42)$$

and where the drop comes when

$$\frac{c_i f}{c_p^2 Q_e} = \frac{1}{500} \quad (21.43)$$

Equation (21.43) can be expressed as

$$\text{Max} \left( \frac{c_i}{c_p} \right) = \frac{c_p Q_e}{500 f} \quad (21.44)$$

### 21.2.2 Formula and numerical analysis for periodic update with PI control

For periodic update as opposed to regular update and from the analysis for proportional control one expects the delay time to be reduced by a factor  $2/\pi$ . For periodic update with interval  $T_{\text{delay}}$  one expects from (21.42) that the delay time is given as

$$T_{\text{delay}} = \frac{Q_e}{\omega_0 c_p} \left( 1 - 250 \frac{c_i f}{c_p^2 Q_e} \right) \quad (\text{periodic update}) \quad (21.45)$$

Putting typical numbers into (21.44) for the ILC crab cavity and computing the delay we get

$$\begin{aligned} \text{frequency} &= 3.9 \times 10^9 \\ Q_e &= 3.0 \times 10^6 \\ c_p &= 37.5 \\ c_i &= 0.003 \\ T_{\text{delay}} &= 1.0012 \times 10^{-6} \end{aligned}$$

Figure 39 shows the computation for this case where PI control is used, the stability limit appears at  $G = 0.625$  hence at the point of instability  $c_{pr} = 37.5$  and  $c_{ir} = 0.003$ . Remarkably this is just about exact. The remark to be made is that there is almost certainly a Z transform analysis similar to the Laplace transform analysis that yields the extra factor of  $2/\pi$ .

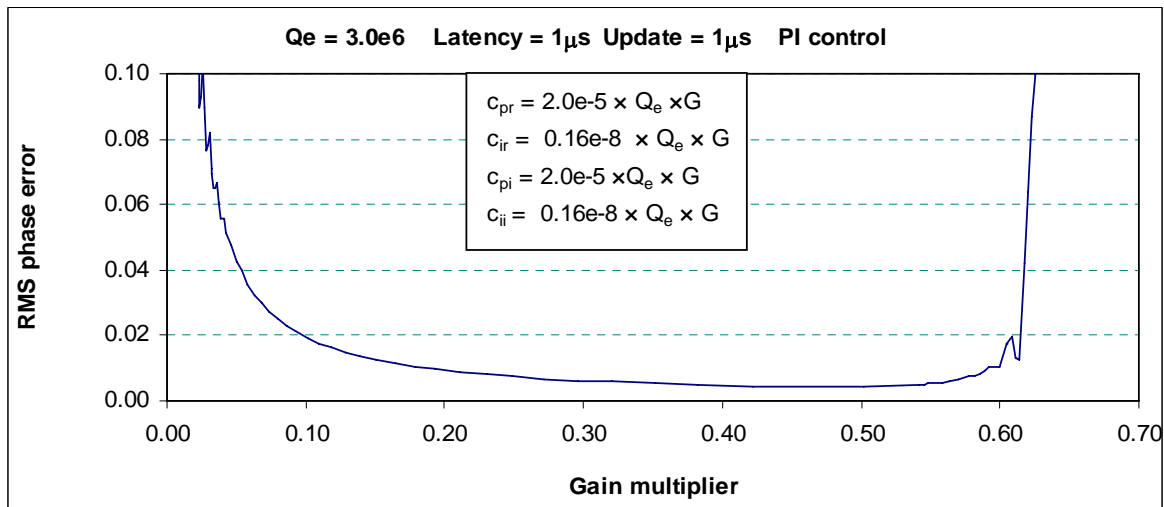


**Figure 39** Calculated stability limit for proportional integral control with periodic update

### 21.2.3 Attempted approximate analysis for PI control

It is of interest to see if this formula can be derived in a simple way. For the case of PI control the condition for stability derived from (21.7) becomes

$$\frac{c_{pr}(A_r(t_o - T_{delay}) - V_{sp}) + c_{ir} \int_{-\infty}^t dt (A_r(t - T_{delay}) - V_{sp})}{Q_e(A_r(t_o) - V_{sp})} < \frac{1}{\omega_o T_{latency}} - \frac{A_r(t_o)}{2Q_L \{A_r(t_o) - V_{sp}\}} \quad (21.46)$$

For a PI controller the steady state error can be zero as the integral provides whatever steady force is necessary to maintain the set point. In steady state we have  $\varepsilon = A_r - V_{sp} = 0$  and  $\dot{A}_r = 0$ , hence from (21.2a) and (18.1) we have the steady state value of the integral determined as

$$\frac{A_r}{2Q_L} = -\frac{c_{ir}}{Q_e} \int_{-\infty}^t dt (A_r(t - T_{delay}) - V_{sp}) \quad (\text{Steady state constraint}) \quad (21.47)$$

Putting (21.47) in (21.46) gives

$$\frac{c_{pr}(A_r(t_o - T_{delay}) - V_{sp}) - \frac{Q_e}{2Q_L} A_r(t_o)}{Q_e(A_r(t_o) - V_{sp})} < \frac{1}{\omega_o T_{latency}} - \frac{A_r(t_o)}{2Q_L \{A_r(t_o) - V_{sp}\}} \quad (21.48)$$

Cancelling terms gives

$$\frac{c_{pr}(A_r(t_o - T_{delay}) - V_{sp})}{Q_e(A_r(t_o) - V_{sp})} < \frac{1}{\omega_o T_{delay}} \quad (21.49)$$

Comparison with (21.45) for update at the delay frequency suggests that

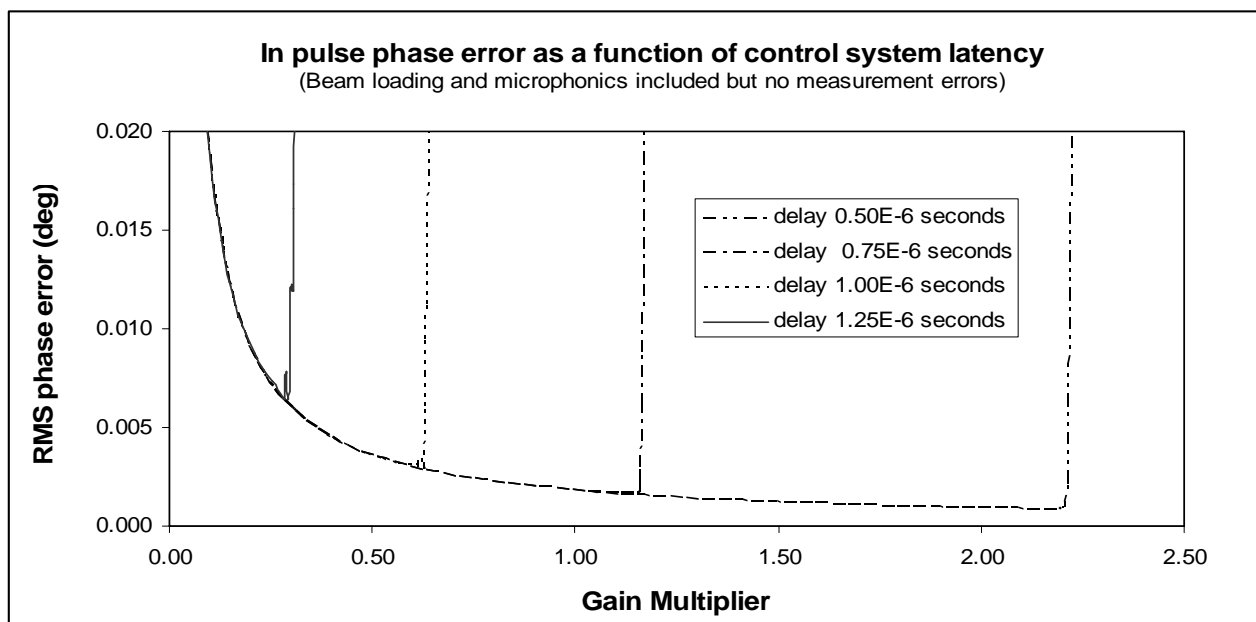
$$\frac{(A_r(t_o) - V_{sp})}{(A_r(t_o - T_{delay}) - V_{sp})} = 1 - \frac{250 c_i f}{c_p^2 Q_L} \quad (21.50)$$

As yet we do not have a simple argument to get this formula.

## 22. Ultimate Phase Performance for the Single Mode Cavity

One expects the ultimate phase stabilisation performance of the cavity to depend on a number of factors. These include control system delay (latency), cavity Q factor, measurement error and the level and rate of change of disturbance from beamloading and microphonics. The analysis in this section and section 23 which use parameters consistent with available digital technology will eventually show that the most significant constraint on phase control is likely to be measurement accuracy. The accuracy to which one can determine the phase and amplitude of the operating mode can be seriously limited by the presence of modes with frequencies close to the operating mode and which are simultaneously detected by the output couplers. This multi-mode case will be considered in section 23.

In this section the effect of the latency, Q factor, disturbance and measurement error on control phase performance is studied for the single mode cavity. The ILC requirement for phase stability of an individual crab cavity is nominally better than 0.05 degrees. Figure 40 shows how RMS phase error depends on control system time delay. Here the control update is set to match the delay, i.e. a measurement is requested, the value is returned to the controller, the controller computes and applies a new phase and amplitude correction for the drive and the update is made at end of the delay period associated with measurement and control. Parameters used for figure 40 are the same as those used in section 19.4 see figure 29.



Drive frequency in GHz	=	3.900 GHz	Bunch charge (ILC=3.2 nC)	=	3.200 nC
Centre cavity frequency in GHz	=	3.900 GHz	RF cycles between bunches	=	1200
Cavity Q factor	=	1.0000E+09	Bunch train length	=	1.000 ms
External Q factor	=	3.0000E+06	Cavity frequency shift from microphonics	=	600.000 Hz
Cavity R over Q (2xFNAL=53 per cell)	=	53.000 ohms	Cavity vibration frequency	=	230.000 Hz
Energy point ILC crab~0.0284J per cell)	=	28.400 mJ	Initial vibration phase (degrees)	=	20.000 deg
Amplitude set point	=	301.675 kV	Phase measurement error(degrees)	=	0.00000 deg
Maximum Amplifier Power per cell	=	1200.000 W	Fractional err in amplitude measurement	=	0.00000
Maximum voltage set point (no beam)	=	1235.476 kV	Time delay (latency) for control system	=	see figure 38
Maximum beam offset	=	1.000 mm	Control update interval	=	time delay
Maximum bunch phase error	=	1.000 deg	Initial gain constant for controller	=	0.0020
Beam offset frequency	=	2000.000 Hz	Amplifier bandwidth	=	1.0000E+07

**Figure 40** In pulse RMS phase error as a function of control system latency for cavity and beam parameters as defined in list and where the update is made after the given time delay.

It is seen straight away from figure 40 that latency is a major constraint on the maximum gain. The curve has a knee such that phase performance deteriorates very quickly when the

latency rises above  $1.25 \mu\text{s}$ . The curves in figure 40 were produced for an external  $Q$  of  $3.0 \times 10^6$ . When minimal power consumption is not the key issue one has some flexibility in the choice of external  $Q$ . It is therefore of interest to investigate whether phase performance can be enhanced by changing the external  $Q$ . In sections 19.1 and 19.2 it was seen for a specific case that similar control performance is obtained by increasing gain in proportion to  $Q_e$  as  $Q_e$  is increased. As ultimate performance depends on the gain at the stability limit it is of interest to see how the stability limit depends on  $Q_e$ . The results of section 22.1 show this dependency. The three figures are for  $Q$  externals of  $0.3 \times 10^6$ ,  $1 \times 10^6$  and  $3 \times 10^6$ . The phase performance is plotted against gain multiplier. The actual gain is obtained as the gain multiplier times the external  $Q$ , times some fixed coefficients used for all cases as illustrated in the inset box of figures 35 and 36. The control coefficients given in the tables under each figure are the values where RMS phase error is minimised. Where there is no measurement error the RMS phase error is minimised at the stability limit. The three plots of section 22.1 are almost identical. This means that the stability limit is a function of the ratio of the gain to the external  $Q$  and that choosing a different external  $Q$  does not necessarily allow an improved phase control performance. Note that the third figure of section 22.1 was given as one of the curves in figure 40.

Section 22.2 repeats the calculations of 22.1 with phase and amplitude measurement errors. Again the three curves are almost identical indicating that the scaling law with  $Q_e$  and gain still applies. With measurement errors the minimum phase error no longer occurs at the stability limit.

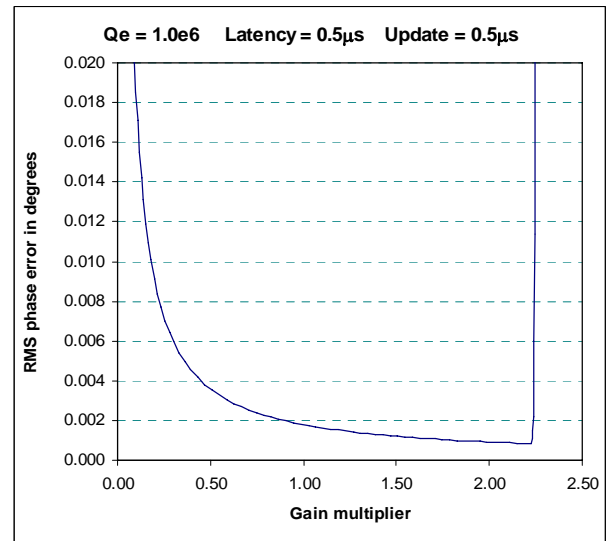
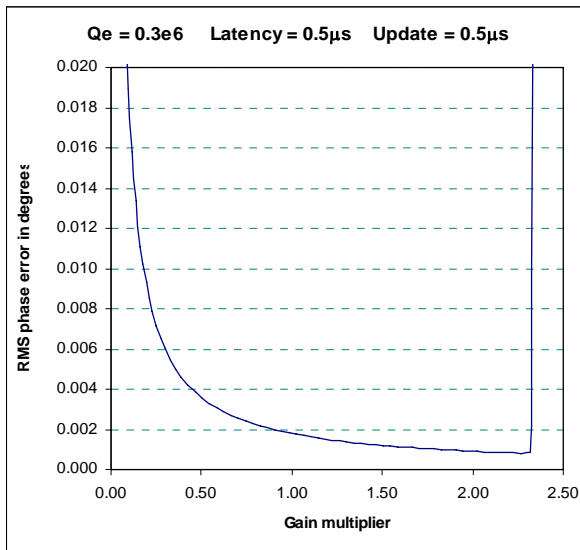
Section 22.3 repeats the calculations of 22.1 with an increased latency. The third figure has already been shown in figure 38. The fourth figure in this section has beamloading switched off. As the figure is almost identical to the third figure with beamloading included one might guess that phase errors are driven by microphonics rather than beamloading. Section 22.4 follows this up by switching off microphonics but including beamloading. According phase control is greatly enhanced. Section 22.5 turns off beamloading and microphonics. In the absence of disturbance, phase control is perfect up to the stability limit.

Section 22.6 repeats the calculations of 22.2 with an increased latency.

Section 22.7 shows that phase control performance is improved if the frequency of the disturbance is reduced.

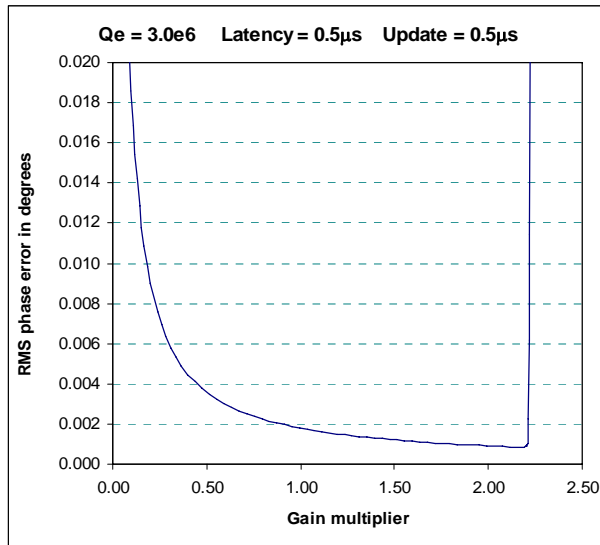
Section 22.8 again considers phase control performance as a function  $Q_e$  as in section 22.2 and 22.6 but with further increased latency going below the knee in figure 38. In this case one loses the result of phase control performance being independent of  $Q_e$  when gain is increased in proportion to the  $Q_e$ .

Section 22.9 goes to an even higher latency but allows update to be more frequent than the latency. This might be achieved by using parallel processors with staggered operation.

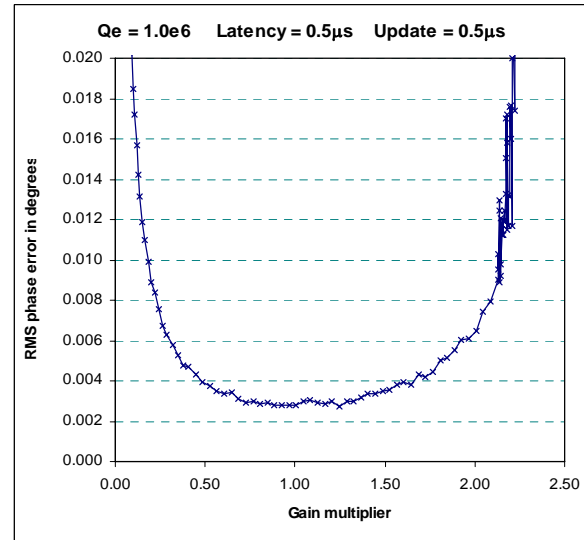
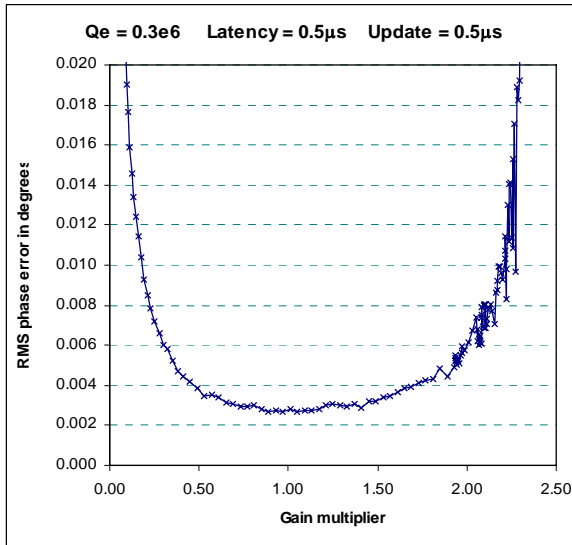
22.1 No measurement error, Latency = 0.5  $\mu$ s, Update = 0.5  $\mu$ s, vary Q

Drive frequency in GHz	=	3.900 GHz
Centre cavity frequency in GHz	=	3.900 GHz
Cavity Q factor	=	1.0000E+09
External Q factor	=	0.3000E+06
Cavity R over Q (2xFNAL=53 per cell)	=	53.000 ohms
Energy point ILC crab-0.0284J per cell)	=	28.400 mJ
Amplitude set point	=	301.675 kV
Maximum Amplifier Power per cell	=	1200.000 W
Maximum voltage set point (no beam)	=	390.692 kV
Maximum beam offset	=	1.000 mm
Maximum bunch phase error	=	1.000 deg
Beam offset frequency	=	2000.000 Hz
Bunch charge (ILC=3.2 nC)	=	3.200 nC
RF cycles between bunches	=	1200
Bunch train length	=	1.000 ms
Cavity frequency shift from microphonics	=	600.000 Hz
Cavity vibration frequency	=	23.000 Hz
Initial vibration phase (degrees)	=	20.000 deg
Phase measurement error(degrees)	=	0.00000 deg
Fractional err in amplitude measurement	=	0.00000
Time delay (latency) for control system	=	0.5000E-06 s
Control update interval	=	0.5000E-06 s
Amplifier bandwidth	=	1.0000E+07
Optimal gain constant for controller	=	2.2643
Minimum rms phase error	=	0.00082
Maximum power delivered	=	822.8670
Proportional coef for real component	=	3.3965E+00
Integral coef for real component	=	1.3586E-04
Proportional coef for imag component	=	1.3586E+01
Integral coef for imag component	=	1.0869E-03

Drive frequency in GHz	=	3.900 GHz
Centre cavity frequency in GHz	=	3.900 GHz
Cavity Q factor	=	1.0000E+09
External Q factor	=	1.0000E+06
Cavity R over Q (2xFNAL=53 per cell)	=	53.000 ohms
Energy point ILC crab-0.0284J per cell)	=	28.400 mJ
Amplitude set point	=	301.675 kV
Maximum Amplifier Power per cell	=	1200.000 W
Maximum voltage set point (no beam)	=	713.302 kV
Maximum beam offset	=	1.000 mm
Maximum bunch phase error	=	1.000 deg
Beam offset frequency	=	2000.000 Hz
Bunch charge (ILC=3.2 nC)	=	3.200 nC
RF cycles between bunches	=	1200
Bunch train length	=	1.000 ms
Cavity frequency shift from microphonics	=	600.000 Hz
Cavity vibration frequency	=	230.000 Hz
Initial vibration phase (degrees)	=	20.000 deg
Phase measurement error(degrees)	=	0.00000 deg
Fractional err in amplitude measurement	=	0.00000
Time delay (latency) for control system	=	0.5000E-06 s
Control update interval	=	0.5000E-06 s
Initial gain constant for controller	=	0.0020
Amplifier bandwidth	=	1.0000E+07
Minimum rms phase error	=	0.00085
Maximum power delivered	=	335.6143
Proportional coef for real component	=	1.0938E+01
Integral coef for real component	=	4.3750E-04
Proportional coef for imag component	=	4.3750E+01
Integral coef for imag component	=	3.5000E-03

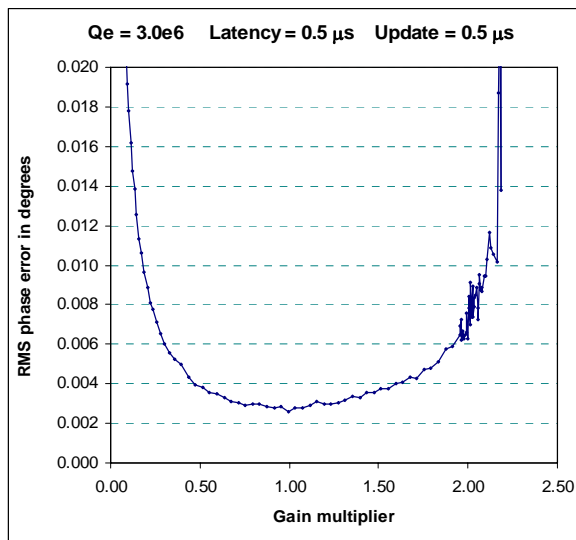


Drive frequency in GHz = 3.900 GHz  
 Centre cavity frequency in GHz = 3.900 GHz  
 Cavity Q factor = 1.0000E+09  
 External Q factor = 3.0000E+06  
 Cavity R over Q (2xFNAL=53 per cell) = 53.000 ohms  
 Energy point ILC crab-0.0284J per cell= 28.400 mJ  
 Amplitude set point = 301.675 kV  
 Maximum Amplifier Power per cell = 1200.000 W  
 Maximum voltage set point (no beam) = 1235.476 kV  
 Maximum beam offset = 1.000 mm  
 Maximum bunch phase error = 1.000 deg  
 Beam offset frequency = 2000.000 Hz  
 Bunch charge (ILC=3.2 nC) = 3.200 nC  
 RF cycles between bunches = 1200  
 Bunch train length = 1.000 ms  
 Cavity frequency shift from microphonics= 600.000 Hz  
 Cavity vibration frequency = 230.000 Hz  
 Initial vibration phase (degrees) = 20.000 deg  
 Phase measurement error(degrees) = 0.00000 deg  
 Fractional err in amplitude measurement = 0.00000  
 Time delay (latency) for control system = 5.0000E-07 s  
 Control update interval = 5.0000E-07 s  
 Amplifier bandwidth = 1.0000E+07  
 Optimal gain constant for controller = 2.1539  
 Minimum rms phase error = 0.00086  
 Maximum power delivered = 231.3614  
 Proportional coef for real component = 3.2309E+01  
 Integral coef for real component = 1.2924E-03  
 Proportional coef for imag component = 1.2924E+02  
 Integral coef for imag component = 1.0339E-02

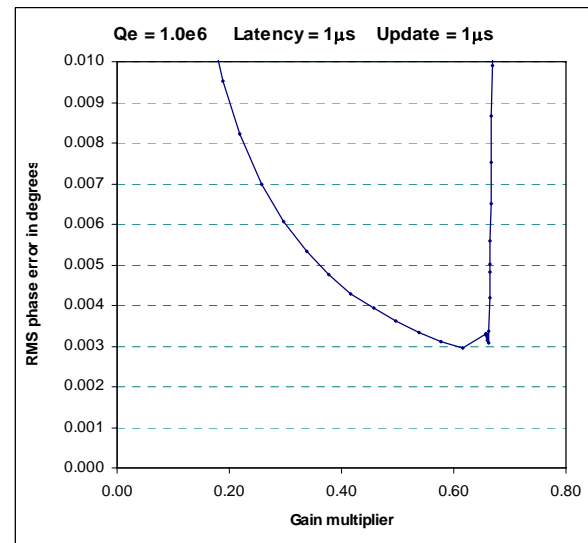
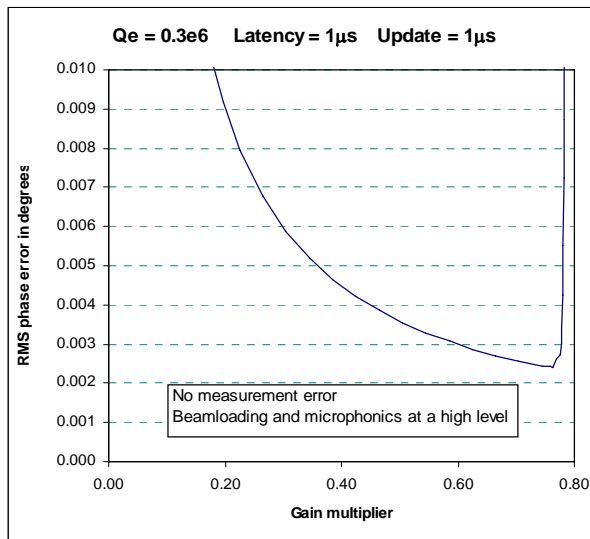
22.2 Measurement error = 0.005 degrees, Latency = 0.5  $\mu$ s, Update = 0.5  $\mu$ s, vary Q

Drive frequency in GHz	=	3.900 GHz
Centre cavity frequency in GHz	=	3.900 GHz
Cavity Q factor	=	1.0000E+09
External Q factor	=	0.3000E+06
Cavity R over Q (2xFNAL=53 per cell)	=	53.000 ohms
Energy point ILC crab-0.0284J per cell)	=	28.400 mJ
Amplitude set point	=	301.675 kV
Maximum Amplifier Power per cell	=	1200.000 W
Maximum voltage set point (no beam)	=	390.692 kV
Maximum beam offset	=	1.000 mm
Maximum bunch phase error	=	1.000 deg
Beam offset frequency	=	2000.000 Hz
Bunch charge (ILC=3.2 nC)	=	3.200 nC
RF cycles between bunches	=	1200
Bunch train length	=	1.000 ms
Cavity frequency shift from microphonics	=	600.000 Hz
Cavity vibration frequency	=	230.000 Hz
Initial vibration phase (degrees)	=	20.000 deg
Phase measurement error(degrees)	=	0.00500 deg
Fractional err in amplitude measurement	=	0.00200
Time delay (latency) for control system	=	2.0000E-06 s
Control update interval	=	1.0000E-06 s
Amplifier bandwidth	=	1.0000E+07
Optimal gain constant for controller	=	0.8897
Minimum rms phase error	=	0.00271
Maximum power delivered	=	832.3693
Proportional coef for real component	=	1.3345E+00
Integral coef for real component	=	5.3380E-05
Proportional coef for imag component	=	5.3380E+00
Integral coef for imag component	=	4.2704E-04

Drive frequency in GHz	=	3.900 GHz
Centre cavity frequency in GHz	=	3.900 GHz
Cavity Q factor	=	1.0000E+09
External Q factor	=	1.0000E+06
Cavity R over Q (2xFNAL=53 per cell)	=	53.000 ohms
Energy point ILC crab-0.0284J per cell)	=	28.400 mJ
Amplitude set point	=	301.675 kV
Maximum Amplifier Power per cell	=	1200.000 W
Maximum voltage set point (no beam)	=	713.302 kV
Maximum beam offset	=	1.000 mm
Maximum bunch phase error	=	1.000 deg
Beam offset frequency	=	2000.000 Hz
Bunch charge (ILC=3.2 nC)	=	3.200 nC
RF cycles between bunches	=	1200
Bunch train length	=	1.000 ms
Cavity frequency shift from microphonics	=	600.000 Hz
Cavity vibration frequency	=	230.000 Hz
Initial vibration phase (degrees)	=	20.000 deg
Phase measurement error(degrees)	=	0.00500 deg
Fractional err in amplitude measurement	=	0.00200
Time delay (latency) for control system	=	0.5000E-06 s
Control update interval	=	0.5000E-06 s
Amplifier bandwidth	=	1.0000E+07
Optimal gain constant for controller	=	1.2461
Minimum rms phase error	=	0.00317
Maximum power delivered	=	350.8633
Proportional coef for real component	=	6.2305E+00
Integral coef for real component	=	2.4922E-04
Proportional coef for imag component	=	2.4922E+01
Integral coef for imag component	=	1.9938E-03

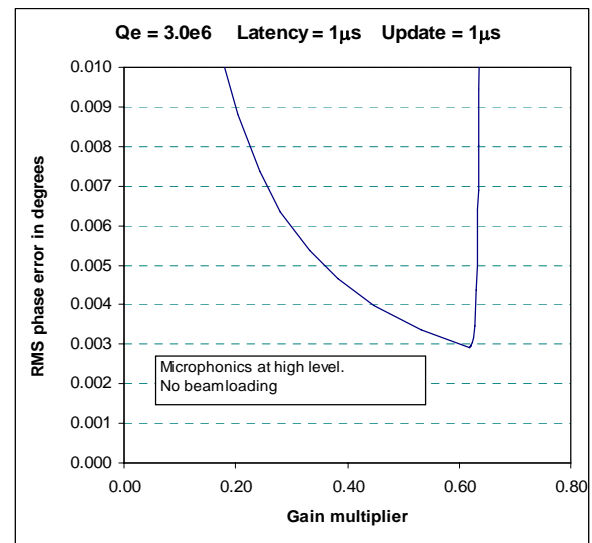
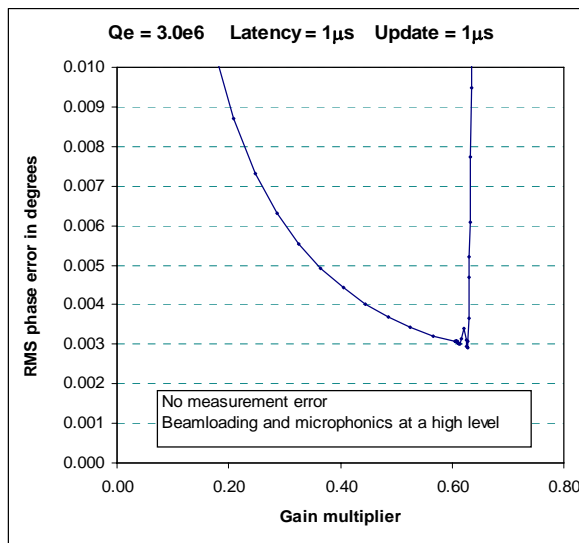


Drive frequency in GHz	=	3.900 GHz
Centre cavity frequency in GHz	=	3.900 GHz
Cavity Q factor	=	1.0000E+09
External Q factor	=	3.0000E+06
Cavity R over Q (2xFNAL=53 per cell)	=	53.000 ohms
Energy point ILC crab-0.0284J per cell)	=	28.400 mJ
Amplitude set point	=	301.675 kV
Maximum Amplifier Power per cell	=	1200.000 W
Maximum voltage set point (no beam)	=	1235.476 kV
Maximum beam offset	=	1.000 mm
Maximum bunch phase error	=	1.000 deg
Beam offset frequency	=	2000.000 Hz
Bunch charge (ILC=3.2 nC)	=	3.200 nC
RF cycles between bunches	=	1200
Bunch train length	=	1.000 ms
Cavity frequency shift from microphonics	=	600.000 Hz
Cavity vibration frequency	=	23.000 Hz
Initial vibration phase (degrees)	=	20.000 deg
Phase measurement error(degrees)	=	0.00500 deg
Fractional err in amplitude measurement	=	0.00200
Time delay (latency) for control system	=	0.5000E-06 s
Control update interval	=	0.5000E-06 s
Amplifier bandwidth	=	1.0000E+07
Optimal gain constant for controller	=	0.9942
Minimum rms phase error	=	0.00297
Maximum power delivered	=	248.0229
Proportional coef for real component	=	1.4913E+01
Integral coef for real component	=	5.9654E-04
Proportional coef for imag component	=	5.9654E+01
Integral coef for imag component	=	4.7723E-03

22.3 No measurement error, Latency = 1  $\mu$ s, Update = 1  $\mu$ s, vary Q

Drive frequency in GHz	=	3.900 GHz
Centre cavity frequency in GHz	=	3.900 GHz
Cavity Q factor	=	1.0000E+09
External Q factor	=	0.3000E+06
Cavity R over Q (2xFNAL=53 per cell)	=	53.000 ohms
Energy point ILC crab~0.0284J per cell)	=	28.400 mJ
Amplitude set point	=	301.675 kV
Maximum Amplifier Power per cell	=	1200.000 W
Maximum voltage set point (no beam)	=	390.692 kV
Maximum beam offset	=	1.000 mm
Maximum bunch phase error	=	1.000 deg
Beam offset frequency	=	2000.000 Hz
Bunch charge (ILC=3.2 nC)	=	3.200 nC
RF cycles between bunches	=	1200
Bunch train length	=	1.000 ms
Cavity frequency shift from microphonics	=	600.000 Hz
Cavity vibration frequency	=	23.000 Hz
Initial vibration phase (degrees)	=	20.000 deg
Phase measurement error(degrees)	=	0.00000 deg
Fractional err in amplitude measurement	=	0.00000
Time delay (latency) for control system	=	2.0000E-06 s
Control update interval	=	1.0000E-06 s
Amplifier bandwidth	=	1.0000E+07
Optimal gain constant for controller	=	0.7633
Minimum rms phase error	=	0.00242
Maximum power delivered	=	823.2286
Proportional coef for real component	=	1.1450E+00
Integral coef for real component	=	4.5800E-05
Proportional coef for imag component	=	4.5800E+00
Integral coef for imag component	=	3.6640E-04

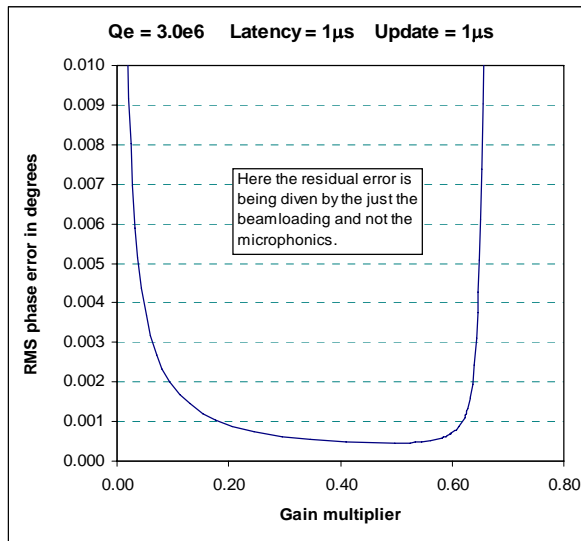
Drive frequency in GHz	=	3.900 GHz
Centre cavity frequency in GHz	=	3.900 GHz
Cavity Q factor	=	1.0000E+09
External Q factor	=	1.0000E+06
Cavity R over Q (2xFNAL=53 per cell)	=	53.000 ohms
Energy point ILC crab~0.0284J per cell)	=	28.400 mJ
Amplitude set point	=	301.675 kV
Maximum Amplifier Power per cell	=	1200.000 W
Maximum voltage set point (no beam)	=	713.302 kV
Maximum beam offset	=	1.000 mm
Maximum bunch phase error	=	1.000 deg
Beam offset frequency	=	2000.000 Hz
Bunch charge (ILC=3.2 nC)	=	3.200 nC
RF cycles between bunches	=	1200
Bunch train length	=	1.000 ms
Cavity frequency shift from microphonics	=	600.000 Hz
Cavity vibration frequency	=	23.000 Hz
Initial vibration phase (degrees)	=	20.000 deg
Phase measurement error(degrees)	=	0.00000 deg
Fractional err in amplitude measurement	=	0.00000
Time delay (latency) for control system	=	1.0000E-06 s
Control update interval	=	1.0000E-06 s
Amplifier bandwidth	=	1.0000E+07
Optimal gain constant for controller	=	0.6169
Minimum rms phase error	=	0.00295
Maximum power delivered	=	336.5188
Proportional coef for real component	=	3.0843E+00
Integral coef for real component	=	1.2337E-04
Proportional coef for imag component	=	1.2337E+01
Integral coef for imag component	=	9.8697E-04



Drive frequency in GHz	=	3.900 GHz
Centre cavity frequency in GHz	=	3.900 GHz
Cavity Q factor	=	1.0000E+09
External Q factor	=	3.0000E+06
Cavity R over Q (2xFNAL=53 per cell)	=	53.000 ohms
Energy point ILC crab-0.0284J per cell)	=	28.400 mJ
Amplitude set point	=	301.675 kV
Maximum Amplifier Power per cell	=	1200.000 W
Maximum voltage set point (no beam)	=	1235.476 kV
Maximum beam offset	=	1.000 mm
Maximum bunch phase error	=	1.000 deg
Beam offset frequency	=	2000.000 Hz
Bunch charge (ILC=3.2 nC)	=	3.200 nC
RF cycles between bunches	=	1200
Bunch train length	=	1.000 ms
Cavity frequency shift from microphonics	=	600.000 Hz
Cavity vibration frequency	=	23.000 Hz
Initial vibration phase (degrees)	=	20.000 deg
Phase measurement error(degrees)	=	0.00000 deg
Fractional err in amplitude measurement	=	0.00000
Time delay (latency) for control system	=	1.0000E-06 s
Control update interval	=	1.0000E-06 s
Initial gain constant for controller	=	0.0020
Amplifier bandwidth	=	1.0000E+07
Optimal gain constant for controller	=	0.6274
Minimum rms phase error	=	0.00291
Maximum power delivered	=	232.6412
Proportional coef for real component	=	9.4114E+00
Integral coef for real component	=	3.7646E-04
Proportional coef for imag component	=	3.7646E+01
Integral coef for imag component	=	3.0117E-03

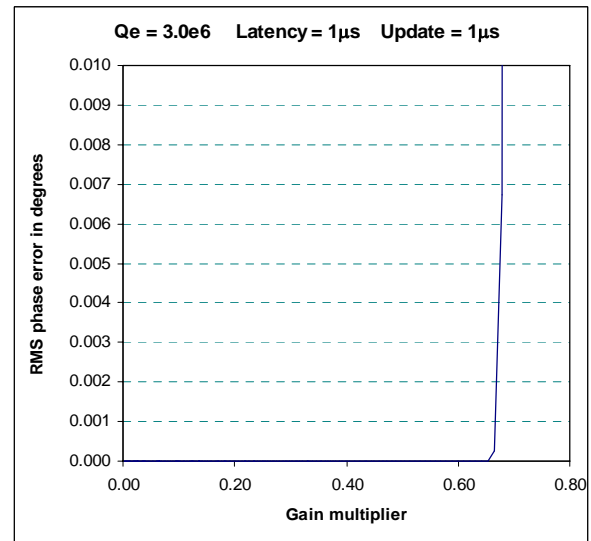
Drive frequency in GHz	=	3.900 GHz
Centre cavity frequency in GHz	=	3.900 GHz
Cavity Q factor	=	1.0000E+09
External Q factor	=	3.0000E+06
Cavity R over Q (2xFNAL=53 per cell)	=	53.000 ohms
Energy point ILC crab-0.0284J per cell)	=	28.400 mJ
Amplitude set point	=	301.675 kV
Maximum Amplifier Power per cell	=	1200.000 W
Maximum voltage set point (no beam)	=	1235.476 kV
Maximum beam offset	=	0.0 mm
Maximum bunch phase error	=	0.0 deg
Beam offset frequency	=	2000.000 Hz
Bunch charge (ILC=3.2 nC)	=	3.200 nC
RF cycles between bunches	=	1200
Bunch train length	=	1.000 ms
Cavity frequency shift from microphonics	=	600.000 Hz
Cavity vibration frequency	=	230.000 Hz
Initial vibration phase (degrees)	=	20.000 deg
Phase measurement error(degrees)	=	0.00000 deg
Fractional err in amplitude measurement	=	0.00000
Time delay (latency) for control system	=	1.0000E-06 s
Control update interval	=	1.0000E-06 s
Initial gain constant for controller	=	0.0020
Amplifier bandwidth	=	1.0000E+07
Optimal gain constant for controller	=	0.6181
Minimum rms phase error	=	0.00292
Maximum power delivered	=	121.8580
Proportional coef for real component	=	9.2721E+00
Integral coef for real component	=	3.7089E-04
Proportional coef for imag component	=	3.7089E+01
Integral coef for imag component	=	2.9671E-03

## 22.4 No microphonics

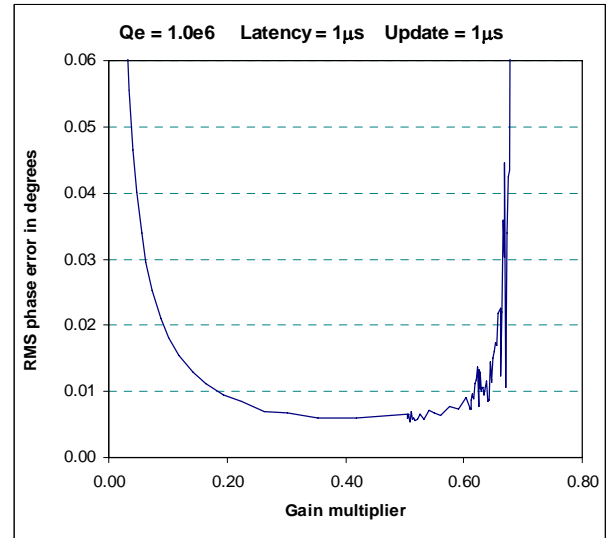
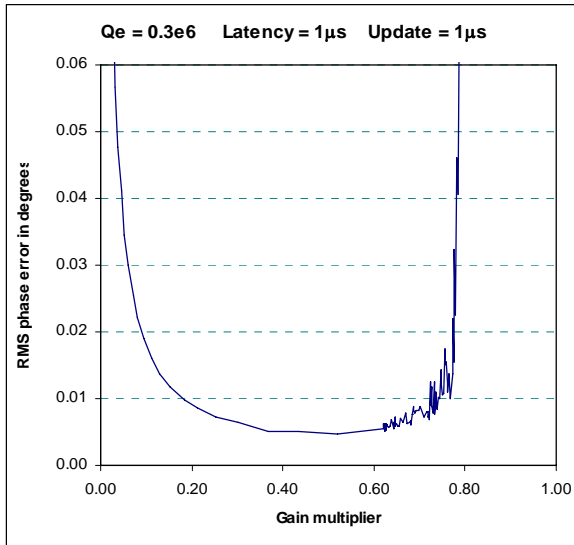


Drive frequency in GHz	=	3.900 GHz
Centre cavity frequency in GHz	=	3.900 GHz
Cavity Q factor	=	1.0000E+09
External Q factor	=	3.0000E+06
Cavity R over Q (2xFNAL=53 per cell)	=	53.000 ohms
Energy point ILC crab-0.0284J per cell)	=	28.400 mJ
Amplitude set point	=	301.675 kV
Maximum Amplifier Power per cell	=	1200.000 W
Maximum voltage set point (no beam)	=	1235.476 kV
Maximum beam offset	=	1.000 mm
Maximum bunch phase error	=	1.000 deg
Beam offset frequency	=	2000.000 Hz
Bunch charge (ILC=3.2 nC)	=	3.200 nC
RF cycles between bunches	=	1200
Bunch train length	=	1.000 ms
Cavity frequency shift from microphonics	=	0.000 Hz
Cavity vibration frequency	=	230.000 Hz
Initial vibration phase (degrees)	=	20.000 deg
Phase measurement error(degrees)	=	0.00000 deg
Fractional err in amplitude measurement	=	0.00000
Time delay (latency) for control system	=	1.0000E-06 s
Control update interval	=	1.0000E-06 s
Amplifier bandwidth	=	1.0000E+07
Optimal gain constant for controller	=	0.4965
Minimum rms phase error	=	0.00045
Maximum power delivered	=	211.2583
Proportional coef for real component	=	7.4479E+00
Integral coef for real component	=	2.9792E-04
Proportional coef for imag component	=	2.9792E+01
Integral coef for imag component	=	2.3833E-03

## 22.5 No beam, no microphonics

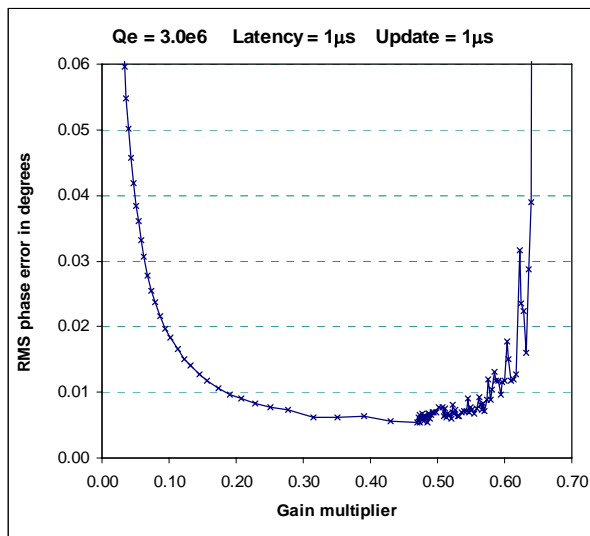


Drive frequency in GHz	=	3.900 GHz
Centre cavity frequency in GHz	=	3.900 GHz
Cavity Q factor	=	1.0000E+09
External Q factor	=	3.0000E+06
Cavity R over Q (2xFNAL=53 per cell)	=	53.000 ohms
Energy point ILC crab-0.0284J per cell)	=	28.400 mJ
Amplitude set point	=	301.675 kV
Maximum Amplifier Power per cell	=	1200.000 W
Maximum voltage set point (no beam)	=	1235.476 kV
Maximum beam offset	=	0.000 mm
Maximum bunch phase error	=	0.000 deg
Beam offset frequency	=	2000.000 Hz
Bunch charge (ILC=3.2 nC)	=	3.200 nC
RF cycles between bunches	=	1200
Bunch train length	=	1.000 ms
Cavity frequency shift from microphonics	=	0.000 Hz
Cavity vibration frequency	=	230.000 Hz
Initial vibration phase (degrees)	=	20.000 deg
Phase measurement error(degrees)	=	0.00000 deg
Fractional err in amplitude measurement	=	0.00000
Time delay (latency) for control system	=	1.0000E-06 s
Control update interval	=	1.0000E-06 s
Amplifier bandwidth	=	1.0000E+07
Optimal gain constant for controller	=	0.3929
Minimum rms phase error	=	0.00000
Maximum power delivered	=	71.9769
Proportional coef for real component	=	5.8929E+00
Integral coef for real component	=	2.3571E-04
Proportional coef for imag component	=	2.3571E+01
Integral coef for imag component	=	1.8857E-03

22.6 Measurement error = 0.005 degrees, Latency = 1  $\mu$ s, Update = 1  $\mu$ s, vary Q

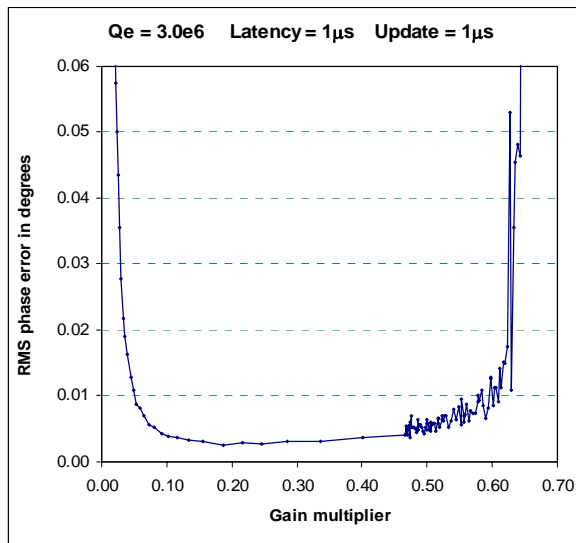
Drive frequency in GHz	=	3.900 GHz
Centre cavity frequency in GHz	=	3.900 GHz
Cavity Q factor	=	1.0000E+09
External Q factor	=	0.3000E+06
Cavity R over Q (2xFNAL=53 per cell)	=	53.000 ohms
Energy point ILC crab-0.0284J per cell)	=	28.400 mJ
Amplitude set point	=	301.675 kV
Maximum Amplifier Power per cell	=	1200.000 W
Maximum voltage set point (no beam)	=	390.692 kV
Maximum beam offset	=	1.000 mm
Maximum bunch phase error	=	1.000 deg
Beam offset frequency	=	2000.000 Hz
Bunch charge (ILC=3.2 nC)	=	3.200 nC
RF cycles between bunches	=	1200
Bunch train length	=	1.000 ms
Cavity frequency shift from microphonics	=	600.000 Hz
Cavity vibration frequency	=	230.000 Hz
Initial vibration phase (degrees)	=	20.000 deg
Phase measurement error(degrees)	=	0.00500 deg
Fractional err in amplitude measurement	=	0.00200
Time delay (latency) for control system	=	2.0000E-06 s
Control update interval	=	1.0000E-06 s
Amplifier bandwidth	=	1.0000E+07
Optimal gain constant for controller	=	0.5195
Minimum rms phase error	=	0.00547
Maximum power delivered	=	828.5186
Proportional coef for real component	=	7.7925E-01
Integral coef for real component	=	3.1170E-05
Proportional coef for imag component	=	3.1170E+00
Integral coef for imag component	=	2.4936E-04

Drive frequency in GHz	=	3.900 GHz
Centre cavity frequency in GHz	=	3.900 GHz
Cavity Q factor	=	1.0000E+09
External Q factor	=	1.0000E+06
Cavity R over Q (2xFNAL=53 per cell)	=	53.000 ohms
Energy point ILC crab-0.0284J per cell)	=	28.400 mJ
Amplitude set point	=	301.675 kV
Maximum Amplifier Power per cell	=	1200.000 W
Maximum voltage set point (no beam)	=	713.302 kV
Maximum beam offset	=	1.000 mm
Maximum bunch phase error	=	1.000 deg
Beam offset frequency	=	2000.000 Hz
Bunch charge (ILC=3.2 nC)	=	3.200 nC
RF cycles between bunches	=	1200
Bunch train length	=	1.000 ms
Cavity frequency shift from microphonics	=	600.000 Hz
Cavity vibration frequency	=	230.000 Hz
Initial vibration phase (degrees)	=	20.000 deg
Phase measurement error(degrees)	=	0.00500 deg
Fractional err in amplitude measurement	=	0.00200
Time delay (latency) for control system	=	1.0000E-06 s
Control update interval	=	1.0000E-06 s
Amplifier bandwidth	=	1.0000E+07
Optimal gain constant for controller	=	0.5089
Minimum rms phase error	=	0.00569
Maximum power delivered	=	343.8641
Proportional coef for real component	=	2.5447E+00
Integral coef for real component	=	1.0179E-04
Proportional coef for imag component	=	1.0179E+01
Integral coef for imag component	=	8.1429E-04



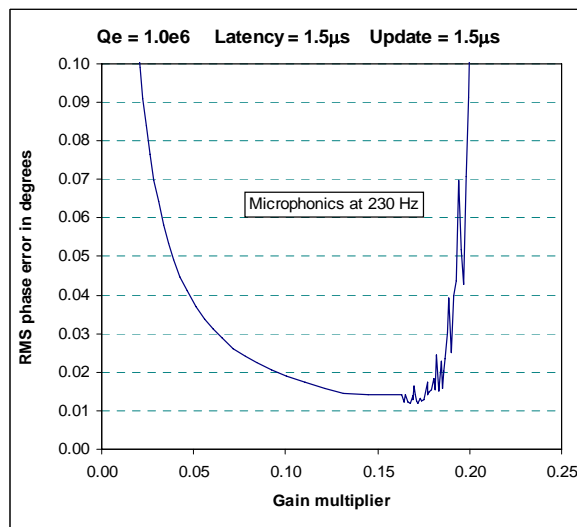
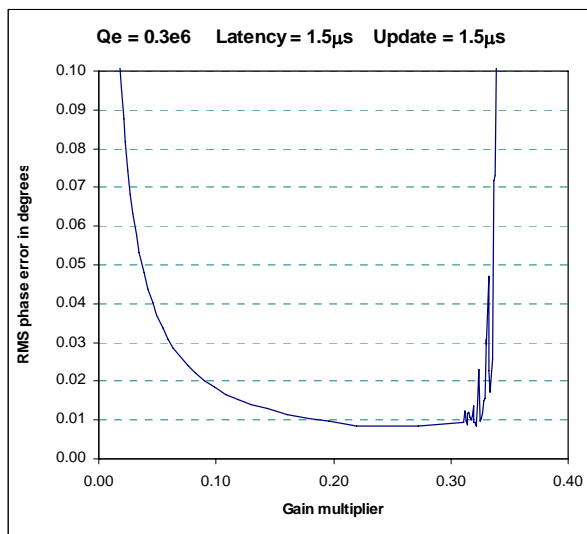
Drive frequency in GHz	=	3.900 GHz
Centre cavity frequency in GHz	=	3.900 GHz
Cavity Q factor	=	1.0000E+09
External Q factor	=	3.0000E+06
Cavity R over Q (2xFNAL=53 per cell)	=	53.000 ohms
Energy point ILC crab-0.0284J per cell)	=	28.400 mJ
Amplitude set point	=	301.675 kV
Maximum Amplifier Power per cell	=	1200.000 W
Maximum voltage set point (no beam)	=	713.302 kV
Maximum beam offset	=	1.000 mm
Maximum bunch phase error	=	1.000 deg
Beam offset frequency	=	2000.000 Hz
Bunch charge (ILC=3.2 nC)	=	3.200 nC
RF cycles between bunches	=	1200
Bunch train length	=	1.000 ms
Cavity frequency shift from microphonics	=	600.000 Hz
Cavity vibration frequency	=	230.000 Hz
Initial vibration phase (degrees)	=	20.000 deg
Phase measurement error(degrees)	=	0.00500 deg
Fractional err in amplitude measurement	=	0.00200
Time delay (latency) for control system	=	1.0000E-06 s
Control update interval	=	1.0000E-06 s
Amplifier bandwidth	=	1.0000E+07
Optimal gain constant for controller	=	0.4707
Minimum rms phase error	=	0.00625
Maximum power delivered	=	238.9978
Proportional coef for real component	=	7.0600E+00
Integral coef for real component	=	2.8240E-04
Proportional coef for imag component	=	2.8240E+01
Integral coef for imag component	=	2.2592E-03

## 22.7 Reduce Microphonic frequency from 230 Hz to 23 Hz



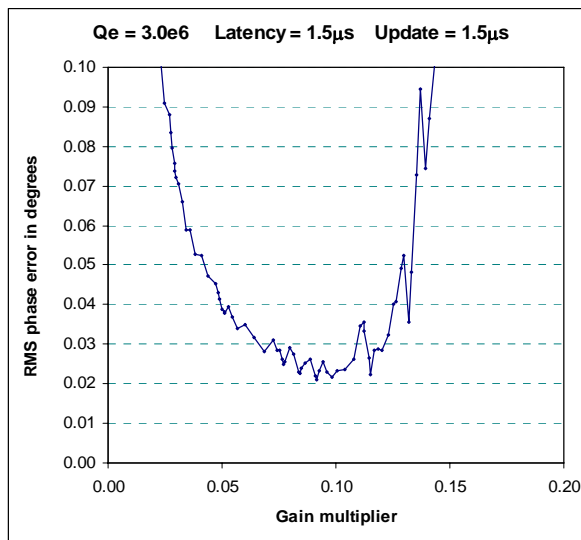
Drive frequency in GHz	=	3.900 GHz
Centre cavity frequency in GHz	=	3.900 GHz
Cavity Q factor	=	1.0000E+09
External Q factor	=	3.0000E+06
Cavity R over Q (2xFNAL=53 per cell)	=	53.000 ohms
Energy point ILC crab-0.0284J per cell)	=	28.400 mJ
Amplitude set point	=	301.675 kV
Maximum Amplifier Power per cell	=	1200.000 W
Maximum voltage set point (no beam)	=	1235.476 kV
Maximum beam offset	=	1.000 mm
Maximum bunch phase error	=	1.000 deg
Beam offset frequency	=	2000.000 Hz
Bunch charge (ILC=3.2 nC)	=	3.200 nC
RF cycles between bunches	=	1200
Bunch train length	=	1.000 ms
Cavity frequency shift from microphonics	=	600.000 Hz
Cavity vibration frequency	=	23.000 Hz
Initial vibration phase (degrees)	=	20.000 deg
Phase measurement error(degrees)	=	0.00500 deg
Fractional err in amplitude measurement	=	0.00200
Time delay (latency) for control system	=	1.0000E-06 s
Control update interval	=	1.0000E-06 s
Amplifier bandwidth	=	1.0000E+07
Optimal gain constant for controller	=	0.1862
Minimum rms phase error	=	0.00280
Maximum power delivered	=	242.5511
Proportional coef for real component	=	2.7924E+00
Integral coef for real component	=	1.1170E-04
Proportional coef for imag component	=	1.1170E+01
Integral coef for imag component	=	8.9357E-04

22.8 Measurement error = 0.005 degrees, Latency = 1.5 μs, Update = 1.5 μs, vary Q

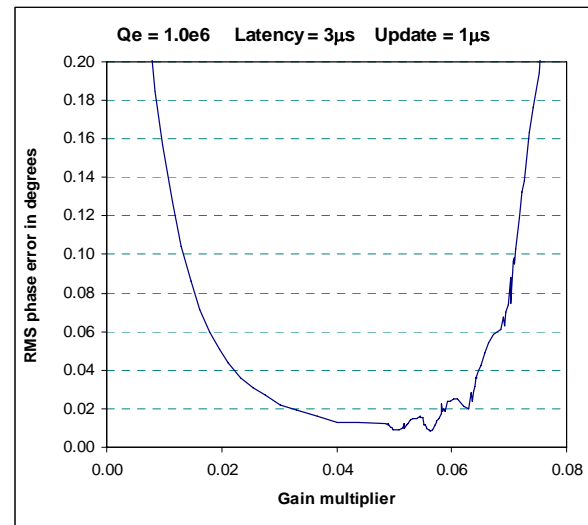
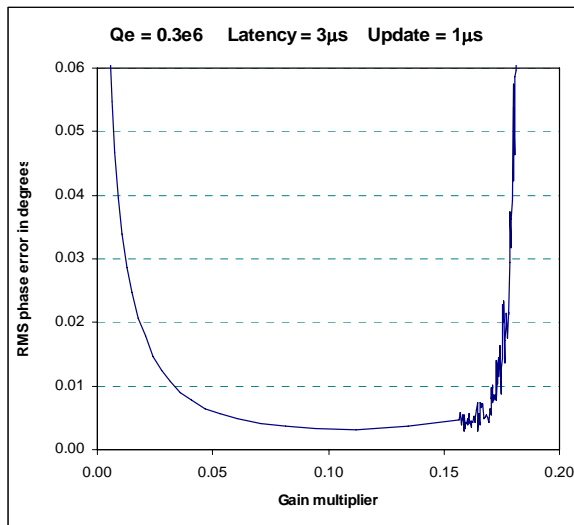


Drive frequency in GHz = 3.900 GHz  
 Centre cavity frequency in GHz = 3.900 GHz  
 Cavity Q factor = 1.0000E+09  
 External Q factor = 0.3000E+06  
 Cavity R over Q (2xFNAL=53 per cell) = 53.000 ohms  
 Energy point ILC crab-0.0284J per cell) = 28.400 mJ  
 Amplitude set point = 301.675 kV  
 Maximum Amplifier Power per cell = 1200.000 W  
 Maximum voltage set point (no beam) = 390.692 kV  
 Maximum beam offset = 1.000 mm  
 Maximum bunch phase error = 1.000 deg  
 Beam offset frequency = 2000.000 Hz  
 Bunch charge (ILC=3.2 nC) = 3.200 nC  
 RF cycles between bunches = 1200  
 Bunch train length = 1.000 ms  
 Cavity frequency shift from microphonics= 600.000 Hz  
 Cavity vibration frequency = 23.000 Hz  
 Initial vibration phase (degrees) = 20.000 deg  
 Phase measurement error(degrees) = 0.00500 deg  
 Fractional err in amplitude measurement = 0.00200  
 Time delay (latency) for control system = 1.5000E-06 s  
 Control update interval = 1.5000E-06 s  
 Amplifier bandwidth = 1.0000E+07  
 Optimal gain constant for controller = 0.2523  
 Minimum rms phase error = 0.00788  
 Maximum power delivered = 827.3736  
 Proportional coef for real component = 3.7852E-01  
 Integral coef for real component = 1.5141E-05  
 Proportional coef for imag component = 1.5141E+00  
 Integral coef for imag component = 1.2112E-04

Drive frequency in GHz = 3.900 GHz  
 Centre cavity frequency in GHz = 3.900 GHz  
 Cavity Q factor = 1.0000E+09  
 External Q factor = 1.0000E+06  
 Cavity R over Q (2xFNAL=53 per cell) = 53.000 ohms  
 Energy point ILC crab-0.0284J per cell) = 28.400 mJ  
 Amplitude set point = 301.675 kV  
 Maximum Amplifier Power per cell = 1200.000 W  
 Maximum voltage set point (no beam) = 713.302 kV  
 Maximum beam offset = 1.000 mm  
 Maximum bunch phase error = 1.000 deg  
 Beam offset frequency = 2000.000 Hz  
 Bunch charge (ILC=3.2 nC) = 3.200 nC  
 RF cycles between bunches = 1200  
 Bunch train length = 1.000 ms  
 Cavity frequency shift from microphonics= 600.000 Hz  
 Cavity vibration frequency = 23.000 Hz  
 Initial vibration phase (degrees) = 20.000 deg  
 Phase measurement error(degrees) = 0.00500 deg  
 Fractional err in amplitude measurement = 0.00200  
 Time delay (latency) for control system = 1.5000E-06 s  
 Control update interval = 1.0500E-06 s  
 Amplifier bandwidth = 1.0000E+07  
 Optimal gain constant for controller = 0.1525  
 Minimum rms phase error = 0.00408  
 Maximum power delivered = 343.4789  
 Proportional coef for real component = 7.6246E-01  
 Integral coef for real component = 3.0499E-05  
 Proportional coef for imag component = 3.0499E+00  
 Integral coef for imag component = 2.4399E-04

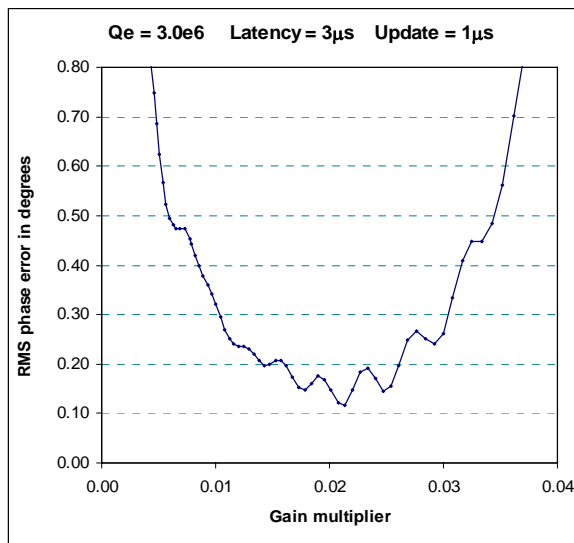


Drive frequency in GHz	=	3.900 GHz
Centre cavity frequency in GHz	=	3.900 GHz
Cavity Q factor	=	1.0000E+09
External Q factor	=	3.0000E+06
Cavity R over Q (2xFNAL=53 per cell)	=	53.000 ohms
Energy point ILC crab-0.0284J per cell)	=	28.400 mJ
Amplitude set point	=	301.675 kV
Maximum Amplifier Power per cell	=	1200.000 W
Maximum voltage set point (no beam)	=	1235.476 kV
Maximum beam offset	=	1.000 mm
Maximum bunch phase error	=	1.000 deg
Beam offset frequency	=	2000.000 Hz
Bunch charge (ILC=3.2 nC)	=	3.200 nC
RF cycles between bunches	=	1200
Bunch train length	=	1.000 ms
Cavity frequency shift from microphonics	=	600.000 Hz
Cavity vibration frequency	=	23.000 Hz
Initial vibration phase (degrees)	=	20.000 deg
Phase measurement error(degrees)	=	0.00500 deg
Fractional err in amplitude measurement	=	0.00200
Time delay (latency) for control system	=	1.5000E-06 s
Control update interval	=	1.5000E-06 s
Amplifier bandwidth	=	1.0000E+07
Optimal gain constant for controller	=	0.1242
Minimum rms phase error	=	0.02200
Maximum power delivered	=	241.4754
Proportional coef for real component	=	1.8627E+00
Integral coef for real component	=	7.4510E-05
Proportional coef for imag component	=	7.4510E+00
Integral coef for imag component	=	5.9608E-04

22.9 Measurement error = 0.005 degrees, Latency = 3.0  $\mu$ s, Update = 1.0  $\mu$ s, vary Q

Drive frequency in GHz	=	3.900 GHz
Centre cavity frequency in GHz	=	3.900 GHz
Cavity Q factor	=	1.0000E+09
External Q factor	=	0.3000E+06
Cavity R over Q (2xFNAL=53 per cell)	=	53.000 ohms
Energy point ILC crab-0.0284J per cell)	=	28.400 mJ
Amplitude set point	=	301.675 kV
Maximum Amplifier Power per cell	=	1200.000 W
Maximum voltage set point (no beam)	=	390.692 kV
Maximum beam offset	=	1.000 mm
Maximum bunch phase error	=	1.000 deg
Beam offset frequency	=	2000.000 Hz
Bunch charge (ILC=3.2 nC)	=	3.200 nC
RF cycles between bunches	=	1200
Bunch train length	=	1.000 ms
Cavity frequency shift from microphonics	=	600.000 Hz
Cavity vibration frequency	=	23.000 Hz
Initial vibration phase (degrees)	=	20.000 deg
Phase measurement error(degrees)	=	0.00500 deg
Fractional err in amplitude measurement	=	0.00200
Time delay (latency) for control system	=	3.0000E-06 s
Control update interval	=	1.0000E-06 s
Amplifier bandwidth	=	1.0000E+07
Optimal gain constant for controller	=	0.1648
Minimum rms phase error	=	0.00446
Maximum power delivered	=	827.3696
Proportional coef for real component	=	2.4719E-01
Integral coef for real component	=	9.8876E-06
Proportional coef for imag component	=	9.8876E-01
Integral coef for imag component	=	7.9101E-05

Drive frequency in GHz	=	3.900 GHz
Centre cavity frequency in GHz	=	3.900 GHz
Cavity Q factor	=	1.0000E+09
External Q factor	=	1.0000E+06
Cavity R over Q (2xFNAL=53 per cell)	=	53.000 ohms
Energy point ILC crab-0.0284J per cell)	=	28.400 mJ
Amplitude set point	=	301.675 kV
Maximum Amplifier Power per cell	=	1200.000 W
Maximum voltage set point (no beam)	=	713.302 kV
Maximum beam offset	=	1.000 mm
Maximum bunch phase error	=	1.000 deg
Beam offset frequency	=	2000.000 Hz
Bunch charge (ILC=3.2 nC)	=	3.200 nC
RF cycles between bunches	=	1200
Bunch train length	=	1.000 ms
Cavity frequency shift from microphonics	=	600.000 Hz
Cavity vibration frequency	=	23.000 Hz
Initial vibration phase (degrees)	=	20.000 deg
Phase measurement error(degrees)	=	0.00500 deg
Fractional err in amplitude measurement	=	0.00200
Time delay (latency) for control system	=	3.0000E-06 s
Control update interval	=	1.0000E-06 s
Amplifier bandwidth	=	1.0000E+07
Optimal gain constant for controller	=	0.0563
Minimum rms phase error	=	0.00703
Maximum power delivered	=	354.8504
Proportional coef for real component	=	2.8150E-01
Integral coef for real component	=	1.1260E-05
Proportional coef for imag component	=	1.1260E+00
Integral coef for imag component	=	9.0079E-05



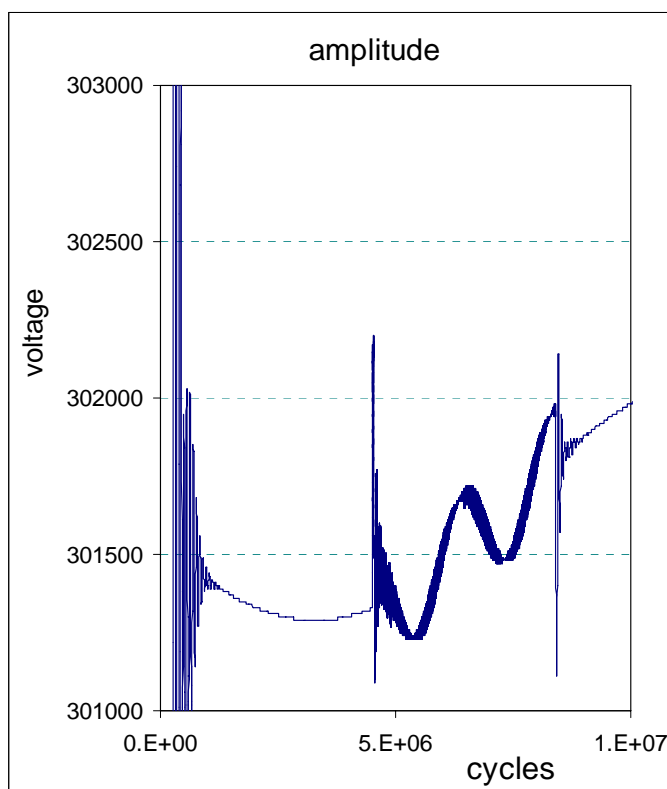
Drive frequency in GHz	=	3.900 GHz
Centre cavity frequency in GHz	=	3.900 GHz
Cavity Q factor	=	1.0000E+09
External Q factor	=	3.0000E+06
Cavity R over Q (2xFNAL=53 per cell)	=	53.000 ohms
Energy point ILC crab-0.0284J per cell)	=	28.400 mJ
Amplitude set point	=	301.675 kV
Maximum Amplifier Power per cell	=	1200.000 W
Maximum voltage set point (no beam)	=	1235.476 kV
Maximum beam offset	=	1.000 mm
Maximum bunch phase error	=	1.000 deg
Beam offset frequency	=	2000.000 Hz
Bunch charge (ILC=3.2 nC)	=	3.200 nC
RF cycles between bunches	=	1200
Bunch train length	=	1.000 ms
Cavity frequency shift from microphonics	=	600.000 Hz
Cavity vibration frequency	=	23.000 Hz
Initial vibration phase (degrees)	=	20.000 deg
Phase measurement error(degrees)	=	0.00500 deg
Fractional err in amplitude measurement	=	0.00200
Time delay (latency) for control system	=	3.0000E-06 s
Control update interval	=	1.0000E-06 s
Amplifier bandwidth	=	1.0000E+07
Optimal gain constant for controller	=	0.0214
Minimum rms phase error	=	0.11827
Maximum power delivered	=	403.8752
Proportional coef for real component	=	3.2060E-01
Integral coef for real component	=	1.2824E-05
Proportional coef for imag component	=	1.2824E+00
Integral coef for imag component	=	1.0259E-04

## 23. Three Mode Simulation for ILC Cavities

Section 11 developed the theory for the case where several modes can be excited by the RF power amplifier or the beam. A proposal for the ILC crab cavity is to use a nine cell cavity. In this design the nearest two modes to the operating mode are the  $8\pi/9$  mode at + 2 MHz and the  $7\pi/9$  mode at + 9 MHz. Modes with frequencies further from the operating mode have less influence on control of the phase and amplitude of the operating mode. In this section calculations with the first 3 modes are made and can be compared with previous results where only one mode was included. Figures 41(a-c) of section 23.1 show the amplitude control, the phase control and the power requirement for near optimal gain. RMS amplitude control is less than 0.1% and this is far better than the ILC requirement. RMS phase control has significantly deteriorated with respect to the single mode case, it has deteriorated from 7 milli-degrees (see figure 42) to 26 milli-degrees.

Section 23.2 gives more realistic performance for measurements made with 3.9 GHz to 1.3 GHz dividers and 1.3 GHz digital phase detector. Measurements made in this way would introduce jitter of 8 milli-degrees in a bandwidth of 1 MHz. The simulation is not completely realistic as the noise introduced by the program has not been tailored to the actual noise spectrum of the digital phase detectors.

### 23.1 Microphonics and oscillatory beamloading but no measurement error



Drive frequency in GHz	=	3.900 GHz
Centre cavity frequency in GHz	=	3.900 GHz
Number of cavity modes	=	3
Cavity Q factor	=	1.0E+09
External Q factor	=	3.0E+06
Cavity R over Q (2xFNAL=53 per cell)	=	53.0 ohms
Energy point ILC crab-0.0284J per cell)	=	28.400 mJ
Amplitude set point	=	301.675 kV
Maximum Amplifier Power per cell	=	1200.000 W
Maximum voltage set point (no beam)	=	1235.476 kV
Maximum beam offset	=	0.6 mm
Maximum bunch phase jitter	=	1.0 deg
Beam offset frequency	=	2000.0 Hz
Bunch charge (ILC=3.2 nC)	=	3.2 nC
RF cycles between bunches	=	1200.0
Bunch train length	=	1.0 ms
Cavity frequency shift from microphonics	=	600 Hz
Cavity vibration frequency	=	230 Hz
Initial vibration phase (degrees)	=	20 deg
Phase measurement error(degrees)	=	0 deg
Fractional err in amplitude measurement	=	0
Time delay (latency) for control system	=	1.0E-06 s
Control update interval	=	1.0E-06 s
Gain constant for controller	=	0.7
Amplifier bandwidth	=	1.0E+07
maximum power delivered	=	167.34
In pulse rms phase err	=	0.02560 degrees
In pulse rms amplitude err	=	0.07966 %
Relative excitation of 2nd mode	=	0.03260 %
Relative excitation of 3rd mode	=	0.01756 %
Proportional coef for real component	=	4.20E+01
Integral coef for real component	=	1.26E-03
Proportional coef for imag component	=	4.20E+01
Integral coef for imag component	=	1.26E-03

**Figure 41** Amplitude control performance of a multi-cell crab cavity when three modes are considered

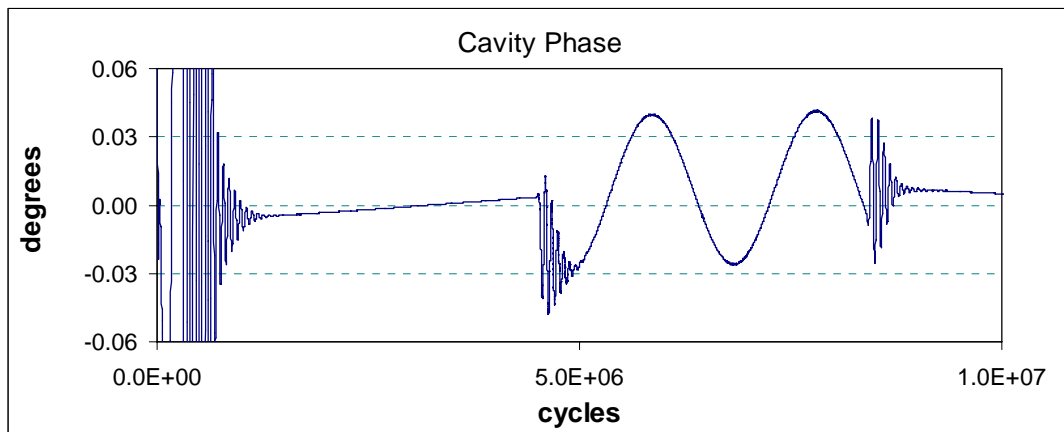


**Figure 41b** Phase control performance for computation of figure 41a

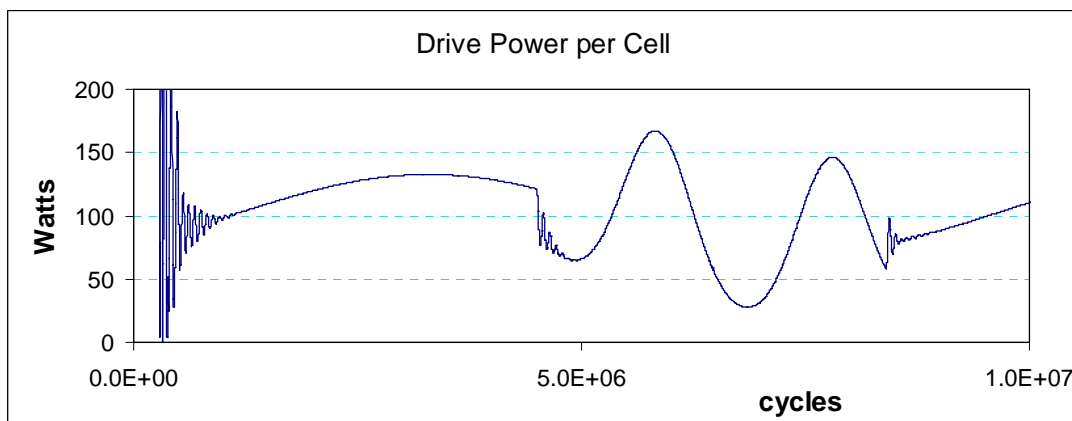


**Figure 41c** Drive power requirement for computation of figure 41a

The striking feature of figure 41b is that when 3 modes are present the coupling to the beam is much stronger. Comparison can be made with figure 34 paying attention to the scale. Figures 41c and 34 were made with slightly differing control parameters. Figure 42 is the phase control for an identical calculation used for figure 41 with the exception that only the operating mode is included.

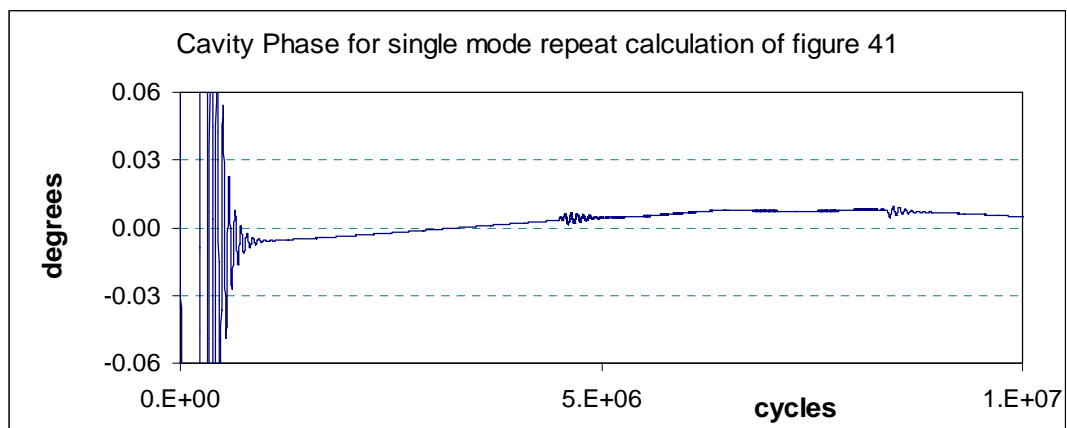


**Figure 42** Phase control single mode case

We make the supposition that the increased error comes from the fact that amplitude and phase is determined from the total field in the cavity rather than that for the operating mode. This is easily examined by modifying the measurement model in the code. Results are shown in figure 43.

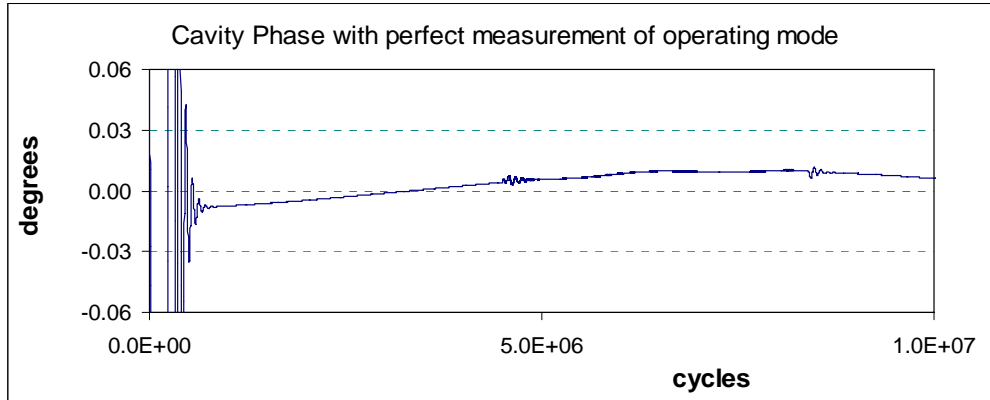
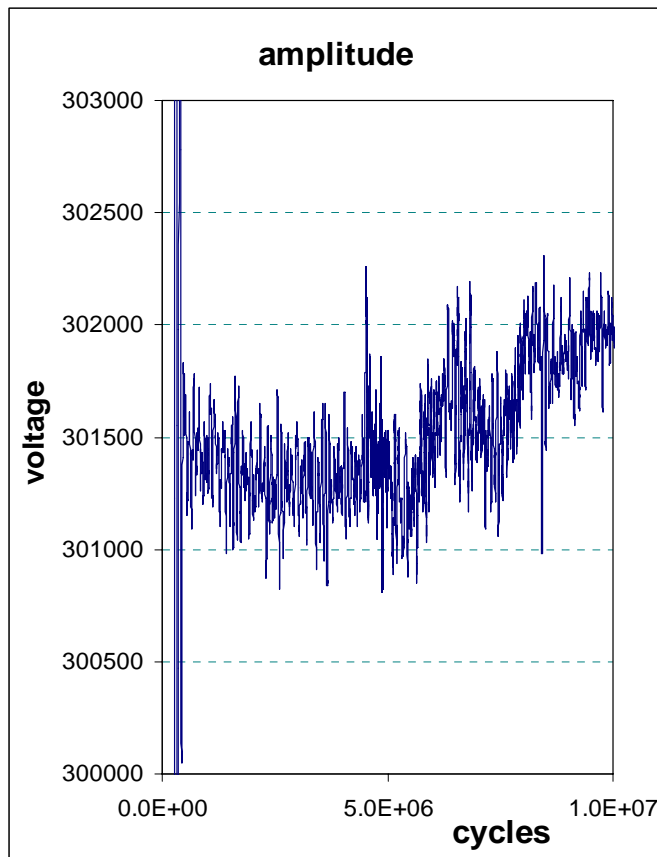


**Figure 43** Phase control for three mode case when by some clever filter one determines the amplitude and phase of just the operating mode.

23.2 Measurement error, microphonics and oscillatory beamloading



Drive frequency in GHz	=	3.900 GHz
Centre cavity frequency in GHz	=	3.900 GHz
Number of cavity modes	=	3
Cavity Q factor	=	1.0000E+09
External Q factor	=	3.0000E+06
Cavity R over Q (2xFNAL=53 per cell)	=	53.000 ohms
Energy point ILC crab-0.0284J per cell)	=	28.400 mJ
Amplitude set point	=	301.675 kV
Maximum Amplifier Power per cell	=	1200.000 W
Maximum voltage set point (no beam)	=	1235.476 kV
Maximum beam offset	=	0.600 mm
Maximum bunch phase jitter	=	1.000 deg
Beam offset frequency	=	2000.000 Hz
Bunch charge (ILC=3.2 nC)	=	3.200 nC
RF cycles between bunches	=	1200.000
Bunch train length	=	1.000 ms
Cavity frequency shift from microphonics	=	600.000 Hz
Cavity vibration frequency	=	230.000 Hz
Initial vibration phase (degrees)	=	20.000 deg
Phase measurement error(degrees)	=	0.02000 deg
Fractional err in amplitude measurement	=	0.00100
Time delay (latency) for control system	=	1.0000E-06 s
Control update interval	=	1.0000E-06 s
Gain constant for controller	=	0.5500
Amplifier bandwidth	=	1.0000E+07
Measurement filter bandwidth	=	5.0000E+05
maximum power delivered	=	193.34
In pulse rms phase err	=	0.02967 deg
In pulse rms amplitude err	=	0.10155 %
Relative excitation of 2nd mode	=	0.03289 %
Relative excitation of 3rd mode	=	0.01768 %
Proportional coef for real component	=	3.3000E+01
Integral coef for real component	=	9.9000E-04
Proportional coef for imag component	=	3.3000E+01
Integral coef for imag component	=	9.9000E-04

**Figure 43a** Amplitude control performance of a multi-cell crab cavity when three modes with measurement errors are considered

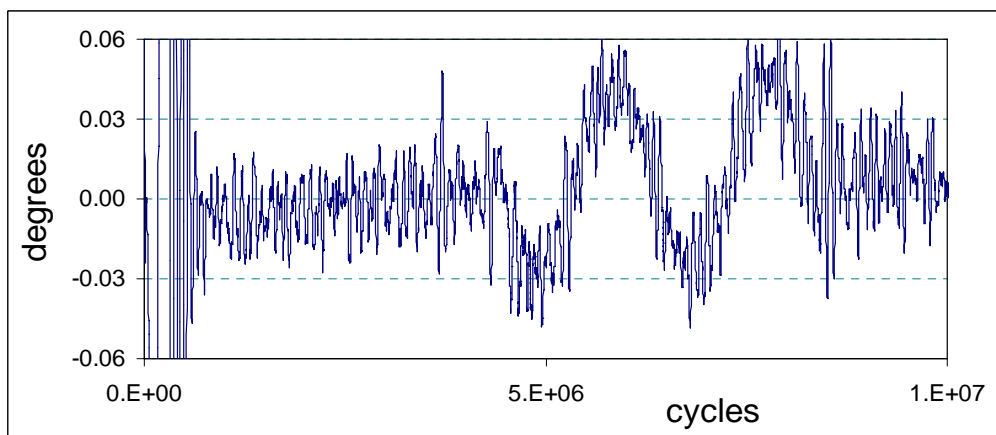


**Figure 43b** Phase control performance for computation of figure 43a

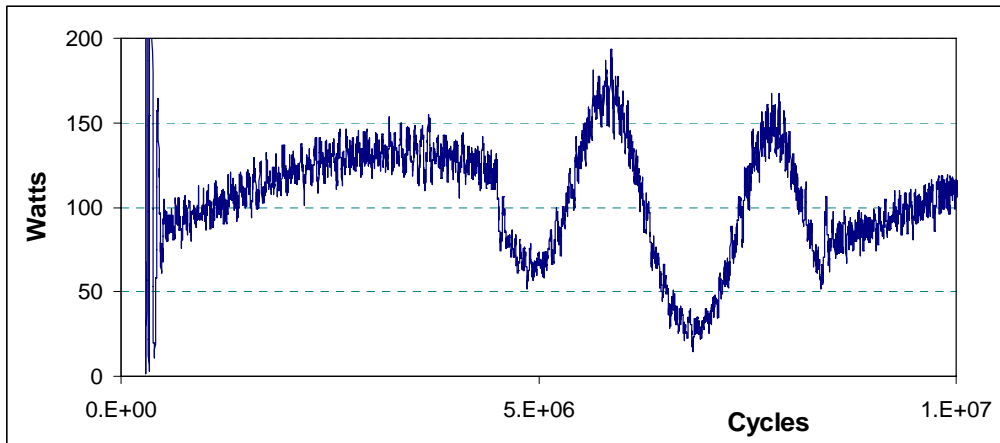


**Figure 43c** Power per cell for computation of figure 43a

## 24. Conclusions

Particle accelerators and light sources have a range of amplitude and stability requirements for the control of their RF cavities. The theory and code developed in this report has far more general application than to just the ILC crab cavities. None the theory developed in sections 3-16 is essentially new however we are not aware of another publication where it is conveniently grouped together. New results are numerical prediction of phase stabilisation performance of superconducting crab cavities. The simulations assume a digital control system where the updated control output has a fixed delay with respect the input. By nature of the numerical solution, realistic measurement errors and incremental beamloading are easily included.

A highly significant result from this work is the added difficulty of getting precise phase control for an operating mode when adjacent modes have even quite small levels of excitation. For a single mode crab cavity operated with ILC beam parameters and in the absence of measurement errors, the phase stability performance is determined by how well the control system compensates microphonics which are present; beam-loading has no significant effect on the phase. This ceases to be true for the multi-mode cavity when the measurement of amplitude and phase detects modes other than the operating mode.

A second result which was new to us (but not necessarily new to the community) is that the optimum phase control performance is almost independent of the cavity external Q for significant range of beamloading, microphonic, digital time delay and measurement error parameters around the preferred operating point.

A third result which may be new are some the formulae given in section 21.2 for the stability limit of the PI algorithm and in particular the empirical approximations.

A final concern requiring further work is the simplistic measurement error model we have used. Preliminary data from cavity control experiments indicate that the random errors we have in our model do not give representative fluctuations on a kHz timescale. Accurate measurements of the noise spectrum need to be made for incorporation into the model.

## 25. References

- [1] C. Adolphsen, C. Beard, L. Bellantoni, G. Burt, R. Carter, B. Chase, M. Church, A. Dexter, M. Dykes, H. Edwards, P. Gouket, R. Jenkins, R. M. Jones, A. Kalinin, T. Khabiboulline, K. Ko, A. Latina, Z. Li, L. Ma, P. McIntosh, C. Ng, A. Seryi, D. Schulte, N. Solyak, I. Tahir, L. Xiao, "Design of the ILC Crab Cavity System" EUROTeV Report 2007-010
- [2] Delayan J.R. "Phase and Amplitude Stabilization of Superconducting Resonators", Ph.D. thesis, California Institute of technology, 1978
- [3] A. Dexter, I. Tahir, G. Burt, R. Carter, P. Ambattu, C. Beard, P. Gouket, P. McIntosh, S. Pattalwar, P. Corlett, "ILC Crab Cavity Phase Control System Development and Synchronisation Testing in a Vertical Cryostat Facility", EUROTeV Report 2008-073
- [4] G. Burt, R.M. Jones, A. Dexter, "Analysis of Damping Requirements for Dipole Wake-Fields in RF Crab Cavities." IEEE Trans. Nuc. Sci. Vol. 54, 2007
- [5] Slater J.C. "Microwave Electronics", Dover Publications Inc, 1969 (Re-print of 1950 ed with corrections)
- [6] Adler R. "A study of locking phenomena in oscillators", Proc IRE, vol. 34, 1946.
- [7] Panofsky W.K.H., Wenzel W., Rev. Sci. Instrum., vol. 27 pg 967, 1956
- [8] Palmer R. SLAC-PUB-4707, 1988
- [9] McAshan & Wanzenberg, FERMILAB-TM-2144 May 2001
- [10] Padamsee H., Knobloch J. and Hays T. "RF Superconductivity for Accelerators", Wiley NY 1998
- [11] ILC design report, <http://www.linearcollider.org/cms/?pid=1000437>
- [12] G. Burt, A. Dexter and P Gouket "Effect and tolerances of RF phase and amplitude errors in the ILC Crab cavity", EUROTeV-Report-2006-098.
- [13] Elmar Vogel "High Gain Proportional RF control stability at TESLA cavities, Physical Review Special Topics –Accelerators and Beams vol. 10 (2007)

## 26. Acknowledgements

The authors wish to thank Leo Bellantoni of FNAL for his many helpful comments during the preparation of this report.

This work has been funded by the UK research council STFC as part of the LC-ABD project grant number PP/B500007/1 and by the Commission of European Communities under the FP6 "Research Infrastructure Action - Structuring the European Research Area" EUROTeV DS Project Contract no.011899 RIDS.

## 27. Appendix 1 Code for direct integration (see section 6)

```

c      Driven oscillator with beam load
c      *****
c      Last modified 26th Oct 2006

c      This program solves the equation

c       $C*dV/dt+V*(1/Zext+1/R)+(1/L)*Integral(V*dt)=2*Forw*cos(wd*t+psi)/Zext$ 

c      Where the voltage V takes a step change at t = 0 and V0 and psi can be
c      changed to minimise recovery time. Forw is the voltage in the forward wave.

c      For solution the differential equation is written in the form

c       $d^2V/dt^2+(wc/QL)*dV/dt+wc**2*V=-2*Forw*(wd*wc/QE)*sin(wd*t+psi)$ 

c      in this program the time derivative Forw is neglected as Forw is usually
c      and when it changes it will change over about 100 cycles hence its values is
c      on hundredth of the other term.

c      The differential equation is solved by 4th or Runge Kutta
c      In the solution E~V, F~dV/dt, Vd0 = Forw for t<0, Vd1 = Forw for t>0

c      The solution starts at a time before t=0 so equilib is established

c23456789012345678901234567890123456789012345678901234567890123456789012

      real*8 Vdr0, Vdr1, Vdi0, Vdi1, Vd0, Vd1, vjump
      real*8 vdr, Vdr_last, vdi, Vdi_last, vdr_dot, vdi_dot
      real*8 wc0, wc1, wc, wd0, wd1, wd
      real*8 QE, QC, QL0, QL1, QE0, QE1, QC0, QC1
      real*8 bL0, bL1, bE0, bE1, bE, bL
      real*8 pi, period, t0, dt, t1, t2, tstart, hdt, dt6, ts, time, tx
      real*8 psi0, psi1, psi0_degrees, psi1_degrees
      real*8 fc0, fc1, fd0, fd1, dfc, dfd
      real*8 E0, E1, E2, E3, E4, F0, F1, F2, F3, F4
      real*8 DF1, DF2, DF3, DF4
      real*8 amplitude, frequency, shift, phase, phase_deg
      real*8 xamplitude
      real*8 driver, drivei, drive
      real*8 tjump, beamloadi, beamloadr

      integer n, ns, nf, its, j, it, nprint, nwrite
      integer ivalue0, ivalue1, ivalue2

c      logical ljump

      intrinsic abs, atan, cos, sin

      open(file='data.txt',unit=42, status='modify')

      pi=4.0d00*atan(1.0d00)

      print*, 'Give forward wave amplitude for t<0'
      read(*,*) vd0
      write(42,949) vd0
949      format('Forward wave amplitude for t<0          =', 1pe11.4)

      print*, 'Give forward wave amplitude for t>0'
      read(*,*) vd1
      write(42,950) vd1
950      format('Forward wave amplitude for t>0          =', 1pe11.4)

```

```

    print*, 'Give beam induced amplitude jump at t=0'
    read(*,*) vjump
    write(42,9501) vjump
9501 format('Voltage jump at t=0                                =', 1pe11.4)

    fd0=3.90e09
    write(42,951) fd0
951  format('Initial drive frequency t<0                        =', 1pe11.4,' Hz')
c    initial drive frequency

    shift = 0.0d00
c    print*, 'Give drive frequency shift at t=0 in MHz'
c    read(*,*) Shift
    dfd=1.0d06*shift

    fd1=fd0+dfd
    write(42,952) fd1
952  format('Drive frequency for t>0                          =', 1pe11.4,' Hz')
c    new drive frequency

    psi0_degrees=0.0d00
    write(42,953) psi0_degrees
953  format('Initial drive phase                               =', 1pe11.4,' deg')
    psi0=psi0_degrees*pi/180.0d00

    shift=0.0d00
    print*, 'Give forward wave phase shift at t=0 in degrees'
    read(*,*) Shift
    psil_degrees=psi0_degrees+shift
    psil=psil_degrees*pi/180.0d00
    write(42,954) psil_degrees
954  format('Phase shift at t=>0 =', 1pe11.4,' deg')

    fc0 =3.9e09
    write(42,955) fd0
955  format('Initial cavity frequency                          =', 1pe11.4,' Hz')
c    initial cavity frequency

    dfc=0.0d00
    fc1 = fc0 + dfc
    write(42,956) fd0
956  format('Cvity frequency for t>0                          =', 1pe11.4,' Hz')
c    new cavity frequency

    wd0=2.0d00*pi*fd0
    wd1=2.0d00*pi*fd1
    wc0=2.0d00*pi*fc0
    wc1=2.0d00*pi*fc1

    write(*,*) 'Give Cavity Q factor'
    read(*,*) QC
    write(42,958) QC
958  format('Cavity Q factor                                    =', 1pe11.4)
    QC0=QC
    QC1=QC

    write(*,*) 'Give External Q factor'
    read(*,*) QE
    write(42,959) QE
959  format('External Q factor                                  =', 1pe11.4)

    QL0=1.0d00/(1.0d00/QE+1.0d00/QC0)
    QL1=1.0d00/(1.0d00/QE+1.0d00/QC1)
    QE0=QE
    QE1=QE

```

```

Close(unit=42,status='keep')

write(*,*) '      '

bL0=wc0/QL0
bL1=wc1/QL1
bE0=wc0/QE0
bE1=wc1/QE1

ns=10000
nf=20000
its=180
ns=100000
nf=200000
its=180
it=0

period=2.0d00*pi/wd0

tjump=0.25d00*period
tjump=0.0d00

beamloadr=0.319324157d00*vjump*QE
beamloadi=0.0d00

tstart=-ns*period
dt=period/its
n=its*(ns+nf)

open(file='results_os.txt',unit=40,status='modify')
open(file='wave_os.txt',unit=41,status='modify')

c   ljump=.false.

t0=tstart
ts=t0
amplitude =0.0d00
xamplitude=amplitude
vdr0 = vd0*cos(psi0)
vdi0 = vd0*sin(psi0)
vdr1 = vd1*cos(psi1)
vdi1 = vd1*sin(psi1)

phase=psi0+0.5d00*pi
c *****
c *   The phase is to be reference to a cosine function.           *
c *   Add 90 degrees to the initial phase as we measure at a going *
c *   positive zero rather than at the peak field.                 *
c *****

write(40,930)
930  format(10x,'time',3x,'amplitude',6x,'frequency',7x,'phase')

write(41,931)
931  format(8x,'time',5x,'      field')

hdt=dt*0.5d00
dt6=dt/6.0d00

E0 = 0.0d00
F0 = 0.0d00

nprint=0
nwrite=10

```

```

if(t0.gt.0.0d00)then
  ivalue0=0
  ivalue1=1
else
  ivalue0=1
  ivalue1=0
end if

vdr=ivalue0*vdr0+ivalue1*vdr1
vdi=ivalue0*vdi0+ivalue1*vdi1

vdr_last=vdr
vdi_last=vdi
vdr_dot=(vdr-vdr_last)/period
vdi_dot=(vdi-vdi_last)/period

do 1 j=1,n

  if(t0.gt.0.0d00)then
    ivalue0=0
    ivalue1=1
  else
    ivalue0=1
    ivalue1=0
  end if

  ivalue2=0
  if((t0.gt.tjump-0.25*period).and.(t0.lt.tjump+0.25*period))then
    ivalue2=1
  end if

  Vdr=ivalue0*Vdr0 + ivalue1*Vdr1 + ivalue2*beamloadr
  Vdi=ivalue0*Vdi0 + ivalue1*Vdi1 + ivalue2*beamloadi
  wd=ivalue0*wd0 + ivalue1*wd1
  wc=ivalue0*wc0 + ivalue1*wc1
  bL=ivalue0*bL0 + ivalue1*bL1
  bE=ivalue0*bE0 + ivalue1*bE1

  driver=(vdr_dot+wd*Vdi)*cos(wd*t0)
  drivei=(vdi_dot-wd*Vdr)*sin(wd*t0)
  drive=driver+drivei

  t1 =t0+hdt
  E1 =E0+hdt*F0
  DF1=-bL*F0+2.0d00*bE*drive-wc**2*E0
  F1 =F0+hdt*DF1

  driver=(vdr_dot+wd*Vdi)*cos(wd*t1)
  drivei=(vdi_dot-wd*Vdr)*sin(wd*t1)
  drive=driver+drivei

  E2 =E0+hdt*F1
  DF2=-bL*F1+2.0d00*bE*drive-wc**2*E1
  F2 =F0+hdt*DF2

  E3 =E0+dt*F2
  DF3=-bL*F2+2.0d00*bE*drive-wc**2*E2
  F3 =F0+dt*DF3

  t2 = t0+dt

  driver=(vdr_dot+wd*Vdi)*cos(wd*t2)
  drivei=(vdi_dot-wd*Vdr)*sin(wd*t2)
  drive=driver+drivei

  E4 = E0 + dt6*(F0 + 2.0d00*(F1+F2) + F3)

```

```

DF4=-bL*F3+2.0d00*bE*drive-wc**2*E3
F4 = F0 + dt6*(DF1 + 2.0d00*(DF2+DF3) + DF4)

if(abs(E4).gt.amplitude) amplitude = abs(E4)

if((E0.lt.0).and.(E4.gt.0.0d00))then
  tx = (t0*E4-t2*E0)/(E4-E0)
  period = tx-ts
  frequency=1.0d-09/period
  phase=phase + wd0*period-2.0d00*pi
  phase_deg=phase*180.0d00/pi

  time = t2*1.0d09

  if(it.gt.nprint)then
    write(*,901) time, amplitude, frequency, phase_deg
901   format('time=',f11.3,' amplitude=',f8.4,
+       ' frequency=', f13.9,' phase=', e11.4)
    nprint=nprint+2000
  end if

  if(it.gt.nwrite)then
902   write(40,902) time, amplitude, frequency, phase_deg
    format(3x,f11.3,3x,f9.5,3x,f13.9,3x,e13.6)
    nwrite=nwrite+100
  end if

  ts=tx
  amplitude=0.0d00
  it=it+1
end if

if((t2.gt.-3.0d00*period).and.(t2.lt.3.0d00*period))then
  time = t2*1.0d09
903   write(41,903) time, E4
  format(3x,f11.3,3x,f11.5)
end if

t0=t2
E0=E4
F0=F4

c   Old code for introducing a voltage jump without a driving current.
c   *****
c   if(.not.ljump)then
c     if(t0.gt.(tjump-hdt))then
c       ljump=.true.
c       E0=E0+0.0d00*Vjump
c     endif
c   endif

1   continue

close(unit=40,status='keep')
close(unit=41,status='keep')

stop

end

```



```

write(42,9501) vjump
9501 format('Voltage jump at t=0           =', 1p11.4)

fd0=3.90e09
write(42,951) fd0
951 format('Inital drive frequency       =', 1p11.4,' Hz')
c initial drive frequency

shift = 0.0d00
c print*, 'Give drive frequency shift at t=0 in MHz'
c read(*,*) Shift
dfd=1.0d06*shift

fd1=fd0+dfd
write(42,952) fd1
952 format('Drive frequency for t>0     =', 1p11.4,' Hz')
c new drive frequency

fc0 =3.9e09
write(42,955) fd0
955 format('Inital cavity frequency     =', 1p11.4,' Hz')
c initial cavity frequency

dfc=0.0d00
fc1 = fc0 + dfc
write(42,956) fd0
956 format('Cavity frequency for t>0    =', 1p11.4,' Hz')
c new cavity frequency

wd0=2.0d00*pi*fd0
wd1=2.0d00*pi*fd1
wc0=2.0d00*pi*fc0
wcl=2.0d00*pi*fc1

write(*,*) 'Give Cavity Q factor'
read(*,*) QC
write(42,958) QC
958 format('Cavity Q factor             =', 1p11.4)
QC0=QC
QC1=QC

write(*,*) 'Give External Q factor'
read(*,*) QE
write(42,959) QE
959 format('External Q factor           =', 1p11.4)

QL0=1.0d00/(1.0d00/QE+1.0d00/QC0)
QL1=1.0d00/(1.0d00/QE+1.0d00/QC1)
QE0=QE
QE1=QE

Close(unit=42,status='keep')

write(*,*) '      '

ns=100000
nf=200000
its=0.1
it=0

period=2.0d00*pi/wd0

tjump=0.0d00

```

```

tstart=-ns*period
dt=period/its
n=its*(ns+nf)

open(file='results_os.txt',unit=40,status='modify')
open(file='wave_os.txt',unit=41,status='modify')

ljump=.false.

t0=tstart
amplitude =0.0d00
vdr = 0.0d00
vdi = 0.0d00
time_step = 1.0d00

write(40,930)
930  format(10x,'time',3x,'amplitude',6x,'phase',
+       9x,'Rcontrol',9x,'Icontrol')

write(41,931)
931  format(8x,'time',5x,'      field')

hdt=dt*0.5d00
dt6=dt/6.0d00

AR0 = 0.0d00
AI0 = 0.0d00

nprint=0
nwrite=1

cpr=5.0d00
cir=5.0d-04
cpi=5.0d00
cii=5.0d-04
sumr=0.0d00
sumi=0.0d00
summax=0.6d00*V_set_point/cir
Vmax=0.55d00*V_set_point

g10=(2.0d00*wd0/wc0)**2+(1.0d00/QL0)**2
g11=(2.0d00*wd1/wc1)**2+(1.0d00/QL1)**2

g20=((wd0/wc0)**2+1.0d00)*(1.0d00/QL0)
g21=((wd1/wc1)**2+1.0d00)*(1.0d00/QL1)

g30=((1.0d00/QL0)**2-(2.0d00*wd0/wc0)*(wc0/wd0-wd0/wc0))*(wd0/wc0)
g31=((1.0d00/QL1)**2-(2.0d00*wd1/wc1)*(wc1/wd1-wd1/wc1))*(wd1/wc1)

g40=2.0d00/(QE0*QL0)
g41=2.0d00/(QE1*QL1)

g50=4.0d00*(wd0/wc0)*(1.0d00/QE0)
g51=4.0d00*(wd1/wc1)*(1.0d00/QE1)

f10=g20/g10
f11=g21/g11

f20=g30/g10
f21=g31/g11

f30=g40/g10
f31=g41/g11

f40=g50/g10

```

```

f41=g51/g10

do 1 j=1,n

  if(t0.gt.0.0d00)then
    ivalue0=0
    ivalue1=1
  else
    ivalue0=1
    ivalue1=0
  end if

  wd=ivalue0*wd0 + ivalue1*wd1
  wc=ivalue0*wc0 + ivalue1*wc1
  fd=ivalue0*fd0 + ivalue1*fd1
  fc=ivalue0*fc0 + ivalue1*fc1
  f1=ivalue0*f10 + ivalue1*f11
  f2=ivalue0*f20 + ivalue1*f21
  f3=ivalue0*f30 + ivalue1*f31
  f4=ivalue0*f40 + ivalue1*f41

c      PI Control
c      *****
  vdr_last=vdr
  vdi_last=vdi
  Rerror=V_set_point-AR0
  Ierror=-AI0
  sumr=sumr+fd*Rerror*dt
  sumi=sumi+fd*Ierror*dt
  if(sumr.gt.summax) sumr=summax
  if(sumr.lt.-summax) sumr=-summax
  if(sumi.gt.summax) sumi=summax
  if(sumi.lt.-summax) sumi=-summax

  Vdr=cpr*Rerror+cir*sumr
  Vdi=cpi*Ierror+cii*sumi

  if(Vdr.gt.Vmax) Vdr=Vmax
  if(Vdr.lt.-Vmax) Vdr=-Vmax
  if(Vdi.gt.Vmax) Vdi=Vmax
  if(Vdi.lt.-Vmax) Vdi=-Vmax

c      development code fixd stimulus
c      *****
c      vdr=10.0d00
c      vdi=0.0d00

  vdr_dot=(vdr-vdr_last)/time_step
  vdi_dot=(vdi-vdi_last)/time_step

  driver=(f3*(vdr_dot+wd*Vdi)-f4*(vdi_dot-wd*Vdr))/wc
  drivei=(f3*(vdi_dot-wd*Vdr)+f4*(vdr_dot+wd*Vdi))/wc

  t1 = t0+hdt
  DAR1=-f1*AR0-f2*AI0+driver
  AR1 = AR0+wc*hdt*DAR1
  DAI1=-f1*AI0+f2*AR0+drivei
  AI1 = AI0+wc*hdt*DAI1

  DAR2=-f1*AR1-f2*AI1+driver
  AR2 = AR0+wc*hdt*DAR2
  DAI2=-f1*AI1+f2*AR1+drivei
  AI2 = AI0+wc*hdt*DAI2

  DAR3=-f1*AR2-f2*AI2+driver

```

```

AR3 = AR0+wc*dt*DAR3
DAI3=-f1*AI2+f2*AR2+drivei
AI3 = AI0+dt*DAI3

t2 = t0+dt
DAR4=-f1*AR3-f2*AI3+driver
AR4 = AR0+wc*dt6*(DAR1+2.0d00*(DAR2+DAR3)+DAR4)
DAI4=-f1*AI3+f2*AR3+drivei
AI4 = AI0+wc*dt6*(DAI1+2.0d00*(DAI2+DAI3)+DAI4)

amplitude = sqrt(AR4*AR4+AI4*AI4)
phase = atan(AI4/AR4)
phase_deg=phase*180.0d00/pi

time = t2*1.0d09

if(it.gt.nprint)then
  write(*,901) time, amplitude, phase_deg, vdr, vdi
901   format('time=',f11.3,' amp=',f10.3,
+       ' pha=', e11.4,' Rcntr=', f7.3,' Icntr=', f7.3)
  nprint=nprint+400*its
end if

if(it.gt.nwrite)then
902   write(40,902) time, amplitude, phase_deg, vdr, vdi
  format(3x,f11.3,3x,f9.3,3x,e13.6,3x,f9.5,3x,f9.5)
  nwrite=nwrite+10*its
end if

it=it+its

if((n.gt.0).and.(n.lt.5000))then
903   time = t2*1.0d09
  write(41,903) time, AR0
  format(3x,f11.3,3x,f11.5)
end if

time_step=t2-t0
t0=t2
AR0=AR4
AI0=AI4

if(.not.ljump)then
  if(t0.gt.tjump)then
    ljump=.true.
    AR0=AR0+Vjump
  endif
endif

1   continue

close(unit=40,status='keep')
close(unit=41,status='keep')

stop

end

```

## 29. Appendix 3 Code to integrate envelope equations

```

c   Driven multi-mode cavity with beamloading, microphonics & delayed PI control.
c   ****
c   Program last modified 29th October 2007

c   29/10/2007 adjustment to mode beam couplings.
c   The 8pi/9 mode is +2MHz, The ratio of its QE to that of the pi mode is 1.667
c   hence the voltage coupling is root this value = 1.29. The relative beam to
c   cavity voltage coupling for the 8pi/9 mode is 0.032

c   The 7pi/9 mode is +9MHz, The ratio of its QE to that of the pi mode is 4.5
c   hence the voltage coupling is root this value = 2.12. The relative beam to
c   cavity voltage coupling for the 7pi/9 mode is 0.024

c   The 6pi/9 mode is +20.6MHz, The ratio of its QE to that of the pi mode is 0.67
c   hence the voltage coupling is root this value = 0.816. The relative beam to
c   cavity voltage coupling for the 6pi/9 mode is 0.0259

c   1/9/07 add measurement filter bandwidth as an input (previously determined from
c   the update interval.)

c   Program still requires a more realistic amplifier model (current modelled as a
c   band pass filter with gain).

c   Program now includes measurement model, amplifier model, multi-mode cavity
c   and beamloading of all modes (the bunch arrival can be an arbitrary phase
c   with respect to the peak mode voltage).

c   This program solves the envelope equations for
c    $C \cdot dV/dt + V/Z_{ext} + (1/L) \cdot \text{Integral}(V \cdot dt) = 2 \cdot \text{Forw} \cdot \cos(\omega d \cdot t + \psi) / Z_{ext}$ 
c   which are formed by setting  $V = (A_r + j \cdot A_i) \cdot \exp(-j \cdot \omega d \cdot t)$  and neglecting second
c   derivatives of  $A_r$  and  $A_i$ 

c   Forw is the amplitude of the forward wave and is determined by a PI controller

c   Two differential equations per mode are solved by 4th order Runge Kutta
c2345678901234567890123456789012345678901234567890123456789012345678901234567890123456789012

integer*4 jic, jm
parameter(jic=100000)
parameter(jm=3)
c   jm sets maximum number of modes
c   jic sets the maximum delay for the control system in cycles

real*8 V_set_point(jm), vjump, drive_amp, drive_max, V_max_point
real*8 energy_set_point
real*8 Vkick, Max_power, drive_pow, drive_phase, bunch_phase, c
real*8 Offset, bunch_phase_err, cos_err, sin_err, bunch_charge
real*8 bunch_phase_jitter
real*8 vdr, Vdr_last, vdi, Vdi_last, vdr_dot, vdi_dot
real*8 wd, wc(jm), wc0(jm), QC(jm), QE(jm)
real*8 wa, QA, ROQ, amp_bandwidth, meas_bandwidth
real*8 pi, period, t0, dt, t2, tstart, hdt, dt6, time
real*8 time_step, time_last, time_step1, time_step2
real*8 fc(jm), fd
real*8 f0(jm), fe(jm), g1(jm), g2(jm), g3(jm)
real*8 gal, ga2, ga3, ga4, ga5
real*8 fal, fa2, fa3, fa4
real*8 AR(jm), AI(jm), AR_sum, AI_sum
real*8 amp_AR0, amp_AR
real*8 amp_AI0, amp_AI

```

```

real*8 amp_AR_dot, amp_AI_dot
real*8 outr(jm), outi(jm)
real*8 AR0_meas, AI0_meas, rand_phase, rand_mag, mag_factor
real*8 meas_phase_jitter, meas_amp_jitter, meas_phase_jitter_deg
real*8 amplitude(jm), phase(jm), phase_deg(jm)
real*8 driver(jic), drivei(jic)
real*8 dr_ramp, di_ramp, dr_flat, di_flat
real*8 cntr_delay, update_interval
real*8 c_prop_Ar, c_intl_Ar, c_prop_Ai, c_intl_Ai
real*8 sumr, sumi, Rerror, Ierror, summax
real*8 cycle
real*8 xrandom
real*8 random
real*8 aa
real*8 offset_freq, w_offset
real*8 pulse_length
real*8 drive_freq, cavity_freq, cavity_vib_freq, cavity_freq_shift
real*8 initial_vib_phase
real*8 wshift, wcav, vph
real*8 sum_sq_ph_err(jm), sum_sq_amp_err(jm), amp_err(jm), value
real*8 gain, max_power_used
real*8 Qmeas, AR0_filter, AI0_filter
real*8 testr, testi
real*8 mode_coupler_coupling(jm), mode_beam_coupling(jm)
real*8 cycles_between_bunches, cycle_of_next_bunch
real*8 cycle_offset_first_bunch

integer*4 n_iterations, ncycle, icycle, j, js, nprint, nwrite
integer*4 its_per_cycle, idelay, ic_delay, ic
integer*4 nbeam_on, nbeam_off, ndetail
integer*4 cycles_per_train
integer*4 count, control_update, cnt_param, nsettle
integer*4 normalise(jm)
integer*4 n_vec_mod
integer*4 nerror, modes

character*80 anything

logical lrandom

intrinsic abs, atan, cos, sin, sqrt, acos, asin
external random, RK, RKM

pi=4.0*atan(1.0d00)

c=2.998d08

c      Read input data from file
c      *****
open(file='indata.txt',unit=45,status='old')
open(file='outdata.txt',unit=46,status='modify')

900   format(a)

read(45,900) anything
nerror=952
read(anything(41:),*,err=3000) drive_freq
write(*,952) drive_freq
write(46,952) drive_freq
fd=drive_freq*1.0d09
952   format('Drive frequency in GHz',f11.3,' GHz')

read(45,900) anything
nerror=953

```

```

    read(anything(41:),*,err=3000) cavity_freq
    write(*,953) cavity_freq
    write(46,953) cavity_freq
    fc(1)=cavity_freq*1.0d09
953  format('Centre cavity frequency in GHz           =',f11.3,' GHz')

    modes=3
    write(46,9539) modes
9539 format('Number of cavity modes                 =',i2)

    fc(2)=fc(1)+2.0d+06
    fc(3)=fc(1)+9.0d+06

    mode_coupler_coupling(1)=1.0d00
    mode_coupler_coupling(2)=1.29d00
    mode_coupler_coupling(3)=2.12d00

    mode_beam_coupling(1)=1.0d00
    mode_beam_coupling(2)=0.032d00
    mode_beam_coupling(3)=0.024d00

    wd=2.0d00*pi*fd
    do 61 js=1,modes
        wc0(js)=2.0d00*pi*fc(js)
61  continue

    aa=0.5d00*c*pi/wd
c  reference radius to get voltage setpoint (aa*w/c)=pi/2

    read(45,900) anything
    nerror=954
    read(anything(41:),*,err=3000) QC(1)
    write(*,954) QC(1)
    write(46,954) QC(1)
954  format('Cavity Q factor                         =',lpe11.4)
    do 62 js=1,modes
        QC(js)=QC(1)
62  continue

    read(45,900) anything
    nerror=955
    read(anything(41:),*,err=3000) QE(1)
    write(*,955) QE(1)
    write(46,955) QE(1)
955  format('External Q factor                       =',lpe11.4)
    do 63 js=1,modes
        QE(js)=QE(1)/mode_coupler_coupling(js)**2
63  continue

    read(45,900) anything
    nerror=956
    read(anything(41:),*,err=3000) ROQ
    write(*,956) ROQ
    write(46,956) ROQ
956  format('Cavity R over Q   (2xFNAL=53 per cell) =',f11.3,' ohms')

    read(45,900) anything
    nerror=957
    read(anything(41:),*,err=3000) energy_set_point
    value=energy_set_point*1000.0d00
    write(*,957) value
    write(46,957) value
957  format('Energy point   ILC crab-0.0284J per cell) =',f11.3,' mJ')

    do 52 js=1,modes
        v_set_point(js)=0.0d00

```

```

52  continue

    v_set_point(1)=(aa*wd/c)*sqrt(energy_set_point*wd*ROQ)
    value=v_set_point(1)/1000.0d00

    write(*,958) value
    write(46,958) value
958  format('Amplitude set point                =',f11.3,' kV')

    read(45,900) anything
    nerror=959
    read(anything(41:),*,err=3000) Max_power
    write(*,959) Max_power
    write(46,959) Max_power
959  format('Maximum Amplifier Power per cell    =',f11.3,' W')

    drive_max= sqrt(2.0d00*QE(1)*ROQ*Max_power)
c***** drive_max is the maximum amplitude of the forward wave *****

    V_max_point=2.0d00*drive_max
    value=V_max_point/1000.0d00
    write(*,960) value
    write(46,960) value
960  format('Maximum voltage set point (no beam) =',f11.3,' kV')

    read(45,900) anything
    nerror=961
    read(anything(41:),*,err=3000) offset
    write(*,961) offset
    write(46,961) offset
961  format('Maximum beam offset                =',f11.3,' mm')

    read(45,900) anything
    nerror=962
    read(anything(41:),*,err=3000) bunch_phase_jitter
    write(*,962) bunch_phase_jitter
    write(46,962) bunch_phase_jitter
962  format('Maximum bunch phase jitter        =',f11.3,' deg')

    read(45,900) anything
    nerror=963
    read(anything(41:),*,err=3000) xrandom

    lrandom=.false.
    if(xrandom.gt.0.5d00) lrandom=.true.
    if(lrandom)then
c      this line contains a offset period which is not used
        read(45,900) anything
        offset_freq=0.0d00
        write(*,963)
        write(46,963)
963  format('Random offset')
    else
        read(45,900) anything
        nerror=964
        read(anything(41:),*,err=3000) offset_freq
        write(*,964) offset_freq
        write(46,964) offset_freq
964  format('Beam offset frequency            =',
+ f11.3,' Hz')
    end if
    w_offset=2.0d00*pi*offset_freq

    read(45,900) anything
    nerror=965
    read(anything(41:),*,err=3000) bunch_charge

```

```

value=bunch_charge*1.0d09
write(*,965) value
write(46,965) value
965 format('Bunch charge (ILC=3.2 nC)                =',f11.3,' nC')
cos_err=cos(bunch_phase_jitter*pi/180.0d00)
sin_err=sin(bunch_phase_jitter*pi/180.0d00)
vjump=0.5d00*(aa*wd/c)*(offset*1.0d-03*wd/c)*wd*ROQ*bunch_charge
write(*,966) vjump
966 format('Voltage jump at t=0                        =', 1pe11.4,' V')

read(45,900) anything
nerror=967
read(anything(41:),*,err=3000) cycles_between_bunches
write(*,967) cycles_between_bunches
write(46,967) cycles_between_bunches
967 format('RF cycles between bunches                =', f11.3)

read(45,900) anything
nerror=969
read(anything(41:),*,err=3000) pulse_length
value=pulse_length*1000.0d00
write(*,969) value
write(46,969) value
969 format('Bunch train length                        =',f11.3,' ms')

read(45,900) anything
nerror=970
read(anything(41:),*,err=3000) cavity_freq_shift
write(*,970) cavity_freq_shift
write(46,970) cavity_freq_shift
970 format('Cavity frequency shift from microphonics=',f11.3,' Hz')
wshift=2.0d00*pi*cavity_freq_shift

read(45,900) anything
nerror=971
read(anything(41:),*,err=3000) cavity_vib_freq
write(*,971) cavity_vib_freq
write(46,971) cavity_vib_freq
971 format('Cavity vibration frequency              =',f11.3,' Hz')
wcav=2.0d00*pi*cavity_vib_freq

read(45,900) anything
nerror=972
read(anything(41:),*,err=3000) initial_vib_phase
write(*,972) initial_vib_phase
write(46,972) initial_vib_phase
972 format('Initial vibration phase (degrees)        =',f11.3,' deg')
vph=initial_vib_phase*pi/180.0d00

read(45,900) anything
nerror=973
read(anything(41:),*,err=3000) meas_phase_jitter_deg
write(*,973) meas_phase_jitter_deg
write(46,973) meas_phase_jitter_deg
973 format('Phase measurement error(degrees)        =',f11.5,' deg')
meas_phase_jitter=meas_phase_jitter_deg*2.0d00*pi/360.00d00

read(45,900) anything
nerror=974
read(anything(41:),*,err=3000) meas_amp_jitter
write(*,974) meas_amp_jitter
write(46,974) meas_amp_jitter
974 format('Fractional err in amplitude measurement =',f11.5)

read(45,900) anything
nerror=968

```

```

read(anything(41:),*,err=3000) cntr_delay
idelay=cntr_delay*fd
if(idelay.gt.jic) idelay=jic
if(idelay.lt.1) idelay=1
write(*,968) cntr_delay
write(46,968) cntr_delay
968 format('Time delay (latency) for control system =',1p11.4,' s')

read(45,900) anything
nerror=975
read(anything(41:),*,err=3000) update_interval
write(*,975) update_interval
write(46,975) update_interval
975 format('Control update interval =',1p11.4,' s')

control_update=fd*update_interval

read(45,900) anything
nerror=9766
read(anything(41:),*,err=3000) gain
write(*,9766) gain
write(46,9766) gain
9766 format('Gain constant for controller =',f9.4)

read(45,900) anything
nerror=9767
read(anything(41:),*,err=3000) amp_bandwidth
write(*,9767) amp_bandwidth
write(46,9767) amp_bandwidth
9767 format('Amplifier bandwidth =',1p11.4)

meas_bandwidth=1.0d00/update_interval
read(45,900,end=101) anything
nerror=9768
read(anything(41:),*,err=3000) meas_bandwidth
write(*,9768) meas_bandwidth
write(46,9768) meas_bandwidth
9768 format('Measurement filter bandwidth =',1p11.4)

101 cycle_offset_first_bunch=0.0d00
c first bunch can arrive part way through an RF cycle

n_vec_mod=20
c number of RF cycles over which the vector modulator ramps to a new value

QA=fd/amp_bandwidth
c Amplifier Q factor

c PI Controller coefficients
c *****
cnt_param=3
if(cnt_param.eq.1)then
c OK from QE=6e6 to high QE=1.75e7 with 3900 delay
c_prop_ar= 250.00d-8*QE(1)
c_intl_ar= 0.01d-8*QE(1)*0.2
c_prop_ai= 250.00d-8*QE(1)
c_intl_ai= 0.01d-8*QE(1)*0.2
else if(cnt_param.eq.2)then
c c_prop_Ar= 500.00d-8*QE(1)*gain
c_intl_Ar= 0.02d-8*QE(1)*gain
c_prop_Ai=2000.00d-8*QE(1)*gain
c_intl_Ai= 0.16d-8*QE(1)*gain
else
c increased values for Ai
c_prop_Ar=2000.00d-8*QE(1)*gain

```

```

    c_intl_Ar= 0.06d-8*QE(1)*gain
    c_prop_Ai=2000.00d-8*QE(1)*gain
    c_intl_Ai= 0.06d-8*QE(1)*gain
endif

write(46,976) c_prop_ar
976 format('Proportional coef for real component   =',1p11.4)
write(46,977) c_intl_ar
977 format('Integral coef for real component     =',1p11.4)
write(46,978) c_prop_ai
978 format('Proportional coef for imag component =',1p11.4)
write(46,979) c_intl_ai
979 format('Integral coef for imag component     =',1p11.4)

close(unit=45,status='keep')

write(*,*) '      '

icycle=0

cycles_per_train=1.0e-3*fd
c number of cycle in a bunch train = lms * frequency

if(QE(1).lt.3.0d06)then
    nbeam_on=2.0d00*QE(1)
else
    nbeam_on=1.5d00*QE(1)
end if
if(nbeam_on.gt.10000000)then
    nbeam_on=10000000
c limit size for plotting in Excel
end if
nbeam_on=4500000
nbeam_off=nbeam_on+cycles_per_train
nsettle=0.05d00*cycles_per_train
ncycle=nbeam_off+0.5d00*cycles_per_train
ndetail=0.5d00*(nbeam_on+nbeam_off)
c cycle when next bunch is due

its_per_cycle=1
c time iterations per cycle

period=2.0d00*pi/wd

tstart=0.0d00
dt=period/its_per_cycle
n_its=its_per_cycle*ncycle

open(file='results_os.txt',unit=40,status='modify')
open(file='wave_os.txt',unit=41,status='modify')

t0=tstart
amplitude(1) =0.0d00
vdr = 0.0d00
vdi = 0.0d00
time_step = 1.0d00

write(40,930)
930 format(9x,'cycle',10x,'time',5x,'amplitude',6x,'phase',
+       11x,'Rcontrol',6x,'Icontrol',6x,'DrvPower',6x,'DrvPhase')

write(41,931)
931 format(8x,'time',5x,'      field')

```

```

    hdt=dt*0.5d00
    dt6=dt/6.0d00

    Qmeas=dt*meas_bandwidth
c    filter parameter for measurement model

    do 31 js=1,modes
      AR(js) = 0.0d00
      AI(js) = 0.0d00
31    continue
    amp_AR = 0.0d00
    amp_AI = 0.0d00
    AR0_filter=0.0d00
    AI0_filter=0.0d00

    nprint=0
    nwrite=1

    sumr=0.0d00
    sumi=0.0d00
    summax=drive_max/c_intl_Ar

    cycle=0.0d00
c    when cycle gets to one the number of cycles=icycle increments

    do 10 ic=1,idelay
      driver(ic)=0.0d00
      drivei(ic)=0.0d00
10    continue

    cycle_of_next_bunch=nbeam_on + cycle_offset_first_bunch
    max_power_used=0.0d00

    do 70 js=1,modes
      sum_sq_ph_err(js)=0.0d00
      sum_sq_amp_err(js)=0.0d00
      normalise(js)=0
70    continue

    ic=2
    ic_delay=1
    count=control_update

c    evaluate amplifier coefficients
c    *****
    wa=wd
    ga1=(2.0d00*wd/wa)**2+(1.0d00/QA)**2
    ga2=((wd/wa)**2+1.0d00)*(1.0d00/QA)
    ga3=((1.0d00/QA)**2-(2.0d00*wd/wa)*(wa/wd-wd/wa))*(wd/wa)
    ga4=1.0d00/(QA*QA)
    ga5=2.0d00*(wd/wa)*(1.0d00/QA)

c***** the coefficients of ga4 and ga5 need checking *****
c***** and also the QA of the amplifier with respect to QE and QL *****

    fa1=wa*ga2/ga1
    fa2=wa*ga3/ga1
    fa3=ga4/ga1
    fa4=ga5/ga1

    do 1 j=1,n_iterations

      t2=t0+dt

```

```

c      set instantaneous cavity frequency and evaluate cavity coefficients
c      *****
do 30 js=1,modes
    wc(js)=wc0(js)+wshift*sin(wcav*t0+vph)

    f0(js)=wc(js)/(4.0d00*QC(js))
    fe(js)=wc(js)/(4.0d00*QE(js))

    g1(js)=(1.0d00+(wc(js)/wd)**2)
    g2(js)=(wc(js)**2-wd**2)/(2.0d00*wd)
    g3(js)=wc(js)/(QE(js)*wd)
30 continue

c      Measurement Model
c      *****
c      Note that the actual measurement model deteriorates at the flash ADC
c      combination points. Still need to put this in.

c      Low Pass Filter to average cavity fields over period between DSP
c      re-calculating the control action
c      *****
c      There will be some sort of low pass filter between the cavity probe and the
c      device that measures amplitude and phase. If the device that measures
c      amplitude and phase delivers its output by means of an ADC to a DSP then it
c      is sensible to chose the low pass cut-off equal to the sample rate. The next
c      two lines implement a first order low pass filter. We also suppose that the
c      filter can select the fundamental mode and discriminate the other modes.

AR_sum=0.0d00
AI_sum=0.0d00
do 73 js=1,modes
    AR_sum=AR_sum+AR(js)*mode_coupler_coupling(js)
    AI_sum=AI_sum+AI(js)*mode_coupler_coupling(js)
73 continue

AR0_filter=AR0_filter*(1.0d00-Qmeas)+AR_sum*Qmeas
AI0_filter=AI0_filter*(1.0d00-Qmeas)+AI_sum*Qmeas

if(count.ge.control_update)then
c      measurement errors depend on bandwidth. The measurement errors that should
c      be inserted are those appropriate to the control update frequency.

    count=1
    rand_phase=meas_phase_jitter*(2.0d00*random()-1.0d00)
    rand_mag=1.0d00 + meas_amp_jitter*(2.0d00*random()-1.0d00)
    mag_factor=rand_mag/sqrt(1.0d00+rand_phase**2)
    AR0_meas=mag_factor*(AR0_filter+rand_phase*AI0_filter)
    AI0_meas=mag_factor*(AI0_filter-rand_phase*AR0_filter)

c      PI Control
c      *****
vdr_last=vdr
vdi_last=vdi
time_last=t0
Rerror=V_set_point(1)-AR0_meas
Ierror=-AI0_meas
sumr=sumr+fd*Rerror*dt*control_update
sumi=sumi+fd*Ierror*dt*control_update
if(sumr.gt.summax) sumr=summax
if(sumr.lt.-summax) sumr=-summax
if(sumi.gt.summax) sumi=summax
if(sumi.lt.-summax) sumi=-summax

```

```

Vdr=c_prop_Ar*Rerror+c_intl_Ar*sumr
Vdi=c_prop_Ai*Ierror+c_intl_Ai*sumi

c      limit drive output
c      *****
drive_amp=sqrt(Vdr**2+Vdi**2)
if(drive_amp.gt.drive_max)then
  Vdr=vdr*drive_max/drive_amp
  Vdi=vdi*drive_max/drive_amp
end if

c      evaluate driver terms in differential equations
c      *****
time_step1=n_vec_mod*dt
time_step2=t0-time_last
if(time_step1.lt.time_step2)then
  time_step=time_step1
else
  time_step=time_step2
end if
if(time_step.le.1.0e-12) time_step=1.0d00
vdr_dot=(vdr-vdr_last)/time_step
vdi_dot=(vdi-vdi_last)/time_step

c      evaluate driver while change is being made and after completion
c      *****
c      everytime the DSP re-calculates the drive, the vector modulator
c      ramps the drive to the new value.
dr_ramp=(fa3*(vdr_dot+wd*Vdi)-fa4*(vdi_dot-wd*Vdr))
di_ramp=(fa3*(vdi_dot-wd*Vdr)+fa4*(vdr_dot+wd*Vdi))
dr_flat=( fa3*wd*Vdi+fa4*wd*Vdr)
di_flat=(-fa3*wd*Vdr+fa4*wd*Vdi)
end if

c      evaluate drive - this stays the same if the controller has not recalculated
c      *****
if(count.le.20)then
  driver(ic_delay)=dr_ramp
  drivei(ic_delay)=di_ramp
else
  driver(ic_delay)=dr_flat
  drivei(ic_delay)=di_flat
endif
c      *****
c      * The drive action is delayed by the processing time *
c      *****

count=count+1

c      amplifier model
c      *****
c      The amplifier is modelled as another cavity hence one needs to solve a
c      second set of envelope functions.

c      4th order Runge Kutta integration for amplifier
c      *****
amp_AR0=amp_AR
amp_AI0=amp_AI

call RK(t0,hdt,dt6,amp_AR,amp_AI,fa1,fa2,driver(ic),drivei(ic))

testr=amp_AR-vdr
testi=amp_AI-vdi

```

```

amp_AR_dot=(amp_AR-amp_AR0)/dt
amp_AI_dot=(amp_AI-amp_AI0)/dt

do 32 js=1,modes
  outr(js)=-g3(js)*(amp_AI_dot-wd*amp_AR)
  outi(js)= g3(js)*(amp_AR_dot+wd*amp_AI)
32 continue

c      4th order Runge Kutta integration for cavity
c      *****
call RKM(t0,hdt,dt6,AR,AI,f0,fe,g1,g2,outr,outi,modes)

do 51 js=1,modes
  amplitude(js) = sqrt(AR(js)*AR(js)+AI(js)*AI(js))
  if(abs(AR(js)).gt.1.0d-9)then
    phase(js) = atan(AI(js)/AR(js))
  else
    phase(js)=0.5d00*pi
  end if
  phase_deg(js)=phase(js)*180.0d00/pi
  if((j.gt.nbeam_on+nsettle).and.(j.lt.nbeam_off))then
    sum_sq_ph_err(js)=sum_sq_ph_err(js)+phase_deg(js)**2
    amp_err(js)=amplitude(js)-v_set_point(js)
    sum_sq_amp_err(js)=sum_sq_amp_err(js)+amp_err(js)**2
    normalise(js)=normalise(js)+1
  endif
51 continue

time = t2*1.0d09

ic=ic+1
ic_delay=ic_delay+1
if(ic_delay.eq.idelay+1) ic_delay=1
if(ic.eq.idelay+1) ic=1

c      output data to files and screen
c      *****
if(j.gt.nprint)then
  write(*,901) time, amplitude(1), phase_deg(1), vdr, vdi
901   format('t=',f11.3,' amp=',f11.1,
+       ' ph=', e11.4,' Rcntr=', f10.1,' Icntr=', f9.1)
  nprint=nprint+100000*its_per_cycle
end if

if(j.gt.nwrite)then
  drive_amp=sqrt(Vdr**2+Vdi**2)
  if(drive_amp.gt.0.0d00)then
    drive_phase=180.0d00*asin(Vdi/drive_amp)/pi
  else
    drive_phase=0.0d00
  end if
  drive_pow=0.5d00*drive_amp**2/(QE(1)*ROQ)
  write(40,902) icycle, time, amplitude(1), phase_deg(1),
+ vdr, vdi,drive_pow,drive_phase
902   format(2x,i12,3x,1pe11.4,3x,1pe11.4,3x,e13.6,3x,1pe11.4,
+       3x,1pe11.4,3x,1pe11.4,3x,1pe11.4)

  if(icycle.gt.nbeam_on)then
    if(drive_pow.gt.max_power_used)then
      max_power_used=drive_pow
    end if
  end if

  if((icycle.gt.ndetail).and.(icycle.lt.ndetail+20000))then
    nwrite=nwrite+20*its_per_cycle

```

```

elseif(icycle.lt.nbeam_on)then
  nwrite=nwrite+2000*its_per_cycle
elseif((icycle.gt.nbeam_on).and.
+   (icycle.lt.(nbeam_on+400000)))then
  nwrite=nwrite+100*its_per_cycle
else
  nwrite=nwrite+2000*its_per_cycle
end if
end if

if((j.gt.0).and.(j.lt.5000))then
  time = t2*1.0d09
  write(41,903) time, AR(1), testr, testi
903  format(3x,f11.3,3x,f11.5,3x,1p11.5,3x,1p11.5)
end if

c  Provision for more than one time step per cycle
c  *****
cycle=cycle+1.0d00/its_per_cycle
if(cycle.gt.0.9999d00)then
  icycle=icycle+cycle*1.00001d00
  cycle=0.0d00
end if

c  Beam loading of modes
c  *****
if(icycle.gt.cycle_of_next_bunch)then
  if((icycle.gt.nbeam_on).and.(icycle.le.nbeam_off))then
    bunch_phase_err=bunch_phase_jitter*pi/180.0d00
    Vkick=Vjump*cos(w_offset*t2)
    if(lrandom)then
      bunch_phase_err=bunch_phase_err*random( )
      Vkick=Vjump*random( )
    end if

c  add in systematic phase advance (zero if bunches synchronised to drive)
c  *****
value=cycle_of_next_bunch-icycle
bunch_phase=bunch_phase_err+2.0d00*value*pi
cos_err=cos(bunch_phase)
sin_err=sin(bunch_phase)

do 152 js=1, modes
  AR(js)=AR(js)-Vkick*mode_beam_coupling(js)*cos_err
  AI(js)=AI(js)-Vkick*mode_beam_coupling(js)*sin_err
152  continue

  cycle_of_next_bunch = cycle_of_next_bunch
+                               + cycles_between_bunches
endif
endif

t0=t2
1  continue

write(*,9977) max_power_used
write(46,9977) max_power_used
9977  format('maximum power delivered           =', f9.2)

value=sqrt(sum_sq_ph_err(1)/normalise(1))
write(*,9978) value
write(46,9978) value
9978  format('In pulse rms phase err           =', f10.5,
+          ' degrees')

```

```

        if(v_set_point(1).gt.0.0d00)then
            value=
+ 100.0d00*sqrt(sum_sq_amp_err(1)/normalise(1))/v_set_point(1)
            write(*,9979) value
            write(46,9979) value
9979 format('In pulse rms amplitude err           =', f10.5,' %')
            value=
+ 100.0d00*sqrt(sum_sq_amp_err(2)/normalise(2))/v_set_point(1)
            write(*,9980) value
            write(46,9980) value
9980 format('Relative excitation of 2nd mode       =', f10.5,' %')

            value=
+ 100.0d00*sqrt(sum_sq_amp_err(3)/normalise(3))/v_set_point(1)
            write(*,9981) value
            write(46,9981) value
9981 format('Relative excitation of 3rd mode       =', f10.5,' %')

        else

            value=sqrt(sum_sq_amp_err(1)/normalise(1))
            write(*,9939) value
            write(46,9939) value
9939 format('In pulse rms amplitude err           =', f10.5,' V')

            value=sqrt(sum_sq_amp_err(2)/normalise(2))
            write(*,9930) value
            write(46,9930) value
9930 format('Relative excitation of 2nd mode       =', f10.5,' V')

            value=sqrt(sum_sq_amp_err(3)/normalise(3))
            write(*,9931) value
            write(46,9931) value
9931 format('Relative excitation of 3rd mode       =', f10.5,' V')
            end if

            close(unit=40,status='keep')
            close(unit=41,status='keep')
            close(unit=46,status='keep')

1000 stop

3000 print*,'error ',nerror,' reading value'
        go to 1001

1001 close(unit=45,status='keep')
        close(unit=46,status='keep')
        go to 1000
        end

        subroutine RK(t0,hdt,dt6,AR0,AI0,f1,f2,outr,outi)
c *****
        real*8 AR0, AR1, AR2, AR3, AR4, AI0, AI1, AI2, AI3, AI4
        real*8 DAR1, DAR2, DAR3, DAR4, DAI1, DAI2, DAI3, DAI4
        real*8 f1, f2, t0, t1, t2, dt6, hdt, outr, outi

        t1 = t0+hdt
        DAR1=-f1*AR0-f2*AI0+outr
        AR1 = AR0+hdt*DAR1
        DAI1=-f1*AI0+f2*AR0+outi
        AI1 = AI0+hdt*DAI1

        DAR2=-f1*AR1-f2*AI1+outr
        AR2 = AR0+hdt*DAR2
        DAI2=-f1*AI1+f2*AR1+outi

```

```

AI2 = AI0+hdt*DAI2

DAR3=-f1*AR2-f2*AI2+outr
AR3 = AR0+2.0d00*hdt*DAR3
DAI3=-f1*AI2+f2*AR2+outi
AI3 = AI0+2.0d00*hdt*DAI3

t2 = t1+hdt
DAR4=-f1*AR3-f2*AI3+outr
AR4 = AR0+dt6*(DAR1+2.0d00*(DAR2+DAR3)+DAR4)
DAI4=-f1*AI3+f2*AR3+outi
AI4 = AI0+dt6*(DAI1+2.0d00*(DAI2+DAI3)+DAI4)

AR0=AR4
AI0=AI4

return
end

subroutine RKM(t0,hdt,dt6,AR0,AI0,f0,fe,g1,g2,outr,outi,modes)
c *****
integer*4 jm
parameter(jm=3)

real*8 AR0(jm), AR1(jm), AR2(jm), AR3(jm), AR4(jm)
real*8 AI0(jm), AI1(jm), AI2(jm), AI3(jm), AI4(jm)
real*8 DAR1(jm), DAR2(jm), DAR3(jm), DAR4(jm)
real*8 DAI1(jm), DAI2(jm), DAI3(jm), DAI4(jm)
real*8 f0(jm), fe(jm), g1(jm), g2(jm)
real*8 outr(jm), outi(jm)
real*8 t0, t1, t2, dt6, hdt, sum

integer*4 j1, j2, modes

t1 = t0+hdt

do 11 j1=1, modes
  sum=0.0d00
  do 12 j2=1, modes
    sum=sum+g1(j2)*AR0(j2)
12  continue
  sum=f0(j1)*g1(j1)*AR0(j1)+fe(j1)*sum
  DAR1(j1)= - sum + g2(j1)*AI0(j1) + outr(j1)
  AR1(j1) = AR0(j1) + hdt*DAR1(j1)

  sum=0.0d00
  do 13 j2=1, modes
    sum=sum+g1(j2)*AI0(j2)
13  continue
  sum=f0(j1)*g1(j1)*AI0(j1)+fe(j1)*sum
  DAI1(j1)= - sum - g2(j1)*AR0(j1) + outi(j1)
  AI1(j1) = AI0(j1)+hdt*DAI1(j1)
11 continue

do 21 j1=1, modes
  sum=0.0d00
  do 22 j2=1, modes
    sum=sum+g1(j2)*AR1(j2)
22  continue
  sum=f0(j1)*g1(j1)*AR1(j1)+fe(j1)*sum
  DAR2(j1)= - sum + g2(j1)*AI1(j1) + outr(j1)
  AR2(j1) = AR0(j1) + hdt*DAR2(j1)

  sum=0.0d00
  do 23 j2=1, modes

```

```

        sum=sum+g1(j2)*AI1(j2)
23      continue
        sum=f0(j1)*g1(j1)*AI1(j1)+fe(j1)*sum
        DAI2(j1)= - sum - g2(j1)*AR1(j1) + outi(j1)
        AI2(j1) =  AI0(j1)+hdt*DAI2(j1)
21      continue

      do 31 j1=1, modes
        sum=0.0d00
        do 32 j2=1, modes
          sum=sum+g1(j2)*AR2(j2)
32        continue
          sum=f0(j1)*g1(j1)*AR2(j1)+fe(j1)*sum
          DAR3(j1)= - sum + g2(j1)*AI2(j1) + outr(j1)
          AR3(j1) =  AR0(j1) + 2.0d00*hdt*DAR3(j1)

          sum=0.0d00
          do 33 j2=1, modes
            sum=sum+g1(j2)*AI2(j2)
33          continue
            sum=f0(j1)*g1(j1)*AI2(j1)+fe(j1)*sum
            DAI3(j1)= - sum - g2(j1)*AR2(j1) + outi(j1)
            AI3(j1) =  AI0(j1) + 2.0d00*hdt*DAI3(j1)
31          continue

          t2 = t1+hdt

          do 41 j1=1, modes
            sum=0.0d00
            do 42 j2=1, modes
              sum=sum+g1(j2)*AR3(j2)
42            continue
              sum=f0(j1)*g1(j1)*AR3(j1)+fe(j1)*sum
              DAR4(j1)= - sum + g2(j1)*AI3(j1) + outr(j1)
              AR4(j1) = AR0(j1) +
+                dt6*(DAR1(j1)+2.0d00*(DAR2(j1)+DAR3(j1))+DAR4(j1))

              sum=0.0d00
              do 43 j2=1, modes
                sum=sum+g1(j2)*AI3(j2)
43              continue
                sum=f0(j1)*g1(j1)*AI3(j1)+fe(j1)*sum
                DAI4(j1)= - sum - g2(j1)*AR3(j1) + outi(j1)
                AI4(j1) = AI0(j1) +
+                dt6*(DAI1(j1)+2.0d00*(DAI2(j1)+DAI3(j1))+DAI4(j1))
41              continue

            do 5 j1=1, modes
              AR0(j1)=AR4(j1)
              AI0(j1)=AI4(j1)
5            continue

          return
          end

```